# Search for supersymmetry in final states with missing transverse momentum and multiple b-jets in proton-proton collisions at s√=13s=13 TeV with the ATLAS detector

ATLAS Collaboration

# Search for supersymmetry in final states with missing transverse momentum and multiple $b$-jets in proton-proton collisions at $\sqrt{s} = 13$ TeV with the ATLAS detector

## The ATLAS collaboration

*E-mail:* atlas.publications@cern.ch

ABSTRACT: A search for supersymmetry involving the pair production of gluinos decaying via third-generation squarks into the lightest neutralino ($\tilde{\chi}_1^0$) is reported. It uses LHC proton-proton collision data at a centre-of-mass energy $\sqrt{s} = 13$ TeV with an integrated luminosity of $36.1\,\mathrm{fb}^{-1}$ collected with the ATLAS detector in 2015 and 2016. The search is performed in events containing large missing transverse momentum and several energetic jets, at least three of which must be identified as originating from $b$-quarks. To increase the sensitivity, the sample is divided into subsamples based on the presence or absence of electrons or muons. No excess is found above the predicted background. For $\tilde{\chi}_1^0$ masses below approximately 300 GeV, gluino masses of less than 1.97 (1.92) TeV are excluded at 95% confidence level in simplified models involving the pair production of gluinos that decay via top (bottom) squarks. An interpretation of the limits in terms of the branching ratios of the gluinos into third-generation squarks is also provided. These results improve upon the exclusion limits obtained with the $3.2\,\mathrm{fb}^{-1}$ of data collected in 2015.

# Contents

# 1 Introduction

Supersymmetry (SUSY) [1–6] is a generalisation of space-time symmetries that predicts new bosonic partners for the fermions and new fermionic partners for the bosons of the Standard Model (SM). If $R$-parity is conserved [7], SUSY particles are produced in pairs and the lightest supersymmetric particle (LSP) is stable. The scalar partners of the left- and right-handed quarks, the squarks $\tilde{q}_{\mathrm{L}}$ and $\tilde{q}_{\mathrm{R}}$, can mix to form two mass eigenstates $\tilde{q}_1$ and $\tilde{q}_2$, ordered by increasing mass. SUSY can solve the hierarchy problem [8–11] reducing unnatural tuning in the Higgs sector by orders of magnitude, provided that the superpartners of the top quark have masses not too far above the weak scale. The large top Yukawa coupling results in significant $\tilde{t}_{\mathrm{L}}$-$\tilde{t}_{\mathrm{R}}$ mixing so that the mass eigenstate $\tilde{t}_1$ is typically

lighter than the other squarks [12, 13]. Because of the SM weak-isospin symmetry, the mass of the lightest bottom squark $\tilde{b}_1$ is also expected to be close to the weak scale. The fermionic partners of the gluons, the gluinos ($\tilde{g}$), are also motivated by naturalness [14] to have a mass around the TeV scale in order to limit their contributions to the radiative corrections to the top squark masses. For these reasons, and because the gluinos are expected to be pair-produced with a high cross-section at the Large Hadron Collider (LHC), the search for gluino production with decays via top and bottom squarks is highly motivated at the LHC.

This paper presents a search for pair-produced gluinos decaying via top or bottom squarks in events with multiple jets originating from the hadronisation of $b$-quarks ($b$-jets in the following), high missing transverse momentum of magnitude $E_T^{miss}$, and potentially additional light-quark jets and/or an isolated charged lepton.[1] The dataset consists of 36.1 fb$^{-1}$ of proton-proton ($pp$) collision data collected with the ATLAS detector [15] at a centre-of-mass energy of 13 TeV in 2015 and 2016. Interpretations are provided in the context of several effective simplified models [16–18] probing various gluino decays into third-generation squarks and the LSP. The latter is assumed to be the lightest neutralino $\tilde{\chi}_1^0$, a linear superposition of the superpartners of the neutral electroweak and Higgs bosons. One model also features the lightest charginos $\tilde{\chi}_1^\pm$, which are linear superpositions of the superpartners of the charged electroweak and Higgs bosons. The results supersede the ones obtained using 3.2 fb$^{-1}$ of data collected in 2015 using the same strategy [19]. Pair-produced gluinos with top-squark-mediated decays have also been searched for using events containing pairs of same-sign leptons or three leptons using 13 TeV data [20, 21]. The same-sign/three lepton search is comparable in sensitivity to the search presented in this paper only when the masses of the gluino and the LSP are very close to each other. Similar searches performed using the 13 TeV dataset collected in 2015 and 2016 by the CMS experiment have produced results comparable to the ATLAS searches [22–25].

## 2 SUSY signal models

Various simplified SUSY models [17, 18] are employed to optimise the event selection and/or interpret the results of the search. In terms of experimental signature, they all contain at least four $b$-jets originating from either gluino or top quark decays, and two $\tilde{\chi}_1^0$, which escape the detector unseen, resulting in high $E_T^{miss}$.

Gluinos are assumed to be pair-produced and to decay either as $\tilde{g} \to \tilde{b}_1 \bar{b}$ or $\tilde{g} \to \tilde{t}_1 \bar{t}$ (the charge conjugate process is implied throughout this paper). The following top and bottom squark decays are then considered: $\tilde{t}_1 \to t \tilde{\chi}_1^0$, $\tilde{t}_1 \to b \tilde{\chi}_1^+$ and $\tilde{b}_1 \to b \tilde{\chi}_1^0$.[2] In all cases, the top or bottom squarks are assumed to be off-shell in order to have simplified models with only two parameters: the gluino and $\tilde{\chi}_1^0$ masses.[3] All other sparticles are decoupled.

---

[1]The term "lepton" refers exclusively to an electron or a muon in this paper.

[2]The decay $\tilde{b}_1 \to t \tilde{\chi}_1^-$ is also possible but, following $\tilde{g} \to \tilde{b}_1 \bar{b}$, it yields the same final state as $\tilde{g} \to \tilde{t}_1^* t \to (\bar{b} \tilde{\chi}_1^-)t$, which is already considered.

[3]The analysis sensitivity is found to be mostly independent of the top and bottom squark masses, except when the top squark is very light [26].
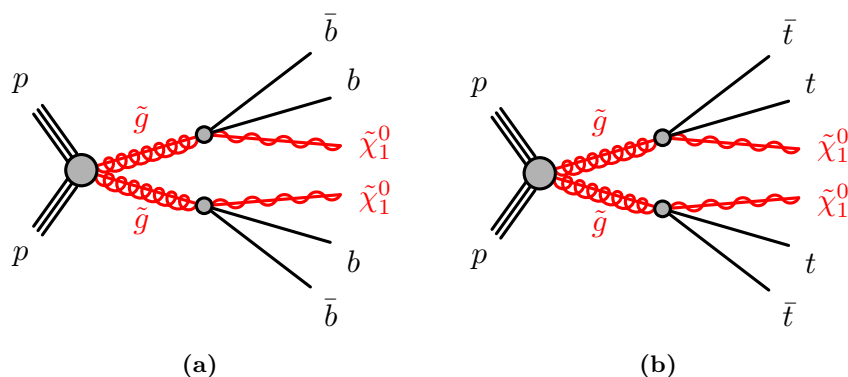
**Figure 1.** The decay topologies in the (a) Gbb and (b) Gtt simplified models.

Two simplified models are used to optimise the event selection and to interpret the results. In the Gbb (Gtt) model, illustrated in figure 1(a) (1(b)), each gluino undergoes an effective three-body decay $\tilde{g} \to b\bar{b}\tilde{\chi}_1^0$ ($\tilde{g} \to t\bar{t}\tilde{\chi}_1^0$) via off-shell bottom (top) squarks, with a branching ratio of 100%. The Gbb model is the simplest in terms of particle multiplicity, resulting in the minimal common features of four $b$-jets and two $\tilde{\chi}_1^0$. In addition to these particles, the Gtt model produces four $W$ bosons originating from the top quark decays: $t \to Wb$. The presence of these four $W$ bosons motivates the design of signal regions with a higher jet multiplicity than for Gbb models, and in some cases with at least one isolated electron or muon.

This paper includes an interpretation that probes the sensitivity of the search as a function of the gluino branching ratio, in addition to the gluino and $\tilde{\chi}_1^0$ masses. Similar interpretations have been performed by the CMS collaboration [24, 27]. For that interpretation a third gluino decay is considered: $\tilde{g} \to t\bar{b}\tilde{\chi}_1^-$ (via the off-shell top squark decay $\tilde{t}_1^* \to \bar{b}\tilde{\chi}_1^-$). The $\tilde{\chi}_1^-$ is then forced to decay as $\tilde{\chi}_1^\pm \to W^*\tilde{\chi}_1^0 \to f\bar{f}'\tilde{\chi}_1^0$ (where $f$ denotes a fermion). To keep the number of model parameters at only two, the mass difference between the $\tilde{\chi}_1^\pm$ and the $\tilde{\chi}_1^0$ is fixed to 2 GeV. Such a small mass-splitting between the $\tilde{\chi}_1^\pm$ and the $\tilde{\chi}_1^0$ is typical of models where the $\tilde{\chi}_1^0$ is dominated by the higgsinos, the superpartners of the neutral Higgs boson. Such models are well motivated by naturalness. The products of the decay $W^* \to f\bar{f}'$ are typically too soft to be detected, except for very large mass differences between the gluino and the $\tilde{\chi}_1^\pm$. Thus, in this model, the gluino can decay as either $\tilde{g} \to b\bar{b}\tilde{\chi}_1^0$, $\tilde{g} \to t\bar{b}\tilde{\chi}_1^-$ (with $\tilde{\chi}_1^- \to f\bar{f}'\tilde{\chi}_1^0$) or $\tilde{g} \to t\bar{t}\tilde{\chi}_1^0$, with the sum of individual branching ratios adding up to 100%. This model probes more realistic scenarios where the branching ratio for either $\tilde{g} \to b\bar{b}\tilde{\chi}_1^0$ or $\tilde{g} \to t\bar{t}\tilde{\chi}_1^0$ is not 100%, and where one, two or three top quarks, and thus on-shell $W$ bosons, are possible in the final state, in between the Gbb (no top quarks) and Gtt (four top quarks) decay topologies. The decay topologies that are considered in the variable branching ratio model are illustrated in figure 2. The model also includes the Gbb and Gtt decay topologies illustrated in figure 1. A limited set of 10 mass points were generated for this variable branching ratio model with $m_{\tilde{g}}$ varying from 1.5 TeV to 2.3 TeV and $m_{\tilde{\chi}_1^0}$ varying from 1 GeV to 1 TeV.
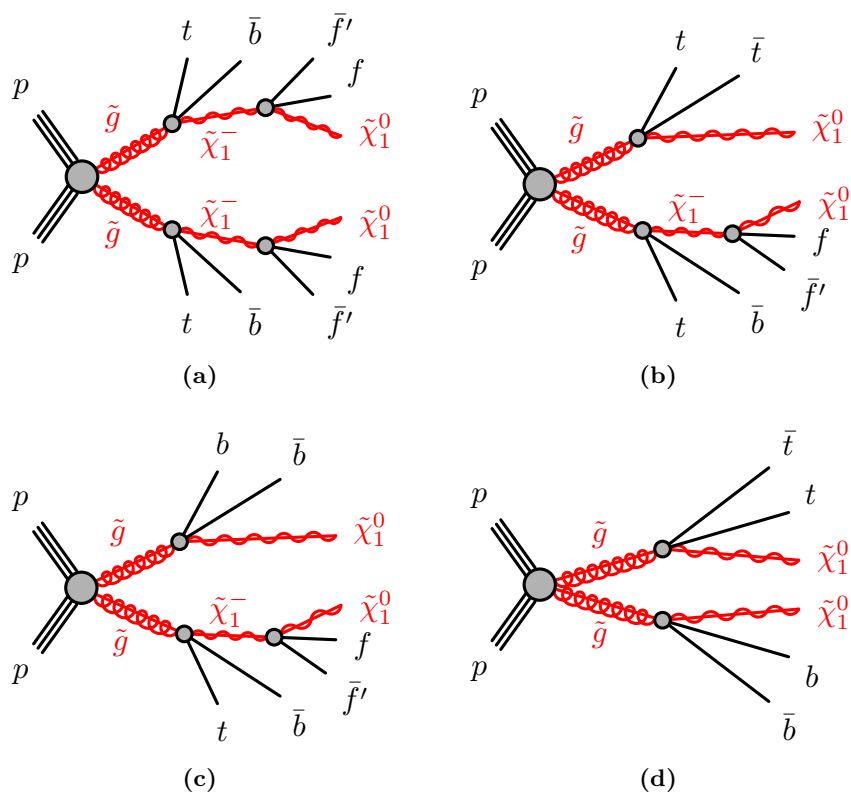
**Figure 2.** The additional decay topologies of the variable gluino branching ratio model in addition to the ones of figure 1. (a) Both gluinos can decay as $\tilde{g} \to t\bar{b}\tilde{\chi}_1^-$ with $\tilde{\chi}_1^- \to f\bar{f}'\tilde{\chi}_1^0$, or only one can with the other decaying as (b) $\tilde{g} \to t\bar{t}\tilde{\chi}_1^0$ or (c) $\tilde{g} \to b\bar{b}\tilde{\chi}_1^0$. (d) Finally, one gluino can decay as $\tilde{g} \to t\bar{t}\tilde{\chi}_1^0$ and the other as $\tilde{g} \to b\bar{b}\tilde{\chi}_1^0$. The charge conjugate processes are implied. The fermions originating from the $\tilde{\chi}_1^\pm$ decay are typically soft because the mass difference between the $\tilde{\chi}_1^\pm$ and the $\tilde{\chi}_1^0$ is fixed to 2 GeV.

The technical implementation of the simulated samples produced from these models is described in section 4.

## 3   ATLAS detector

The ATLAS detector is a multipurpose particle physics detector with a forward-backward symmetric cylindrical geometry and nearly $4\pi$ coverage in solid angle.[4] The inner tracking detector (ID) consists of silicon pixel and microstrip detectors covering the pseudorapidity region $|\eta| < 2.5$, surrounded by a transition radiation tracker, which enhances electron

---

[4]ATLAS uses a right-handed coordinate system with its origin at the nominal interaction point in the centre of the detector. The positive $x$-axis is defined by the direction from the interaction point to the centre of the LHC ring, with the positive $y$-axis pointing upwards, while the beam direction defines the $z$-axis. Cylindrical coordinates $(r, \phi)$ are used in the transverse plane, $\phi$ being the azimuthal angle around the $z$-axis. The pseudorapidity $\eta$ is defined in terms of the polar angle $\theta$ by $\eta = -\ln\tan(\theta/2)$. Rapidity is defined as $y = 0.5\ln[(E + p_z)/(E - p_z)]$ where $E$ denotes the energy and $p_z$ is the component of the momentum along the beam direction.

identification in the region $|\eta| < 2.0$. Before the start of Run 2, the new innermost pixel layer, the insertable B-layer (IBL) [28], was inserted at a mean sensor radius of 3.3 cm. The ID is surrounded by a thin superconducting solenoid providing an axial 2 T magnetic field and by a fine-granularity lead/liquid-argon (LAr) electromagnetic calorimeter covering $|\eta| < 3.2$. A steel/scintillator-tile calorimeter provides coverage for hadronic showers in the central pseudorapidity range ($|\eta| < 1.7$). The endcaps ($1.5 < |\eta| < 3.2$) of the hadronic calorimeter are made of LAr active layers with either copper or tungsten as the absorber material. The forward region ($3.1 < |\eta| < 4.9$) is instrumented with a LAr calorimeter for both the EM and hadronic measurements. A muon spectrometer with an air-core toroidal magnet system surrounds the calorimeters. Three layers of high-precision tracking chambers provide coverage in the range $|\eta| < 2.7$, while dedicated fast chambers allow triggering in the region $|\eta| < 2.4$. The ATLAS trigger system [29] consists of a hardware-based level-1 trigger followed by a software-based high-level trigger (HLT).

## 4 Data and simulated event samples

The data used in this analysis were collected by the ATLAS detector from $pp$ collisions produced by the LHC at a centre-of-mass-energy of 13 TeV and 25 ns proton bunch spacing over the 2015 and 2016 data-taking periods. The full dataset corresponds to an integrated luminosity of 36.1 fb$^{-1}$ after the application of beam, detector and data-quality requirements. The uncertainty in the combined 2015+2016 integrated luminosity is 2.1%. It is derived, following a methodology similar to that detailed in ref. [30], from a preliminary calibration of the luminosity scale using $x$-$y$ beam-separation scans performed in August 2015 and May 2016. Events are required to pass an $E_{\mathrm{T}}^{\mathrm{miss}}$ trigger with thresholds of 70 GeV, 100 GeV and 110 GeV at the HLT level for the 2015, early 2016 and late 2016 datasets, respectively. These triggers are fully efficient for events passing the preselection defined in section 6, which requires the offline reconstructed $E_{\mathrm{T}}^{\mathrm{miss}}$ to exceed 200 GeV. There are on average 24 inelastic $pp$ collisions (the interactions other than the hard scatter are referred to as "pile-up") in the dataset.

Samples of Monte Carlo (MC) simulated events are used to model the signal and background processes in this analysis, except multijet processes, which are estimated from data. SUSY signal samples in which each gluino decays into $b\bar{b}\tilde{\chi}_1^0$, $t\bar{t}\tilde{\chi}_1^0$, or $t\bar{b}\tilde{\chi}_1^-$ were generated with up to two additional partons using MADGRAPH5_aMC@NLO [31] v2.2.2 at leading order (LO) with the NNPDF 2.3 [32] parton distribution function (PDF) set. These samples were interfaced to PYTHIA v8.186 [33] for the modelling of the parton showering, hadronisation and underlying event.

The dominant background in the signal regions is the production of $t\bar{t}$ pairs with additional high transverse momentum ($p_{\mathrm{T}}$) jets. For the generation of $t\bar{t}$ and single top quarks in the $Wt$- and $s$-channels the POWHEG-BOX [34] v2 event generator with the CT10 [35] PDF set in the matrix element calculations was used. Electroweak $t$-channel single-top-quark events were generated using the POWHEG-BOX v1 event generator. This event generator uses the four-flavour scheme for the next-to-leading order (NLO) matrix elements calculations together with the fixed four-flavour PDF set CT10f4. For all processes

involving top quarks, top-quark spin correlations are preserved. In the $t$-channel, top quarks were decayed using MadSpin [36]. The parton shower, fragmentation, and the underlying event were simulated using PYTHIA v6.428 [37] with the CTEQ6L1 PDF set [38]. The $h_{\mathrm{damp}}$ parameter in POWHEG, which controls the $p_T$ of the first additional emission beyond the Born level and thus regulates the $p_T$ of the recoil emission against the $t\bar{t}$ system, was set to the mass of the top quark ($m_{\mathrm{top}} = 172.5$ GeV). All events with at least one leptonically decaying $W$ boson are included. Single-top and $t\bar{t}$ events in which all top quarks decay hadronically do not contain sufficient $E_{\mathrm{T}}^{\mathrm{miss}}$ to contribute significantly to the background.

Smaller backgrounds in the signal region come from the production of $t\bar{t}$ pairs in association with $W/Z/h$ bosons and possibly additional jets, and production of $t\bar{t}t\bar{t}$, $W/Z$+jets and $WW/WZ/ZZ$ (diboson) events. Other potential sources of background, such as the production of three top quarks or three gauge bosons, are expected to be negligible. The production of $t\bar{t}$ pairs in association with electroweak vector bosons $W$ and $Z$ was modelled by samples generated at LO using MADGRAPH5_aMC@NLO v2.2.2 and showered with PYTHIA v8.186, while samples to model $t\bar{t}H$ production were generated using MAD-GRAPH5_aMC@NLO v2.2.1 and showered with HERWIG++ [39] v2.7.1. These samples are described in detail in ref. [40]. MADGRAPH5_aMC@NLO was also used to simulate the $t\bar{t}t\bar{t}$ production and the showering was performed with PYTHIA v8.186. The $W/Z$+jets processes were simulated using the SHERPA v2.2.0 [41] event generator, while SHERPA v2.1.1 was used to simulate diboson production processes. Matrix elements for the $W/Z$+jets and diboson processes were calculated using Comix [42] and OpenLoops [43] and merged with the SHERPA parton shower [44] using the ME+PS@NLO prescription [45]. The SHERPA diboson sample cross-section was scaled down to account for its use of $\alpha_{\mathrm{QED}} = 1/129$ rather than $1/132$, corresponding to the use of current Particle Data Group [46] parameters, as input to the $G_\mu$ scheme [47]. Samples generated using MADGRAPH5_aMC@NLO v2.2.2 were produced with the NNPDF 2.3 PDF set and $W/Z$+jets samples were generated with the NNPDF 3.0 PDF set [48], while all other samples used CT10 PDFs.

For all samples, except the ones generated using SHERPA, the EVTGEN v1.2.0 program [49] was used to simulate the properties of the bottom- and charm-hadron decays. All PYTHIA v6.428 samples used the PERUGIA2012 [50] set of tuned parameters (tune) for the underlying event, while PYTHIA v8.186 and HERWIG++ showering were run with the A14 [51] and UEEE5 [52] underlying-event tunes, respectively. In-time and out-of-time pile-up interactions from the same or nearby bunch-crossings were simulated by overlaying additional $pp$ collisions generated by PYTHIA v8.186 using the A2 tune [53] and the MSTW2008LO parton distribution function set [54] on top of the hard-scattering events. Details of the sample generation and normalisation are summarised in table 1. Additional samples with different event generators and settings are used to estimate systematic uncertainties in the backgrounds, as described in section 7.

All simulated event samples were passed through the full ATLAS detector simulation using GEANT4 [55], with the exception of signal samples in which at least one gluino decays as $\tilde{g} \to b\bar{b}\tilde{\chi}_1^0$ or $\tilde{g} \to t\bar{b}\tilde{\chi}_1^-$, which were passed through a fast simulation that uses a parameterisation for the calorimeter response [56] and GEANT4 for the ID and the muon spectrometer. The simulated events are reconstructed with the same algorithm as that used for data.

| Process | Event Generator + fragmentation/hadronisation | Tune | PDF set | Cross-section order |
|---|---|---|---|---|
| **SUSY signal** | MadGraph5_aMC@NLO v2.2.2 + Pythia v8.186 | A14 | NNPDF2.3 | NLO+NLL [57–62] |
| $t\bar{t}$ | Powheg-Box v2 + Pythia v6.428 | PERUGIA2012 | CT10 | NNLO+NNLL [64] |
| **Single top** | Powheg-Box v1 or v2 + Pythia v6.428 | PERUGIA2012 | CT10 | NNLO+NNLL [65–67] |
| $t\bar{t}W/t\bar{t}Z/$**4-tops** | MadGraph5_aMC@NLO v2.2.2 + Pythia v8.186 | A14 | NNPDF2.3 | NLO [68] |
| $t\bar{t}H$ | MadGraph5_aMC@NLO v2.2.1 + Herwig++ v2.7.1 | UEEE5 | CT10 | NLO [69] |
| **Diboson** $WW, WZ, ZZ$ | Sherpa v2.1.1 | Default | CT10 | NLO [47] |
| $W/Z$+**jets** | Sherpa v2.2.0 | Default | NNPDF3.0 | NNLO [70] |

**Table 1.** List of event generators used for the different processes. Information is given about the underlying-event tunes, the PDF sets and the pQCD highest-order accuracy used for the normalisation of the different samples.

The signal samples are normalised using the best cross-section calculations at NLO in the strong coupling constant, adding the resummation of soft gluon emission at next-to-leading-logarithm (NLL) accuracy [57–61]. The nominal cross-section and the uncertainty are taken from an envelope of cross-section predictions using different PDF sets and factorisation and renormalisation scales, as described in ref. [62]. The cross-section of gluino pair-production in these simplified models is $14 \pm 3$ fb for a gluino mass of 1.5 TeV, falling to $1.0 \pm 0.3$ fb for 2 TeV mass gluinos. All background processes are normalised using the best available theoretical calculation for their respective cross-sections. The order of this calculation in perturbative QCD (pQCD) for each process is listed in table 1. For $t\bar{t}$, the largest background, this corresponds to a cross-section of 831.8 pb.

Finally, contributions from multijet background are estimated from data using a procedure described in ref. [63], which performs a smearing of the jet response in data events with well-measured $E_{\mathrm{T}}^{\mathrm{miss}}$ (so-called "seed events"). The response function is derived in Monte Carlo dijet events and is different for $b$-tagged and non-$b$-tagged jets.

## 5 Event reconstruction

Interaction vertices from the proton-proton collisions are reconstructed from at least two tracks with $p_T > 0.4$ GeV, and are required to be consistent with the beamspot envelope. The primary vertex is identified as the one with the largest sum of squares of the transverse momenta from associated tracks ($\sum |p_{T,track}|^2$) [71].

Basic selection criteria are applied to define candidates for electrons, muons and jets in the event. An overlap removal procedure is applied to these candidates to prevent double-counting. Further requirements are then made to select the final signal leptons and jets from the remaining candidates. The details of the candidate selections and of the overlap removal procedure are given below.

Candidate jets are reconstructed from three-dimensional topological energy clusters [72] in the calorimeter using the anti-$k_t$ jet algorithm [73, 74] with a radius parameter of 0.4 (small-$R$ jets). Each topological cluster is calibrated to the electromagnetic scale response prior to jet reconstruction. The reconstructed jets are then calibrated to the particle level by the application of a jet energy scale (JES) derived from $\sqrt{s} = 13$ TeV data and simulations [75]. Quality criteria are imposed to reject events that contain at least one jet arising from non-collision sources or detector noise [76]. Further selections are applied to reject jets that originate from pile-up interactions by means of a multivariate algorithm using information about the tracks matched to each jet [77]. Candidate jets are required to have $p_T > 20$ GeV and $|\eta| < 2.8$. After resolving overlaps with electrons and muons, selected jets are required to satisfy the stricter requirement of $p_T > 30$ GeV.

A jet is tagged as a $b$-jet candidate by means of a multivariate algorithm using information about the impact parameters of inner detector tracks matched to the jet, the presence of displaced secondary vertices, and the reconstructed flight paths of $b$- and $c$-hadrons inside the jet [78, 79]. The $b$-tagging working point corresponding to an efficiency of 77% to identify $b$-jets with $p_T > 20$ GeV, as determined from a sample of simulated $t\bar{t}$ events, is found to be optimal for the statistical significance of this search. The corresponding rejection factors against jets originating from $c$-quarks, $\tau$-leptons and light quarks and gluons in the same sample at this working point are 6, 22 and 134, respectively.

After resolving the overlap with leptons, the candidate small-$R$ jets are re-clustered [80] into large-$R$ jets using the anti-$k_t$ algorithm with a radius parameter of 0.8. The calibration from the input small-$R$ jets propagates directly to the re-clustered jets. These re-clustered jets are then trimmed [80–83] by removing subjets whose $p_T$ falls below 10% of the $p_T$ of the original re-clustered jet. The resulting large-$R$ jets are required to have $p_T > 100$ GeV and $|\eta| < 2.0$. When it is not explicitly stated otherwise, the term "jets" in this paper refers to small-$R$ jets.

Electron candidates are reconstructed from energy clusters in the electromagnetic calorimeter and inner detector tracks and are required to satisfy a set of "loose" quality criteria [84, 85]. They are also required to have $|\eta| < 2.47$. Muon candidates are reconstructed from matching tracks in the inner detector and muon spectrometer. They are required to meet "medium" quality criteria, as described in ref. [86], and to have $|\eta| < 2.5$. All electron and muon candidates must have $p_T > 20$ GeV.

Leptons are selected from the candidates that survive the overlap removal procedure if they fulfil a requirement on the scalar sum of $p_{\mathrm{T}}$ of additional inner detector tracks in a cone around the lepton track. This isolation requirement is defined to ensure a flat efficiency of around 99% across the whole electron transverse energy and muon transverse momentum ranges. The angular separation between the lepton and the $b$-jet ensuing from a semileptonic top quark decay narrows as the $p_{\mathrm{T}}$ of the top quark increases. This increased collimation is accounted for by setting the radius of the isolation cone to $\min(0.2, 10 \text{ GeV}/p_{\mathrm{T}}^{\mathrm{lep}})$, where $p_{\mathrm{T}}^{\mathrm{lep}}$ is the lepton $p_{\mathrm{T}}$ expressed in GeV. Selected electrons are further required to meet the "tight" quality criteria [84, 85]. Electrons (muons) are matched to the primary vertex by requiring the transverse impact parameter $d_0$ of the associated ID track to satisfy $|d_0|/\sigma_{d_0} < 5$ (3), where $\sigma_{d_0}$ is the measured uncertainty of $d_0$, and the longitudinal impact parameter $z_0$ to satisfy $|z_0 \sin\theta| < 0.5$ mm.[5] In addition, events containing one or more muon candidates with $|d_0|$ ($|z_0|$) $> 0.2$ mm (1 mm) are rejected to suppress cosmic rays.

Overlaps between candidate objects are removed sequentially. Firstly, electron candidates that lie a distance[6] $\Delta R < 0.01$ from muon candidates are removed to suppress contributions from muon bremsstrahlung. Overlaps between electron and jet candidates are resolved next, and finally, overlaps between remaining jets and muon candidates are removed.

Overlap removal between electron and jet candidates aims to resolve two sources of ambiguity: it is designed, firstly, to remove jets that are formed primarily from the showering of a prompt electron and, secondly, to remove electrons that are produced in the decay chains of hadrons. Consequently, any non-$b$-tagged jet whose axis lies $\Delta R < 0.2$ from an electron is discarded. Electrons with $E_{\mathrm{T}} < 50$ GeV are discarded if they lie $\Delta R < 0.4$ from the axis of any remaining jet and the corresponding jet is kept. For higher-$E_{\mathrm{T}}$ electrons, the latter removal is performed using a threshold of $\Delta R = \min(0.4, 0.04 + 10 \text{ GeV}/E_{\mathrm{T}})$ to increase the acceptance for events with collimated top quark decays.

The procedure to remove overlaps between muon and jet candidates is designed to remove those muons that are likely to have originated from the decay of hadrons and to retain the overlapping jet. Jets and muons may also appear in close proximity when the jet results from high-$p_{\mathrm{T}}$ muon bremsstrahlung, and in such cases the jet should be removed and the muon retained. Such jets are characterised by having very few matching inner detector tracks. Therefore, if the angular distance $\Delta R$ between a muon and a jet is lower than 0.2, the jet is removed if it is not $b$-tagged and has fewer than three matching inner detector tracks. Like the electrons, muons with $p_{\mathrm{T}}$ below (above) 50 GeV are subsequently discarded if they lie within $\Delta R = 0.4$ ($\Delta R = \min(0.4, 0.04 + 10 \text{ GeV}/p_{\mathrm{T}})$) of any remaining jet.

The missing transverse momentum ($E_{\mathrm{T}}^{\mathrm{miss}}$) in the event is defined as the magnitude of the negative vector sum ($\vec{p}_{\mathrm{T}}^{\;\mathrm{miss}}$) of the transverse momenta of all selected and calibrated objects in the event, with an extra term added to account for energy deposits that are not associated with any of these selected objects. This "soft" term is calculated from inner detector tracks matched to the primary vertex to make it more resilient to contamination from pile-up interactions [87, 88].

---

[5]Both the transverse and longitudinal impact parameters are defined with respect to the selected primary vertex.

[6]$\Delta R = \sqrt{(\Delta y)^2 + (\Delta\phi)^2}$ defines the distance in rapidity $y$ and azimuthal angle $\phi$.

Corrections derived from data control samples are applied to simulated events to account for differences between data and simulation in the reconstruction efficiencies, momentum scale and resolution of leptons, in the efficiency and fake rate for identifying $b$-jets, and in the efficiency for rejecting jets originating from pile-up interactions.

## 6 Event selection

The event selection criteria are defined based on kinematic requirements for the objects defined in section 5. Other discriminating event-based variables, described in section 6.1, are used to further reject the background. Two sets of preselection criteria targeting the 0-lepton and the 1-lepton channels are presented in section 6.2. The modelling of the data in these regions is also discussed in that section. The general analysis strategy and the treatment of background sources is presented in section 6.3. Finally, the event selection for the cut-and-count and multi-bin analyses are discussed in sections 6.4 and 6.5, respectively.

### 6.1 Discriminating variables

The effective mass variable ($m_{\text{eff}}$) is defined as:

$$m_{\text{eff}} = \sum_i p_{\text{T}}^{\text{jet}_i} + \sum_j p_{\text{T}}^{\ell_j} + E_{\text{T}}^{\text{miss}},$$

where the first and second sums are over the selected jets ($N_{\text{jet}}$) and leptons ($N_{\text{lepton}}$), respectively. It typically has a much higher value in pair-produced gluino events than in background events.

In regions with at least one selected lepton, the transverse mass $m_{\text{T}}$ composed of the $p_{\text{T}}$ of the leading selected lepton ($\ell$) and $E_{\text{T}}^{\text{miss}}$ is defined as:

$$m_{\text{T}} = \sqrt{2p_{\text{T}}^{\ell} E_{\text{T}}^{\text{miss}}\{1 - \cos[\Delta\phi(\vec{p}_{\text{T}}^{\text{miss}}, \vec{p}_{\text{T}}^{\ell})]\}}.$$

It is used to reduce the $t\bar{t}$ and $W$+jets background events in which a $W$ boson decays leptonically. Neglecting resolution effects, the $m_{\text{T}}$ distribution for these backgrounds has an expected upper bound corresponding to the $W$ boson mass and typically has higher values for Gtt events. Another useful transverse mass variable is $m_{\text{T,min}}^{b\text{-jets}}$, the minimum transverse mass formed by $E_{\text{T}}^{\text{miss}}$ and any of the three highest-$p_{\text{T}}$ $b$-tagged jets in the event:

$$m_{\text{T,min}}^{b\text{-jets}} = \min_{i \leq 3}\left(\sqrt{2p_{\text{T}}^{b\text{-jet}_i} E_{\text{T}}^{\text{miss}}\{1 - \cos[\Delta\phi(\vec{p}_{\text{T}}^{\text{miss}}, \vec{p}_{\text{T}}^{b\text{-jet}_i})]\}}\right).$$

The $m_{\text{T,min}}^{b\text{-jets}}$ distribution has an expected upper bound corresponding to the top quark mass for $t\bar{t}$ events with a semileptonic top quark decay, while peaking at higher values for Gbb and Gtt events.

Another powerful variable is the total jet mass variable, defined as:

$$M_J^{\Sigma} = \sum_{i \leq 4} m_{J,i},$$

– 10 –

where $m_{J,i}$ is the mass of the large-radius re-clustered jet $i$ in the event. The decay products of a hadronically decaying boosted top quark can be reconstructed in a single large-radius re-clustered jet, resulting in a jet with a high mass. This variable typically has larger values for Gtt events than for background events. This is because Gtt events contain as many as four hadronically decaying top quarks while the background is dominated by $t\bar{t}$ events with one or two semileptonic top quark decays.

The requirement of a selected lepton, with the additional requirements on jets, $E_T^{\mathrm{miss}}$ and event variables described above, makes the multijet background negligible for the $\geq 1$-lepton signal regions. For the 0-lepton signal regions, the minimum azimuthal angle $\Delta\phi_{\mathrm{min}}^{4\mathrm{j}}$ between $\vec{p}_T^{\mathrm{miss}}$ and the $p_T$ of the four leading small-$R$ jets in the event, defined as:

$$\Delta\phi_{\mathrm{min}}^{4\mathrm{j}} = \min_{i\leq 4}\left(\left|\phi_{\mathrm{jet}_i} - \phi_{\vec{p}_T^{\mathrm{miss}}}\right|\right),$$

is required to be greater than 0.4. This requirement supresses the multijet background, which can produce events with large $E_T^{\mathrm{miss}}$ if containing poorly measured jets or neutrinos emitted close to the axis of a jet. A similar variable, denoted $\Delta\phi^{\mathrm{j1}}$, is also used in the Gbb signal regions targeting small mass differences between the gluino and the neutralino, allowing the identification of events containing a high-$p_T$ jet coming from initial-state radiation (ISR) and recoiling against the gluino pair. It is defined as the absolute value of the azimuthal angle separating the $p_T$ of the leading jet and $\vec{p}_T^{\mathrm{miss}}$, and is expected to have larger values for the targeted signal than for the background.

## 6.2 Modelling of the data

Preselection criteria in the 0-lepton and 1-lepton channels require $E_T^{\mathrm{miss}} > 200$ GeV, in addition to the $E_T^{\mathrm{miss}}$ trigger requirement, and at least four jets of which at least two must be $b$-tagged. The 0-lepton (1-lepton) channel requires the event to contain no (at least one) selected lepton.

In this analysis, correction factors need to be extracted to account for shape discrepancies in the $m_{\mathrm{eff}}$ spectrum between the data and the expected background for the 1-lepton preselection sample. These factors are defined as the ratio of the number of observed events to the predicted number of background events in a given $m_{\mathrm{eff}}$ bin, in a signal-depleted region. This region is defined by applying the 1-lepton preselection criteria and requiring exactly two $b$-tagged jets and $m_{\mathrm{T,min}}^{b\text{-jets}} < 140$ GeV. This kinematic reweighting leads to correction factors ranging from 0.7 to 1.1. They are applied to the background prediction and the full size of the correction is taken as an uncertainty for both the background and signal events.

Figures 3 and 4 show the multiplicity of selected jets and $b$-tagged jets, the distributions of $E_T^{\mathrm{miss}}$, $m_{\mathrm{eff}}$, and $M_J^\Sigma$ for events passing the 0-lepton or the 1-lepton preselection, respectively. Figure 3 (4) also displays the distribution of $m_{\mathrm{T,min}}^{b\text{-jets}}$ ($m_T$) in the 0-lepton (1-lepton) channel. The correction described above is applied in the 1-lepton channel. The uncertainty bands include the statistical and experimental systematic uncertainties, as described in section 7, but not the theoretical uncertainties in the background modelling.

The data and the predicted background are found to agree reasonably well at the preselection level after the kinematic reweighting described above. A discrepancy between

data and prediction is observed for the number of $b$-tagged jets, but it has a negligible impact on the background estimate after the renormalisation of the simulation in dedicated control regions with the same $b$-tagged jets requirements as the signal regions, as described in sections 6.4 and 6.5. Example signal models with enhanced cross-sections are overlaid for comparison.

## 6.3 Analysis strategy and background treatment

In order to enhance the sensitivity to the various signal benchmarks described in section 2, multiple signal regions (SRs) are defined. The main background in all these regions is the production of a $t\bar{t}$ pair in association with heavy- and light-flavour jets. A normalisation factor for this background is extracted for each individual SR from a data control region (CR) that has comparable background composition and kinematics. This is ensured by keeping the kinematic requirements similar in the two regions. The CRs and SRs are defined to be mutually exclusive. Signal contributions in the CRs are suppressed by inverting or relaxing some requirements on the kinematic variables (e.g. $m_{\mathrm{T}}$ or $m_{\mathrm{T,min}}^{b\text{-jets}}$), leading to a signal contamination in the CRs of 6% at most. The $t\bar{t}$ normalisation is cross-checked in validation regions (VRs) that share similar background composition, i.e. jet and lepton flavours, with the SR. The signal contamination in the VRs is found to be lower than 30% for benchmark signal mass points above the already excluded mass range. The $t\bar{t}$ purity is superior to 73% and 53% in the CRs and VRs, respectively.

The non-$t\bar{t}$ backgrounds mainly consist of single-top, $W$+jets, $Z$+jets, $t\bar{t}$ +$W/Z/h$, $t\bar{t}t\bar{t}$ and diboson events. Their normalisation is taken from the simulation normalised using the best available theory prediction. The multijet background is found to be very small or negligible in all regions. It is estimated using a procedure described in ref. [63], in which the jet response is determined from simulated dijet events. This response function is then used to smear the jet response in low-$E_{\mathrm{T}}^{\mathrm{miss}}$ events. The jet response is cross-checked with data where the $E_{\mathrm{T}}^{\mathrm{miss}}$ can be unambiguously attributed to the mismeasurement of one of the jets.

Two analysis strategies are followed, and different SR sets are defined for each:

- A **cut-and-count** analysis, using partially overlapping single-bin SRs, optimised to maximise the expected discovery power for benchmark signal models, and allowing for reinterpretation of the results. The SRs are defined to probe the existence of a signal or to assess model-independent upper limits on the number of signal events.

- A **multi-bin** analysis, using a set of non-overlapping SRs and CRs that are combined to strengthen the exclusion limits on the targeted signal benchmarks. This set of regions is used to assess model-dependent interpretations of the various signal models.

## 6.4 Cut-and-count analysis

The SRs are named in the form SR-$X$-$Y$L-$Z$, where $X$ indicates the target model, $Y$ indicates the number of leptons and $Z$ labels the type of region targeted. The cut-and-count regions labelled B (for "boosted") are optimised for signals with a large mass difference between the gluino and the neutralino ($\Delta m \gtrsim 1.5$ TeV), possibly leading to highly boosted
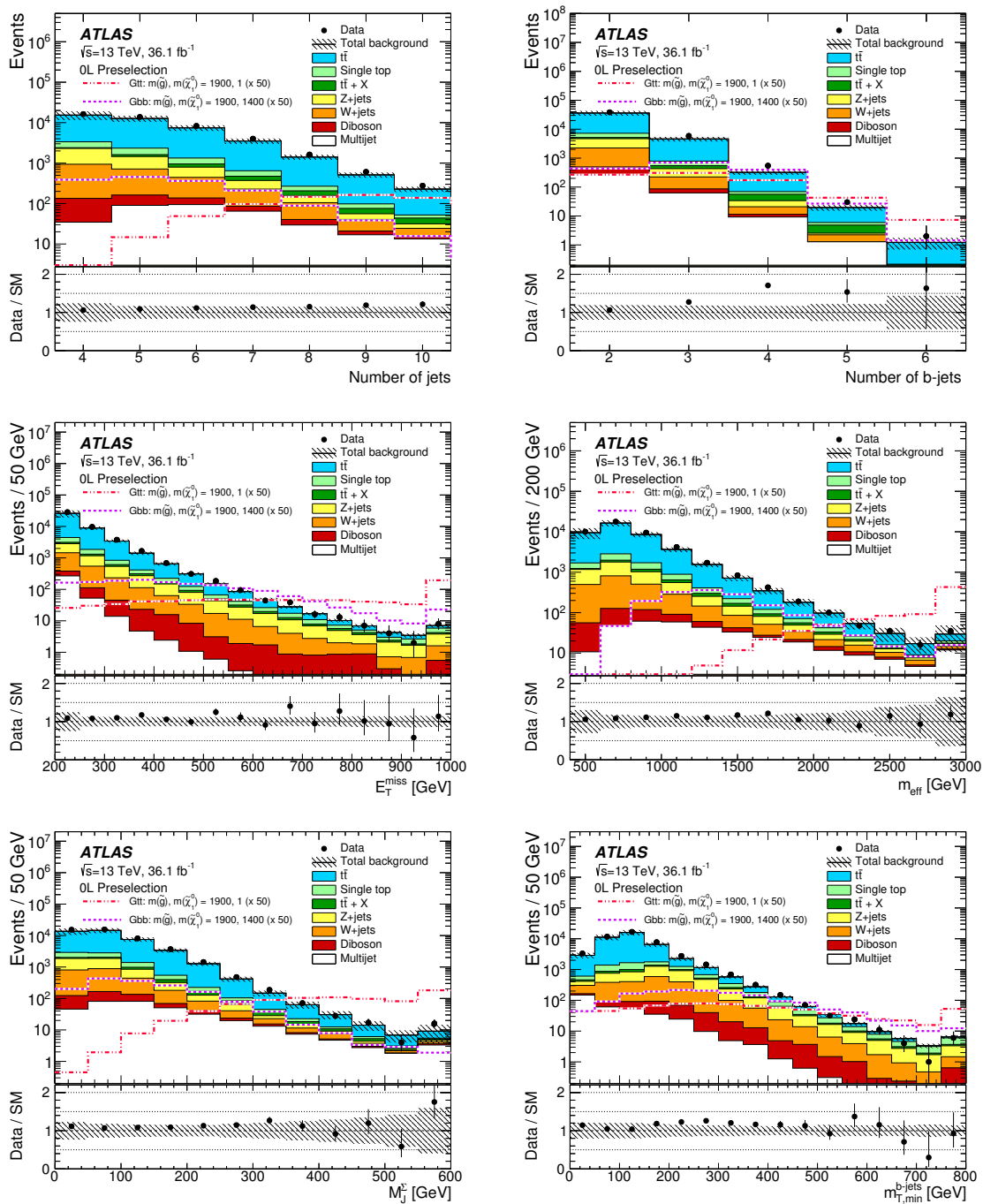
**Figure 3.** Distributions of (top-left) the number of selected jets ($N_{\text{jet}}$), (top-right) the number of selected $b$-tagged jets, (centre-left) $E_{\text{T}}^{\text{miss}}$, (centre-right) $m_{\text{eff}}$, (bottom-left) $M_J^{\Sigma}$ and (bottom-right) $m_{\text{T,min}}^{b\text{-jets}}$ for events passing the 0-lepton preselection criteria. The statistical and experimental systematic uncertainties (as defined in section 7) are included in the uncertainty band. The last bin includes overflow events. The lower part of each figure shows the ratio of data to the background prediction. All backgrounds (including $t\bar{t}$) are normalised using the best available theoretical calculation described in section 4. The background category $t\bar{t} + X$ includes $t\bar{t}W/Z$, $t\bar{t}h$ and $t\bar{t}t\bar{t}$ events. Example signal models with cross-sections enhanced by a factor of 50 are overlaid for comparison.
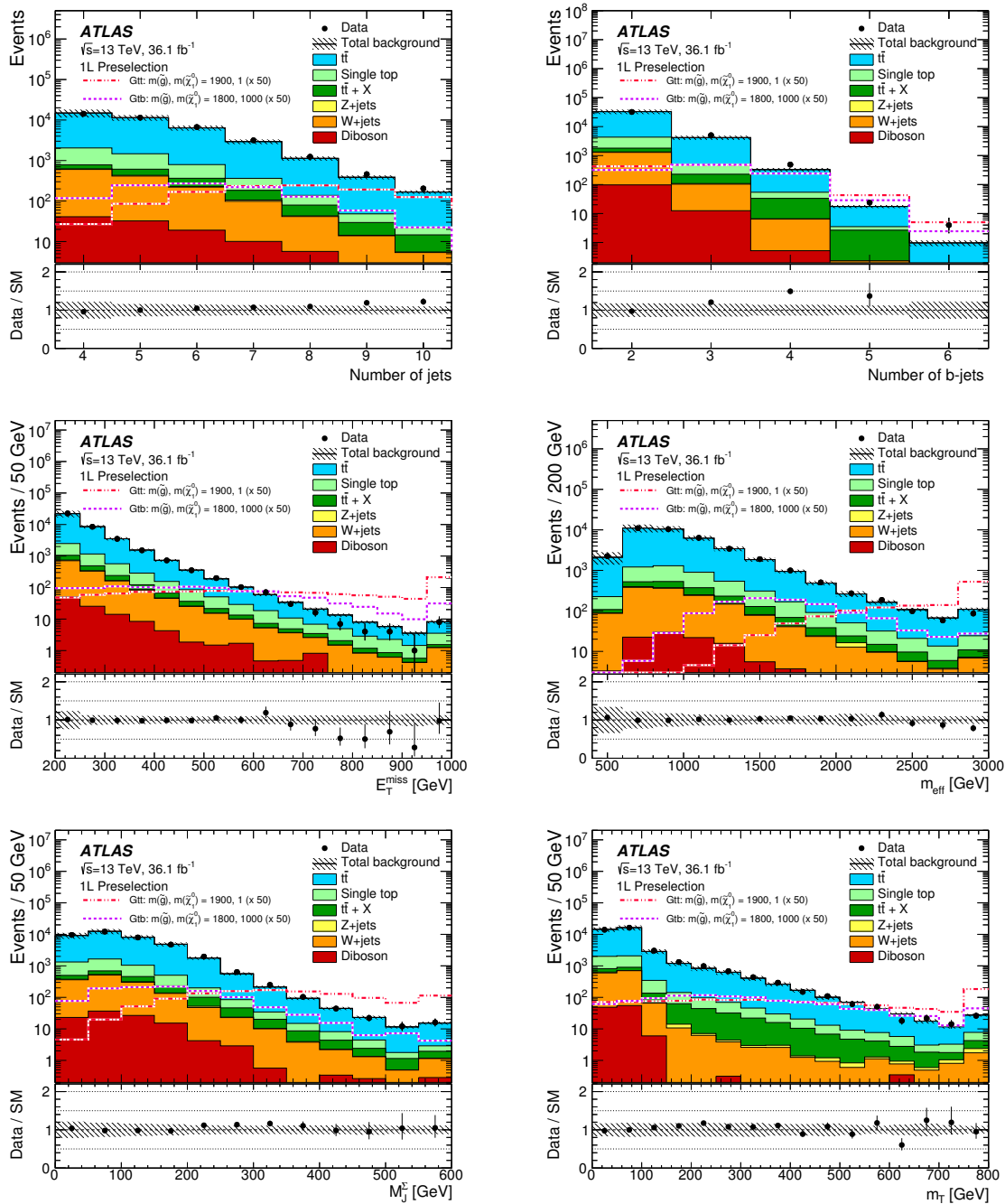
**Figure 4.** Distributions of (top-left) the number of selected jets ($N_{\text{jet}}$), (top-right) the number of selected $b$-tagged jets, (centre-left) $E_{\text{T}}^{\text{miss}}$, (centre-right) $m_{\text{eff}}$, (bottom-left) $M_J^\Sigma$ and (bottom-right) $m_{\text{T}}$ for events passing the 1-lepton preselection criteria, after applying the kinematic reweighting to the $m_{\text{eff}}$ distribution described in the text. The statistical and experimental systematic uncertainties (as defined in section 7) are included in the uncertainty band. The last bin includes overflow events. The lower part of each figure shows the ratio of data to the background prediction. All backgrounds (including $t\bar{t}$) are normalised using the best available theoretical calculation described in section 4. The background category $t\bar{t} + X$ includes $t\bar{t}W/Z$, $t\bar{t}h$ and $t\bar{t}t\bar{t}$ events. Example signal models with cross-sections enhanced by a factor of 50 are overlaid for comparison.

objects in the final state. Conversely, regions C (for "compressed") primarily focus on signals for which the gluino decay products are softer due to the small $\Delta m$ ($\Delta m \lesssim$ 300 GeV). Regions M (for "moderate") target intermediate values of $\Delta m$. SRs targeting the Gtt model in the 1- and 0-lepton channels are presented in table 2.

In the 1-lepton channel, these regions differ mainly in their kinematic selections thresholds: $m_{\text{eff}}$, $E_{\text{T}}^{\text{miss}}$ and $M_J^\Sigma$ selections are relaxed when going from region B to C to improve the acceptance for softer signals. The resulting background increase is compensated for by tightening the requirements on the number of ($b$-tagged) jets or $m_{\text{T,min}}^{b\text{-jets}}$. CRs constraining the $t\bar{t}$ background are defined in the low-$m_{\text{T}}$ region to remove overlaps with the SRs. The requirements on $m_{\text{T,min}}^{b\text{-jets}}$ are removed, and the selections on kinematic variables are relaxed to ensure at least about 10 events in each CR. The requirement of an exclusive jet multiplicity permits the definition of VRs kinematically close to the SRs and mutually exclusive to both the CRs and SRs. VR-$m_{\text{T}}$ validates the background prediction in the high-$m_{\text{T}}$ region. It is kept mutually exclusive with the SR by an inverted selection on $M_J^\Sigma$ or $m_{\text{T,min}}^{b\text{-jets}}$. VR-$m_{\text{T,min}}^{b\text{-jets}}$ checks the background prediction in the high-$m_{\text{T,min}}^{b\text{-jets}}$ regime, with an upper bound on $m_{\text{T}}$ to keep the region mutually exclusive with the corresponding SR. The other kinematic requirements are kept as close as possible to those of the SRs to ensure that the event kinematics are similar, and allow sufficiently large yields.

The signal regions of the 0-lepton channel follow a similar strategy to the 1-lepton channel. Background composition studies performed on simulated event samples show that semileptonic $t\bar{t}$ events, for which the lepton is outside the acceptance or is a hadronically decaying $\tau$-lepton, dominate in the SRs. Thus, CRs to normalise the $t\bar{t}$+jets background make use of the 1-lepton channel, requiring the presence of exactly one signal lepton. An inverted selection on $m_{\text{T}}$ is applied to remove overlaps with the 1-lepton SRs. The background prediction is validated in a 0-lepton region, inverting the $M_J^\Sigma$ selection to remove any overlap with the SRs.

Regions targeting the Gbb model are presented in table 3. The region definition follows the same pattern as for Gtt-0L regions, in particular for regions B, M and C. For very small values of $\Delta m$, the Gbb signal does not lead to a significant amount of $E_{\text{T}}^{\text{miss}}$, except if a hard ISR jet recoils against the gluino pair. Such events are targeted by region VC (for "very compressed") that identifies an ISR-jet candidate as a non-$b$-tagged high-$p_{\text{T}}$ leading jet ($\text{j}_1$), with a large azimuthal separation $\Delta\phi^{\text{j}_1}$ with respect to $\vec{p}_{\text{T}}^{\text{miss}}$. Similarly, the normalisation factor of the $t\bar{t}$ background is extracted from a 1-lepton CR, to which an inverted selection on $m_{\text{T}}$ is applied to remove the overlaps with Gtt 1-lepton SRs and the corresponding signal contamination. The 0-lepton VRs are constructed in the 0-lepton channel with selections very close to the SR ones. They are mutually exclusive due to an inverted $E_{\text{T}}^{\text{miss}}$ selection in the VR.

| Gtt 1-lepton | | | | | | | |
|---|---|---|---|---|---|---|---|
| Criteria common to all regions: $\geq 1$ signal lepton, $p_{\mathrm{T}}^{\mathrm{jet}} > 30$ GeV, $N_{b\text{-jets}} \geq 3$ | | | | | | | |
| Targeted kinematics | Type | $N_{\mathrm{jet}}$ | $m_{\mathrm{T}}$ | $m_{\mathrm{T,min}}^{b\text{-jets}}$ | $E_{\mathrm{T}}^{\mathrm{miss}}$ | $m_{\mathrm{eff}}^{\mathrm{incl}}$ | $M_J^\Sigma$ |
| Region B (Boosted, Large $\Delta m$) | SR | $\geq 5$ | $> 150$ | $> 120$ | $> 500$ | $> 2200$ | $> 200$ |
| | CR | $= 5$ | $< 150$ | $-$ | $> 300$ | $> 1700$ | $> 150$ |
| | VR-$m_{\mathrm{T}}$ | $\geq 5$ | $> 150$ | $-$ | $> 300$ | $> 1600$ | $< 200$ |
| | VR-$m_{\mathrm{T,min}}^{b\text{-jets}}$ | $> 5$ | $< 150$ | $> 120$ | $> 400$ | $> 1400$ | $> 200$ |
| Region M (Moderate $\Delta m$) | SR | $\geq 6$ | $> 150$ | $> 160$ | $> 450$ | $> 1800$ | $> 200$ |
| | CR | $= 6$ | $< 150$ | $-$ | $> 400$ | $> 1500$ | $> 100$ |
| | VR-$m_{\mathrm{T}}$ | $\geq 6$ | $> 200$ | $-$ | $> 250$ | $> 1200$ | $< 100$ |
| | VR-$m_{\mathrm{T,min}}^{b\text{-jets}}$ | $> 6$ | $< 150$ | $> 140$ | $> 350$ | $> 1200$ | $> 150$ |
| Region C (Compressed, small $\Delta m$) | SR | $\geq 7$ | $> 150$ | $> 160$ | $> 350$ | $> 1000$ | $-$ |
| | CR | $= 7$ | $< 150$ | $-$ | $> 350$ | $> 1000$ | $-$ |
| | VR-$m_{\mathrm{T}}$ | $\geq 7$ | $> 150$ | $< 160$ | $> 300$ | $> 1000$ | $-$ |
| | VR-$m_{\mathrm{T,min}}^{b\text{-jets}}$ | $> 7$ | $< 150$ | $> 160$ | $> 300$ | $> 1000$ | $-$ |

| Gtt 0-lepton | | | | | | | | | |
|---|---|---|---|---|---|---|---|---|---|
| Criteria common to all regions: $p_{\mathrm{T}}^{\mathrm{jet}} > 30\,\mathrm{GeV}$ | | | | | | | | | |
| Targeted kinematics | Type | $N_{\mathrm{lepton}}$ | $N_{b\text{-jets}}$ | $N_{\mathrm{jet}}$ | $\Delta\phi_{\mathrm{min}}^{4\mathrm{j}}$ | $m_{\mathrm{T}}$ | $m_{\mathrm{T,min}}^{b\text{-jets}}$ | $E_{\mathrm{T}}^{\mathrm{miss}}$ | $m_{\mathrm{eff}}^{\mathrm{incl}}$ | $M_J^\Sigma$ |
| Region B (Boosted, Large $\Delta m$) | SR | $= 0$ | $\geq 3$ | $\geq 7$ | $> 0.4$ | $-$ | $> 60$ | $> 350$ | $> 2600$ | $> 300$ |
| | CR | $= 1$ | $\geq 3$ | $\geq 6$ | $-$ | $< 150$ | $-$ | $> 275$ | $> 1800$ | $> 300$ |
| | VR | $= 0$ | $\geq 3$ | $\geq 6$ | $> 0.4$ | $-$ | $-$ | $> 250$ | $> 2000$ | $< 300$ |
| Region M (Moderate $\Delta m$) | SR | $= 0$ | $\geq 3$ | $\geq 7$ | $> 0.4$ | $-$ | $> 120$ | $> 500$ | $> 1800$ | $> 200$ |
| | CR | $= 1$ | $\geq 3$ | $\geq 6$ | $-$ | $< 150$ | $-$ | $> 400$ | $> 1700$ | $> 200$ |
| | VR | $= 0$ | $\geq 3$ | $\geq 6$ | $> 0.4$ | $-$ | $-$ | $> 450$ | $> 1400$ | $< 200$ |
| Region C (Compressed, moderate $\Delta m$) | SR | $= 0$ | $\geq 4$ | $\geq 8$ | $> 0.4$ | $-$ | $> 120$ | $> 250$ | $> 1000$ | $> 100$ |
| | CR | $= 1$ | $\geq 4$ | $\geq 7$ | $-$ | $< 150$ | $-$ | $> 250$ | $> 1000$ | $> 100$ |
| | VR | $= 0$ | $\geq 4$ | $\geq 7$ | $> 0.4$ | $-$ | $-$ | $> 250$ | $> 1000$ | $< 100$ |

**Table 2.** Definitions of the Gtt SRs, CRs and VRs of the cut-and-count analysis. All kinematic variables are expressed in GeV except $\Delta\phi_{\mathrm{min}}^{4\mathrm{j}}$, which is in radians. The jet $p_{\mathrm{T}}$ requirement is also applied to $b$-tagged jets.

**Gbb**

Criteria common to all regions: $N_{\mathrm{jet}} \geq 4$, $p_{\mathrm{T}}^{\mathrm{jet}} > 30\,\mathrm{GeV}$

| Targeted kinematics | Type | $N_{\mathrm{lepton}}$ | $N_{b\text{-jets}}$ | $\Delta\phi_{\mathrm{min}}^{4\mathrm{j}}$ | $m_{\mathrm{T}}$ | $m_{\mathrm{T,min}}^{b\text{-jets}}$ | $E_{\mathrm{T}}^{\mathrm{miss}}$ | $m_{\mathrm{eff}}$ | Others |
|---|---|---|---|---|---|---|---|---|---|
| Region B (Boosted, Large $\Delta m$) | SR | $= 0$ | $\geq 3$ | $> 0.4$ | – | – | $> 400$ | $> 2800$ | – |
| | CR | $= 1$ | $\geq 3$ | – | $< 150$ | – | $> 400$ | $> 2500$ | – |
| | VR | $= 0$ | $\geq 3$ | $> 0.4$ | – | – | $> 350$ | 1900–2800 | – |
| Region M (Moderate $\Delta m$) | SR | $= 0$ | $\geq 4$ | $> 0.4$ | – | $> 90$ | $> 450$ | $> 1600$ | – |
| | CR | $= 1$ | $\geq 4$ | – | $< 150$ | – | $> 300$ | $> 1600$ | – |
| | VR | $= 0$ | $\geq 4$ | $> 0.4$ | – | $> 100$ | 250–450 | 1600–1900 | – |
| Region C (Compressed, small $\Delta m$) | SR | $= 0$ | $\geq 4$ | $> 0.4$ | – | $> 155$ | $> 450$ | – | – |
| | CR | $= 1$ | $\geq 4$ | – | $< 150$ | – | $> 375$ | – | – |
| | VR | $= 0$ | $\geq 4$ | $> 0.4$ | – | $> 125$ | 350–450 | – | – |
| Region VC (Very Compressed, very small $\Delta m$) | SR | $= 0$ | $\geq 3$ | $> 0.4$ | – | $> 100$ | $> 600$ | – | $p_{\mathrm{T}}^{\mathrm{j}_1} > 400$, $\mathrm{j}_1 \neq b$, $\Delta\phi^{\mathrm{j}_1} > 2.5$ |
| | CR | $= 1$ | $\geq 3$ | – | $< 150$ | – | $< 600$ | – | |
| | VR | $= 0$ | $\geq 3$ | $> 0.4$ | – | $> 100$ | 225–600 | – | |

**Table 3.** Definitions of the Gbb SRs, CRs and VRs of the cut-and-count analysis. All kinematic variables are expressed in GeV except $\Delta\phi_{\mathrm{min}}^{4\mathrm{j}}$, which is in radians. The jet $p_{\mathrm{T}}$ requirement is applied to the four leading jets, a subset of which are $b$-tagged jets. The $\mathrm{j}_1 \neq b$ requirement specifies that the leading jet is not $b$-tagged.
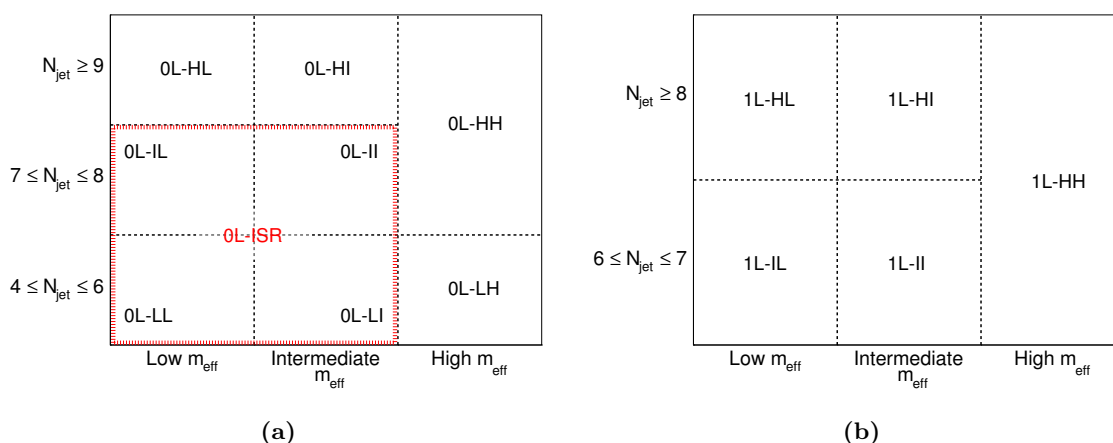
**Figure 5.** Scheme of the multi-bin analysis for the (a) 0-lepton and (b) 1-lepton regions. The 0L-ISR region is represented with the broad red dashed line in (a).

## 6.5 Multi-bin analysis

Figures 3 and 4 show that a good separation between signal and background can be achieved with various kinematic variables. The distribution of $N_{\mathrm{jet}}$ and $m_{\mathrm{eff}}$ for different signal benchmarks and $\Delta m$ values is used to build a two-dimensional slicing of the phase space in a set of non-overlapping SRs, CRs and VRs that can be statistically combined. The slicing scheme is presented in figure 5. The SRs are named in the form SR-$Y$L-$Z_1Z_2$, where $Y$ indicates the number of leptons, $Z_1$ labels the jet multiplicity bin and $Z_2$ labels the $m_{\mathrm{eff}}$ bin. For $Z_1$ and $Z_2$, the letters "H" stands for "high", "I" for "intermediate" and "L" for "low". In the 0-lepton channel, there is also a 0L-ISR region that is a subset of the IL, LL, II and LI regions, and kept mutually exclusive with them as detailed below.

The low-$N_{\mathrm{jet}}$ region probes especially Gbb-like models, for which the number of hard jets is lower than in decay topologies containing top quarks. This category of events is thus only considered in the 0-lepton channel. Gtt events are mostly expected in the high-$N_{\mathrm{jet}}$ bin. The intermediate jet multiplicity bin is built to be sensitive to decay topologies with a number of top quarks intermediate between Gbb and Gtt, but also to Gbb (with additional jets originating from radiation) and to Gtt (when some jets fall outside the acceptance). The $m_{\mathrm{eff}}$ bins are chosen to provide sensitivity to various kinematic regimes: the low-$m_{\mathrm{eff}}$ regions are essentially sensitive to soft signals (low $\Delta m$), while the high-$m_{\mathrm{eff}}$ regions are designed to select highly boosted events.

For each $N_{\mathrm{jet}}$-$m_{\mathrm{eff}}$ region presented in figure 5, the selection was optimised over all the other variables to maximise the exclusion power for the Gbb and Gtt models. For each $m_{\mathrm{eff}}$ bin, a targeted range of $\Delta m$ was used in the optimisation procedure.

The high- and intermediate-$N_{\mathrm{jet}}$ regions are presented in tables 4 and 5, respectively. For each $m_{\mathrm{eff}}$ region, 0- and 1-lepton channels are used to provide sensitivity to the Gtt model and the decay topologies of the variable branching ratio model which contain at least one top quark. In the intermediate-$N_{\mathrm{jet}}$ categories the leading jet is required to be $b$-tagged or the value of $\Delta\phi^{\mathrm{j}1}$ to be lower than 2.9 in order to ensure they are mutually exclusive

with the 0L-ISR regions. Corresponding 0-lepton and 1-lepton SRs share a single CR, hosted in the 1-lepton channel, after the application of an inverted $m_{\mathrm{T}}$ selection to remove the overlap with the 1-lepton SRs. The other kinematic requirements are kept close to the ones of the SR. One VR is defined for each SR in the corresponding lepton channel. Full independence between the signal and VRs is guaranteed by $E_{\mathrm{T}}^{\mathrm{miss}}$ and $m_{\mathrm{T,min}}^{b\text{-jets}}$ requirements.

The low-$N_{\mathrm{jet}}$ regions are presented in table 6. Targeting primarily the Gbb model, the transverse momentum of the fourth jet is required to be larger than 90 GeV in all SRs. In the intermediate and low $m_{\mathrm{eff}}$ regions, the leading jet is required to be $b$-tagged or the value of $\Delta\phi^{\mathrm{j1}}$ to be lower than 2.9 in order to be mutually exclusive with the 0L-ISR regions. The $t\bar{t}$ background dominates in all regions, and is normalised in dedicated 1-lepton regions, defined with a low $m_{\mathrm{T}}$ requirement, as done for the regions of the cut-and-count analysis. VRs are constructed in the 0-lepton channel, closely reproducing the background composition and kinematics of the SR events.

A dedicated set of regions is designed to target very compressed Gbb scenarios in which a hard ISR jet recoils against the gluino pair. The definition of these regions is presented in table 6.

**High-$N_{\mathrm{jet}}$ regions**

Criteria common to all regions: $N_{b\text{-jets}} \geq 3$, $p_{\mathrm{T}}^{\mathrm{jet}} > 30\,\mathrm{GeV}$

| Targeted kinematics | Type | $N_{\mathrm{lepton}}$ | $\Delta\phi_{\mathrm{min}}^{4j}$ | $m_{\mathrm{T}}$ | $N_{\mathrm{jet}}$ | $m_{\mathrm{T,min}}^{b\text{-jets}}$ | $M_J^{\Sigma}$ | $E_{\mathrm{T}}^{\mathrm{miss}}$ | $m_{\mathrm{eff}}$ |
|---|---|---|---|---|---|---|---|---|---|
| High-$m_{\mathrm{eff}}$ (HH) (Large $\Delta m$) | SR-0L | $=0$ | $>0.4$ | $-$ | $\geq 7$ | $>100$ | $>200$ | $>400$ | $>2500$ |
| | SR-1L | $\geq 1$ | $-$ | $>150$ | $\geq 6$ | $>120$ | $>200$ | $>500$ | $>2300$ |
| | CR | $\geq 1$ | $-$ | $<150$ | $\geq 6$ | $>60$ | $>150$ | $>300$ | $>2100$ |
| | VR-0L | $=0$ | $>0.4$ | $-$ | $\geq 7$ | $<100$ if $E_{\mathrm{T}}^{\mathrm{miss}}>300$ | $-$ | $<300$ if $m_{\mathrm{T,min}}^{b\text{-jets}}>100$ | $>2100$ |
| | VR-1L | $\geq 1$ | $-$ | $>150$ | $\geq 6$ | $>140$ if $m_{\mathrm{eff}}>2300$ | $-$ | $<500$ | $>2100$ |
| Intermediate-$m_{\mathrm{eff}}$ (HI) (Intermediate $\Delta m$) | SR-0L | $=0$ | $>0.4$ | $-$ | $\geq 9$ | $>140$ | $>150$ | $>300$ | $[1800, 2500]$ |
| | SR-1L | $\geq 1$ | $-$ | $>150$ | $\geq 8$ | $>140$ | $>150$ | $>300$ | $[1800, 2300]$ |
| | CR | $\geq 1$ | $-$ | $<150$ | $\geq 8$ | $>60$ | $>150$ | $>200$ | $[1700, 2100]$ |
| | VR-0L | $=0$ | $>0.4$ | $-$ | $\geq 9$ | $<140$ if $E_{\mathrm{T}}^{\mathrm{miss}}>300$ | $-$ | $<300$ if $m_{\mathrm{T,min}}^{b\text{-jets}}>140$ | $[1650, 2100]$ |
| | VR-1L | $\geq 1$ | $-$ | $>150$ | $\geq 8$ | $<140$ if $E_{\mathrm{T}}^{\mathrm{miss}}>300$ | $-$ | $<300$ if $m_{\mathrm{T,min}}^{b\text{-jets}}>140$ | $[1600, 2100]$ |
| Low-$m_{\mathrm{eff}}$ (HL) (Small $\Delta m$) | SR-0L | $=0$ | $>0.4$ | $-$ | $\geq 9$ | $>140$ | $-$ | $>300$ | $[900, 1800]$ |
| | SR-1L | $\geq 1$ | $-$ | $>150$ | $\geq 8$ | $>140$ | $-$ | $>300$ | $[900, 1800]$ |
| | CR | $\geq 1$ | $-$ | $<150$ | $\geq 8$ | $>130$ | $-$ | $>250$ | $[900, 1700]$ |
| | VR-0L | $=0$ | $>0.4$ | $-$ | $\geq 9$ | $<140$ | $-$ | $>300$ | $[900, 1650]$ |
| | VR-1L | $\geq 1$ | $-$ | $>150$ | $\geq 8$ | $<140$ | $-$ | $>225$ | $[900, 1650]$ |

**Table 4.** Definition of the high-$N_{\mathrm{jet}}$ SRs, CRs and VRs of the multi-bin analysis. All kinematic variables are expressed in GeV except $\Delta\phi_{\mathrm{min}}^{4j}$, which is in radians.

**Intermediate-$N_{\text{jet}}$ regions**

Criteria common to all regions: $N_{b\text{-jets}} \geq 3$, $p_T^{\text{jet}} > 30\,\text{GeV}$

| Targeted kinematics | Type | $N_{\text{lepton}}$ | $\Delta\phi_{\min}^{4j}$ | $m_T$ | $N_{\text{jet}}$ | $j_1 = b$ or $\Delta\phi^{j1} \leq 2.9$ | $m_{T,\min}^{b\text{-jets}}$ | $M_J^{\Sigma}$ | $E_T^{\text{miss}}$ | $m_{\text{eff}}$ |
|---|---|---|---|---|---|---|---|---|---|---|
| Intermediate-$m_{\text{eff}}$ (II) (Intermediate $\Delta m$) | SR-0L | $=0$ | $>0.4$ | $-$ | $[7,8]$ | ✔ | $>140$ | $>150$ | $>300$ | $[1600, 2500]$ |
| | SR-1L | $\geq 1$ | $-$ | $>150$ | $[6,7]$ | $-$ | $>140$ | $>150$ | $>300$ | $[1600, 2300]$ |
| | CR | $\geq 1$ | $-$ | $<150$ | $[6,7]$ | ✔ | $>110$ | $>150$ | $>200$ | $[1600, 2100]$ |
| | VR-0L | $=0$ | $>0.4$ | $-$ | $[7,8]$ | ✔ | $<140$ | $-$ | $>300$ | $[1450, 2000]$ |
| | VR-1L | $\geq 1$ | $-$ | $>150$ | $[6,7]$ | $-$ | $<140$ | $-$ | $>225$ | $[1450, 2000]$ |
| Low-$m_{\text{eff}}$ (IL) (Low $\Delta m$) | SR-0L | $=0$ | $>0.4$ | $-$ | $[7,8]$ | ✔ | $>140$ | $-$ | $>300$ | $[800, 1600]$ |
| | SR-1L | $\geq 1$ | $-$ | $>150$ | $[6,7]$ | $-$ | $>140$ | $-$ | $>300$ | $[800, 1600]$ |
| | CR | $\geq 1$ | $-$ | $<150$ | $[6,7]$ | ✔ | $>130$ | $-$ | $>300$ | $[800, 1600]$ |
| | VR-0L | $=0$ | $>0.4$ | $-$ | $[7,8]$ | ✔ | $<140$ | $-$ | $>300$ | $[800, 1450]$ |
| | VR-1L | $\geq 1$ | $-$ | $>150$ | $[6,7]$ | $-$ | $<140$ | $-$ | $>300$ | $[800, 1450]$ |

**Table 5.** Definition of the intermediate-$N_{\text{jet}}$ SRs, CRs and VRs of the multi-bin analysis. All kinematic variables are expressed in GeV except $\Delta\phi_{\min}^{4j}$, which is in radians. The $j_1 = b$ requirement specifies that the leading jet is $b$-tagged.

**Low-$N_{\rm jet}$ regions**

Criteria common to all regions: $N_{b\text{-jets}} \geq 3$, $p_T^{\rm jet} > 30$ GeV

| Targeted kinematics | Type | $N_{\rm lepton}$ | $\Delta\phi^{4j}_{\min}$ | $m_T$ | $N_{\rm jet}$ | $j_1 = b$ or $\Delta\phi^{j_1} \leq 2.9$ | $p_T^{j4}$ | $m_{T,\min}^{b\text{-jets}}$ | $E_T^{\rm miss}$ | $m_{\rm eff}$ |
|---|---|---|---|---|---|---|---|---|---|---|
| High-$m_{\rm eff}$ (LH) (Large $\Delta m$) | SR | $= 0$ | $> 0.4$ | – | [4, 6] | – | $> 90$ | – | $> 300$ | $> 2400$ |
| | CR | $\geq 1$ | – | $< 150$ | [4, 5] | – | - | – | $> 200$ | $> 2100$ |
| | VR | $= 0$ | $> 0.4$ | – | [4, 6] | – | $> 90$ if $E_T^{\rm miss} < 300$ | – | $> 200$ | [2000, 2400] |
| Intermediate-$m_{\rm eff}$ (LI) (Intermediate $\Delta m$) | SR | $= 0$ | $> 0.4$ | – | [4, 6] | ✓ | $> 90$ | $> 140$ | $> 350$ | [1400, 2400] |
| | CR | $\geq 1$ | – | $< 150$ | [4, 5] | ✓ | $> 70$ | – | $> 300$ | [1400, 2000] |
| | VR | $= 0$ | $> 0.4$ | – | [4, 6] | ✓ | $> 90$ | $< 140$ | $> 300$ | [1250, 1800] |
| Low-$m_{\rm eff}$ (LL) (Low $\Delta m$) | SR | $= 0$ | $> 0.4$ | – | [4, 6] | ✓ | $> 90$ | $> 140$ | $> 350$ | [800, 1400] |
| | CR | $\geq 1$ | – | $< 150$ | [4, 5] | ✓ | $> 70$ | – | $> 300$ | [800, 1400] |
| | VR | $= 0$ | $> 0.4$ | – | [4, 6] | ✓ | $> 90$ | $< 140$ | $> 300$ | [800, 1250] |

**ISR regions**

Criteria common to all regions: $N_{b\text{-jets}} \geq 3$, $\Delta\phi^{j_1} > 2.9$, $p_{T1}^{j} > 400$ GeV, $p_T^{\rm jet} > 30$ GeV, $j_1 \neq b$

| Type | $N_{\rm lepton}$ | $\Delta\phi^{4j}_{\min}$ | $m_T$ | $N_{\rm jet}$ | $m_{T,\min}^{b\text{-jets}}$ | $E_T^{\rm miss}$ | $m_{\rm eff}$ |
|---|---|---|---|---|---|---|---|
| SR | $= 0$ | $> 0.4$ | – | [4, 8] | $> 100$ | $> 600$ | $< 2200$ |
| CR | $\geq 1$ | – | $< 150$ | [4, 7] | – | $> 400$ | $< 2000$ |
| VR | $= 0$ | $> 0.4$ | – | [4, 8] | $> 100$ | $> 250$ | $< 2000$ |

**Table 6.** Definition of the low-$N_{\rm jet}$ and ISR SRs, CRs and VRs of the multi-bin analysis. All kinematic variables are expressed in GeV except $\Delta\phi^{4j}_{\min}$, which is in radians. The $j_1 = b$ ($j_1 \neq b$) requirement specifies that the leading jet is (not) $b$-tagged.

## 7 Systematic uncertainties

Figures 6a and 6b summarise the relative systematic uncertainties in the background esti-mate for the cut-and-count and multi-bin analyses, respectively. These uncertainties arise from the extrapolation of the $t\bar{t}$ normalisation obtained in the CRs to the SRs as well as from the yields of the minor backgrounds in the SRs, which are predicted by the simulation. The total systematic uncertainties range from approximately 20% to 80% in the various SRs.

The detector-related systematic uncertainties affect both the background estimate and the signal yield. The largest sources in this analysis relate to the jet energy scale, jet energy resolution (JER) and the $b$-tagging efficiencies and mistagging rates. The JES uncertainties for the small-$R$ jets are derived from $\sqrt{s} = 13$ TeV data and simulations while the JER uncertainties are extrapolated from 8 TeV data using MC simulations [89]. These uncertainties are also propagated to the re-clustered large-$R$ jets, which use them as inputs. The jet mass scale and resolution uncertainties have a negligible impact on the re-clustered jet mass. The impact of the JES uncertainties on the expected background yields is between 4% and 35%, while JER uncertainties affect the background yields by approximately 0–26% in the various regions. Uncertainties in the measured $b$-tagging efficiencies and mistagging rates are the subleading sources of experimental uncertainty.

The impact of these uncertainties on the expected background yields is 3–24% de-pending on the considered region. The uncertainties associated with lepton reconstruction and energy measurements have a negligible impact on the final results. All lepton and jet measurement uncertainties are propagated to the calculation of $E_T^{miss}$, and additional uncertainties are included in the scale and resolution of the soft term. The overall impact of the $E_T^{miss}$ soft-term uncertainties is also small.

Since the normalisation of the $t\bar{t}$ background is fit to data in the CRs, uncertainties in the modelling of this background only affect the extrapolation from the CRs to the SRs and VRs. Hadronisation and parton showering model uncertainties are estimated using a sample generated with POWHEG and showered by HERWIG++ v2.7.1 with the UEEE5 underlying-event tune. Systematic uncertainties in the modelling of initial- and final-state radiation are explored with POWHEG samples showered with two alternative settings of PYTHIA v6.428. The first of these uses the PERUGIA2012radHi tune [50] and has the renormalisation and factorisation scales set to twice the nominal value, resulting in more radiation in the final state. In addition, it has $h_{damp}$ set to $2m_{top}$. The second sample, using the PERUGIA2012radLo tune, has $h_{damp} = m_{top}$ and the renormalisation and factorisation scales are set to half of their nominal values, resulting in less radiation in the event. In each case, the uncertainty is taken as the change in the expected yield of $t\bar{t}$ background with respect to the nominal sample. The uncertainty due to the choice of event generator is estimated by comparing the expected yields obtained using a $t\bar{t}$ sample generated with MADGRAPH5_aMC@NLO and one that is generated with POWHEG. Both of these samples are showered with HERWIG++ v2.7.1. The total theoretical uncertainty in the inclusive $t\bar{t}$ background is taken as the sum in quadrature of these individual components. An additional uncertainty is assigned to the fraction of $t\bar{t}$ events produced in association with additional heavy-flavour jets (i.e. $t\bar{t}+ \geq 1b$ and $t\bar{t}+ \geq 1c$), a process which suffers from large
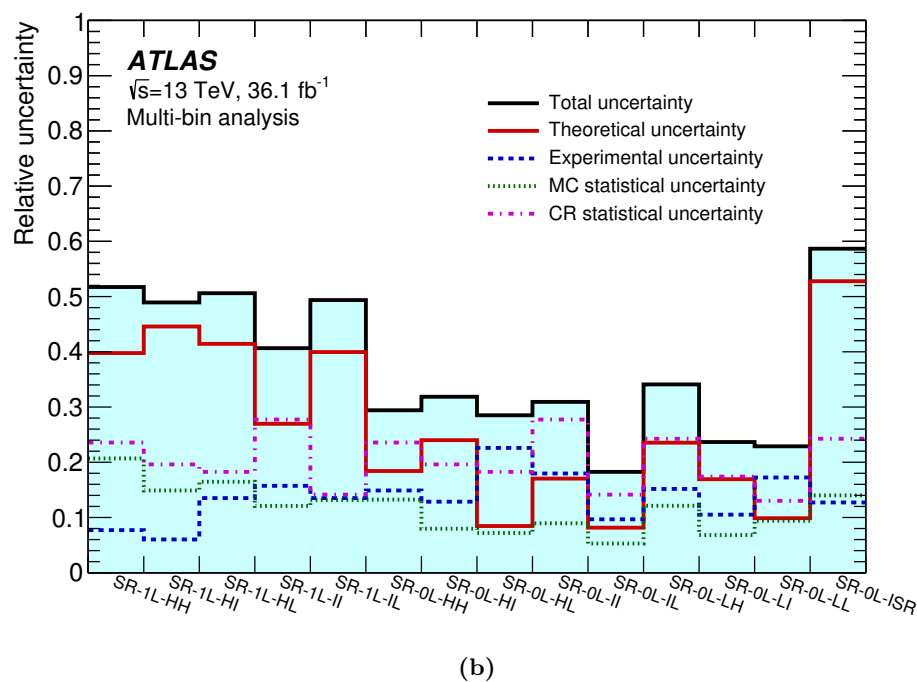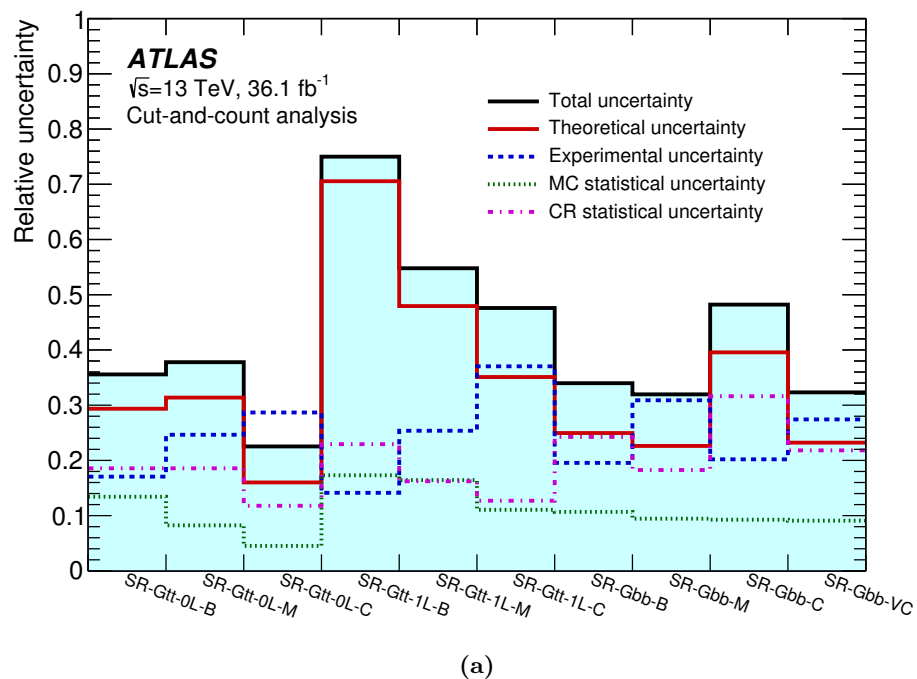
**(a)**



**(b)**

**Figure 6.** Relative systematic uncertainty in the background estimate for the (a) cut-and-count and (b) multi-bin analyses. The individual uncertainties can be correlated, such that the total background uncertainty is not necessarily their sum in quadrature.

theoretical uncertainties. Simulation studies show that the heavy-flavour fractions in each set of SR, CR and VR, which have almost identical $b$-tagged jets requirements, are similar. Therefore, the theoretical uncertainties in this fraction affect these regions in a similar way, and thus largely cancel out in the semi-data-driven $t\bar{t}$ normalisation based on the observed CR yields. The residual uncertainty in the $t\bar{t}$ prediction is taken as the difference between the nominal $t\bar{t}$ prediction and the one obtained after varying the cross-section of $t\bar{t}$ events with additional heavy-flavour jets by 30%, in accordance with the results of the ATLAS measurement of this cross-section at $\sqrt{s} = 8$ TeV [90]. This component typically makes a small contribution (0–8%) to the total impact of the $t\bar{t}$ modelling uncertainties on the background yields, which ranges between 5% and 76% for the various regions. The statistical uncertainty of the CRs used to extract the $t\bar{t}$ normalisation factors, which is included in the systematic uncertainties, ranges from 10% to 30% depending on the SR.

Modelling uncertainties affecting the single-top process arise especially from the interference between the $t\bar{t}$ and $Wt$ processes. This uncertainty is estimated using inclusive $WWbb$ events, generated using MADGRAPH5_aMC@NLO, which are compared with the sum of $t\bar{t}$ and $Wt$ processes. Furthermore, as in the $t\bar{t}$ modelling uncertainties, variations of PYTHIA v6.428 settings increasing or decreasing the amount of radiation are also used. An additional 5% uncertainty is included in the cross-section of single-top processes [91]. Overall, the modelling uncertainties affecting the single-top process lead to changes of approximately 0–11% in the total yields in the various regions. Uncertainties in the $W/Z$+jets backgrounds are estimated by varying independently the scales for factorisation, renormalisation and resummation by factors of 0.5 and 2. The scale used for the matching between jets originating from the matrix element and the parton shower is also varied. The resulting uncertainties in the total yield range from approximately 0 to 50% in the various regions. A 50% normalisation uncertainty is assigned to $t\bar{t} + W/Z/h$, $t\bar{t}t\bar{t}$ and diboson backgrounds and are found to have no significant impact on the sensitivity of this analysis. Uncertainties arising from variations of the parton distribution functions were found to affect background yields by less than 2%, and therefore these uncertainties are neglected here. Uncertainties due to the limited number of events in the MC background samples are included if above 5%. They reach approximately 20% in regions targeting large mass-splitting.

The uncertainties in the cross-sections of signal processes are determined from an envelope of different cross-section predictions, as described in section 4. A systematic uncertainty is also assigned to the kinematic correction described in section 6. The total size of the correction is used as an uncertainty, and is applied to all simulated event samples for the 1-lepton channel.

# 8 Results

The expected SM background is determined separately in each SR with a profile likelihood fit [92] implemented in the HistFitter framework [93], referred to as a background-only fit. The fit uses as a constraint the observed event yield in the associated CR to adjust the $t\bar{t}$ normalisation, assuming that no signal contributes to this yield, and applies that normalisation factor to the number of $t\bar{t}$ events predicted by simulation in the SR. The

values of the normalisation factors, the expected numbers of background events and the observed data yields in all the CRs are shown in figures 7a and 7b for the cut-and-count and multi-bin analyses, respectively.

The inputs to the background-only fit for each SR are the number of events observed in its associated CR and the number of events predicted by simulation in each region for all background processes. The numbers of observed and predicted events in each CR are described by Poisson probability density functions. The systematic uncertainties in the expected values are included in the fit as nuisance parameters. They are constrained by Gaussian distributions with widths corresponding to the sizes of the uncertainties and are treated as correlated, when appropriate, between the various regions. The product of the various probability density functions forms the likelihood, which the fit maximises by adjusting the $t\bar{t}$ normalisation and the nuisance parameters.

Figures 8a and 8b show the results of the background-only fit to the CRs, extrapolated to the VRs for the cut-and-count and multi-bin analyses, respectively. The number of events predicted by the background-only fit is compared to the data in the upper panel. The pull, defined by the difference between the observed number of events ($n_{\mathrm{obs}}$) and the predicted background yield ($n_{\mathrm{pred}}$) divided by the total uncertainty ($\sigma_{\mathrm{tot}}$), is shown for each region in the lower panel. No evidence of significant background mismodelling is observed in the VRs.

The event yields in the SRs for the cut-and-count and multi-bin analyses are presented in figure 9, where the pull is shown for each region in the lower panel. No significant excess is found above the predicted background. The maximum deviation is observed in region SR-0L-HH of the multi-bin analysis with a local significance of 2.3 standard deviations. The background is dominated by $t\bar{t}$ events in all SRs. The subdominant background contributions in the 0-lepton regions are $Z(\rightarrow \nu\nu)$+jets and $W(\rightarrow \ell\nu)$+jets events, where for $W$+jets events the lepton is an unidentified electron or muon or a hadronically decaying $\tau$-lepton. In the 1-lepton SRs, the subdominant backgrounds are single-top, $t\bar{t}W$ and $t\bar{t}Z$.
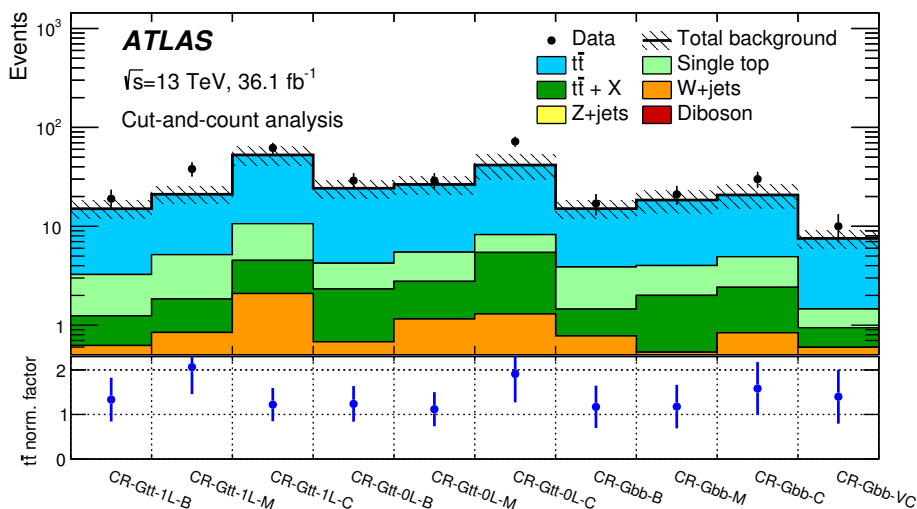
Table 7 shows the observed number of events and predicted number of background events from the background-only fit in the Gtt 1-lepton, Gtt 0-lepton and Gbb regions for the cut-and-count analysis. The central value of the fitted background is in general larger than the MC-only prediction. This is in part due to an underestimation of the cross-section of $t\bar{t}+ \geq 1b$ and $t\bar{t}+ \geq 1c$ processes in the simulation.

## 9 Interpretation

Since no significant excess over the expected background from SM processes is observed, the data are used to derive one-sided upper limits at 95% confidence level (CL). Two levels of interpretation are provided in this paper: model-independent exclusion limits and model-dependent exclusion limits set on the Gbb, Gtt and gluino variable branching ratio models.

### 9.1 Model-independent exclusion limits

Model-independent limits on the number of beyond-the-SM (BSM) events for each SR are derived with pseudoexperiments using the CL$_{\mathrm{s}}$ prescription [94] and neglecting a possible signal contamination in the CR. Only the single-bin regions from the cut-and-count analysis
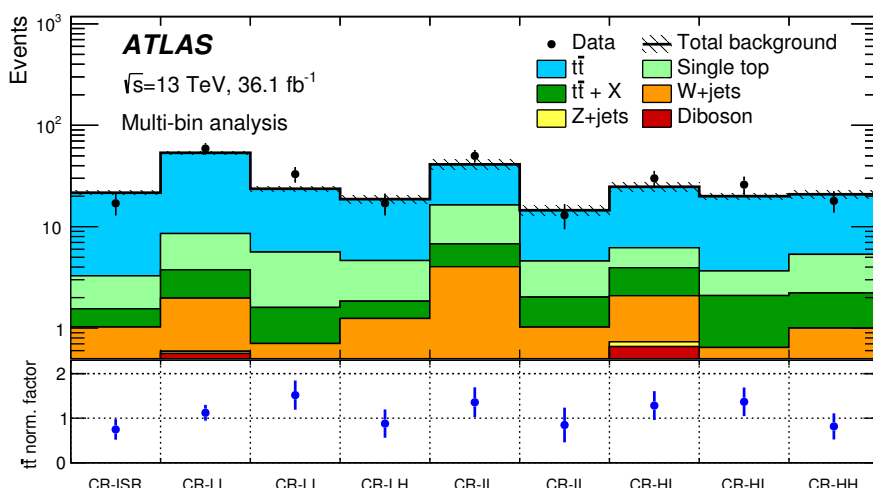
**Figure 7.** Pre-fit event yield in control regions and related $t\bar{t}$ normalization factors after the background-only fit for (a) the cut-and-count and (b) the multi-bin analyses. The upper panel shows the observed number of events and the predicted background yield before the fit. The background category $t\bar{t} + X$ includes $t\bar{t}W/Z$, $t\bar{t}H$ and $t\bar{t}t\bar{t}$ events. All of these regions require at least one signal lepton, for which the multijet background is negligible. All uncertainties describes in section 7 are included in the uncertainty band. The $t\bar{t}$ normalisation is obtained from the fit and is displayed in the bottom panel.
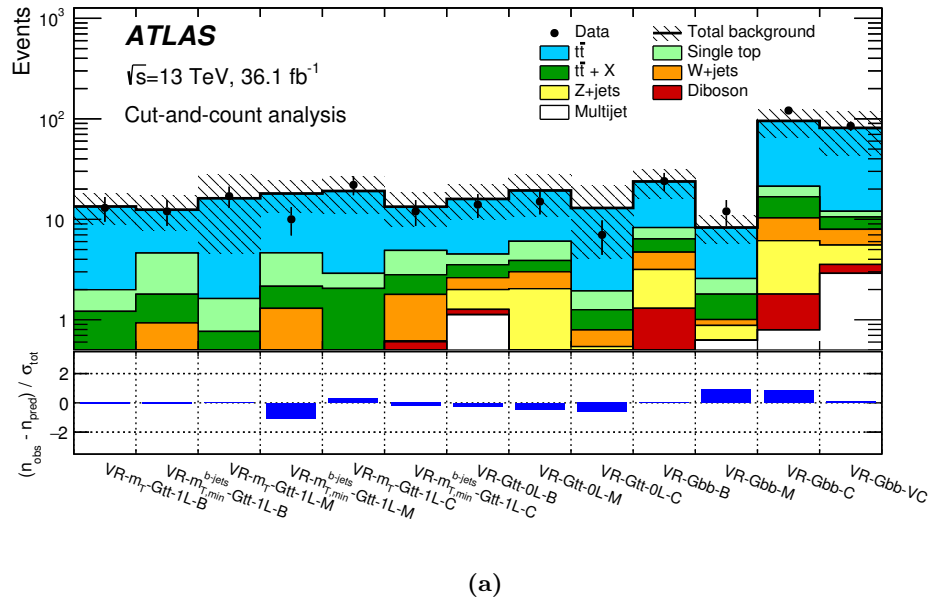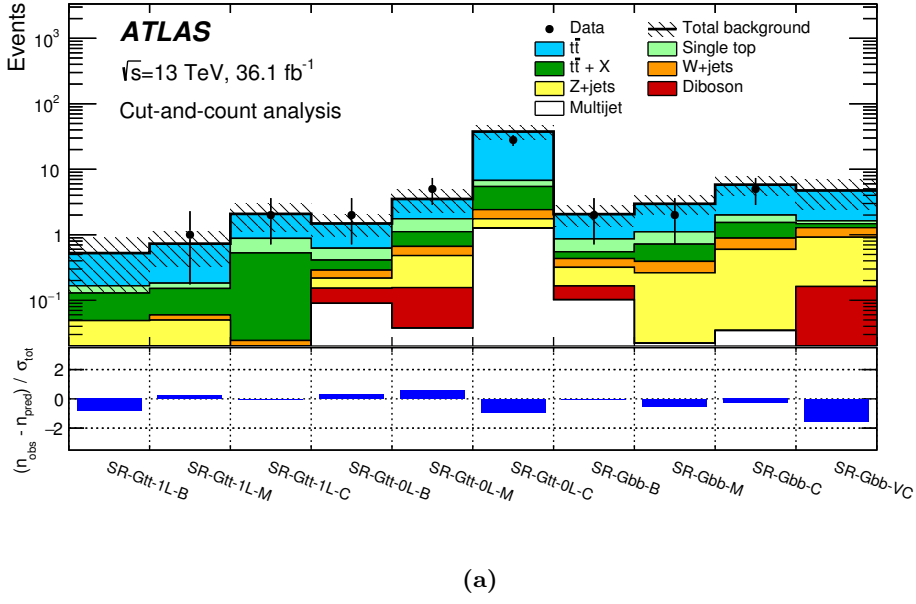
**(a)**
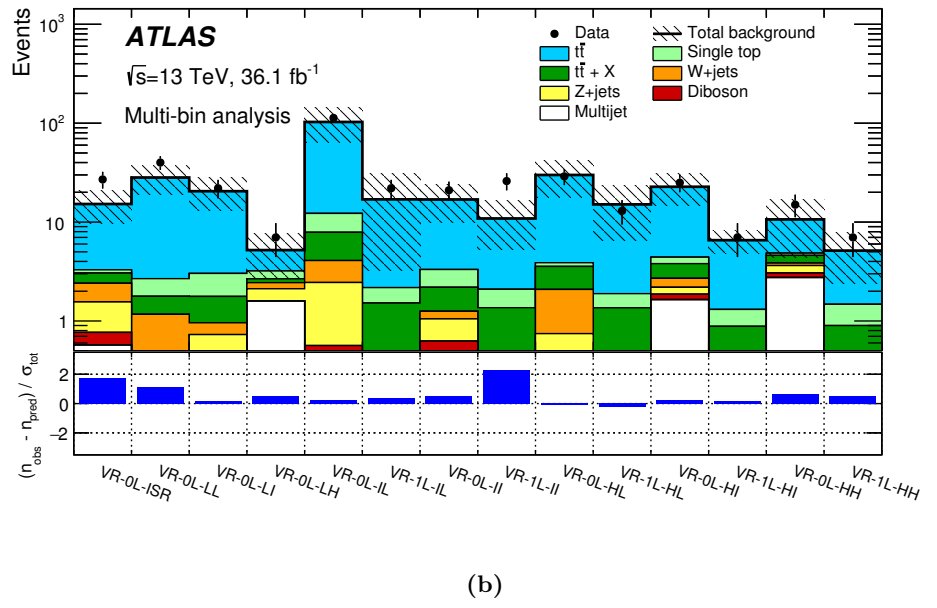


**(b)**

**Figure 8.** Results of the background-only fit extrapolated to the VRs of (a) the cut-and-count and (b) the multi-bin analyses. The $t\bar{t}$ normalisation is obtained from the fit to the CRs shown in figure 7. The upper panel shows the observed number of events and the predicted background yield. All uncertainties defined in section 7 are included in the uncertainty band. The background category $t\bar{t} + X$ includes $t\bar{t}W/Z$, $t\bar{t}H$ and $t\bar{t}t\bar{t}$ events. The lower panel shows the pulls in each VR.
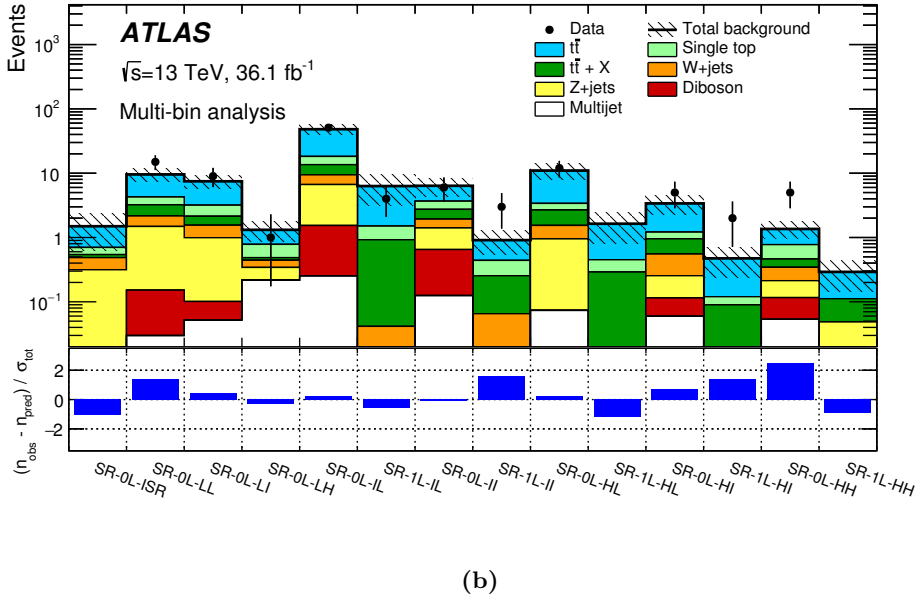
**(a)**



**(b)**

**Figure 9.** Results of the background-only fit extrapolated to the SRs for (a) the cut-and-count and (b) the multi-bin analyses. The data in the SRs are not included in the fit. The upper panel shows the observed number of events and the predicted background yield. All uncertainties defined in section 7 are included in the uncertainty band. The background category $t\bar{t} + X$ includes $t\bar{t}W/Z$, $t\bar{t}H$ and $t\bar{t}t\bar{t}$ events. The lower panel shows the pulls in each SR.

| | SR-Gtt-1L | | |
|---|---|---|---|
| Targeted kinematics | B | M | C |
| Observed events | 0 | 1 | 2 |
| Fitted background | $0.5 \pm 0.4$ | $0.7 \pm 0.4$ | $2.1 \pm 1.0$ |
| $t\bar{t}$ | $0.4 \pm 0.4$ | $0.5 \pm 0.4$ | $1.2 \pm 0.8$ |
| Single-top | $0.04 \pm 0.05$ | $0.03 \pm 0.06$ | $0.35 \pm 0.28$ |
| $t\bar{t} + X$ | $0.08 \pm 0.05$ | $0.09 \pm 0.06$ | $0.50 \pm 0.28$ |
| $Z$+jets | $0.049 \pm 0.023$ | $0.050 \pm 0.023$ | $< 0.01$ |
| $W$+jets | $< 0.01$ | $< 0.01$ | $0.024 \pm 0.026$ |
| Diboson | $< 0.01$ | $< 0.01$ | $< 0.01$ |
| MC-only background | 0.43 | 0.45 | 1.9 |

| | SR-Gtt-0L | | |
|---|---|---|---|
| Targeted kinematics | B | M | C |
| Observed events | 2 | 5 | 28 |
| Fitted background | $1.5 \pm 0.5$ | $3.5 \pm 1.3$ | $38 \pm 8$ |
| $t\bar{t}$ | $0.9 \pm 0.4$ | $1.8 \pm 0.7$ | $31 \pm 8$ |
| Single-top | $0.21 \pm 0.14$ | $0.6 \pm 0.4$ | $1.3 \pm 1.1$ |
| $t\bar{t} + X$ | $0.12 \pm 0.07$ | $0.45 \pm 0.25$ | $3.0 \pm 1.6$ |
| $Z$+jets | $0.06 \pm 0.10$ | $0.3 \pm 0.9$ | $0.49 \pm 0.31$ |
| $W$+jets | $0.07 \pm 0.06$ | $0.18 \pm 0.15$ | $0.67 \pm 0.22$ |
| Diboson | $0.06 \pm 0.07$ | $0.12 \pm 0.07$ | $< 0.01$ |
| Multijet | $0.09 \pm 0.11$ | $0.04 \pm 0.05$ | $1.3 \pm 2.1$ |
| MC-only background | 1.3 | 3.3 | 23 |

| | SR-Gbb | | | |
|---|---|---|---|---|
| Targeted kinematics | B | M | C | VC |
| Observed events | 2 | 2 | 5 | 0 |
| Fitted background | $2.1 \pm 0.7$ | $3.0 \pm 1.0$ | $5.8 \pm 1.9$ | $4.7 \pm 2.3$ |
| $t\bar{t}$ | $1.2 \pm 0.6$ | $1.9 \pm 0.7$ | $3.8 \pm 1.3$ | $3.1 \pm 1.3$ |
| Single-top | $0.31 \pm 0.16$ | $0.39 \pm 0.16$ | $0.46 \pm 0.20$ | $0.15 \pm 0.18$ |
| $t\bar{t} + X$ | $0.12 \pm 0.06$ | $0.33 \pm 0.19$ | $0.6 \pm 0.4$ | $0.19 \pm 0.11$ |
| $Z$+jets | $0.15 \pm 0.34$ | $0.2 \pm 0.6$ | $0.6 \pm 1.3$ | $0.8 \pm 1.9$ |
| $W$+jets | $0.12 \pm 0.09$ | $0.13 \pm 0.12$ | $0.29 \pm 0.19$ | $0.37 \pm 0.30$ |
| Diboson | $0.06 \pm 0.04$ | $< 0.01$ | $< 0.01$ | $0.15 \pm 0.08$ |
| Multijet | $0.10 \pm 0.12$ | $0.022 \pm 0.025$ | $0.03 \pm 0.04$ | $0.016 \pm 0.020$ |
| MC-only background | 1.9 | 2.7 | 4.4 | 3.9 |

**Table 7.** Results of the background-only fit extrapolated to the Gtt 1-lepton, Gtt 0-lepton and Gbb SRs in the cut-and-count analysis, for the total background prediction and breakdown of the main background sources. The uncertainties shown include all systematic uncertainties. The data in the SRs are not included in the fit. The background category $t\bar{t} + X$ includes $t\bar{t}W/Z$, $t\bar{t}H$ and $t\bar{t}t\bar{t}$ events. The row "MC-only background" provides the total background prediction when the $t\bar{t}$ normalisation is obtained from a theoretical calculation [64].

| Signal channel | $p_0$ (Z) | $\sigma_{\mathrm{vis}}^{95}$ [fb] | $S_{obs}^{95}$ | $S_{\exp}^{95}$ |
|---|---|---|---|---|
| SR-Gtt-1L-B | 0.50 (0.00) | 0.08 | 3.0 | $3.0^{+1.0}_{-0.0}$ |
| SR-Gtt-1L-M | 0.34 (0.42) | 0.11 | 3.9 | $3.6^{+1.1}_{-0.4}$ |
| SR-Gtt-1L-C | 0.50 (0.00) | 0.13 | 4.8 | $4.7^{+1.8}_{-0.9}$ |
| SR-Gtt-0L-B | 0.32 (0.48) | 0.13 | 4.8 | $4.1^{+1.7}_{-0.6}$ |
| SR-Gtt-0L-M | 0.25 (0.69) | 0.21 | 7.5 | $6.0^{+2.3}_{-1.4}$ |
| SR-Gtt-0L-C | 0.50 (0.00) | 0.39 | 14.0 | $17.8^{+6.6}_{-4.5}$ |
| SR-Gbb-B | 0.50 (0.00) | 0.13 | 4.6 | $4.6^{+1.7}_{-1.0}$ |
| SR-Gbb-M | 0.50 (0.00) | 0.12 | 4.4 | $5.0^{+1.9}_{-1.1}$ |
| SR-Gbb-C | 0.50 (0.00) | 0.18 | 6.6 | $6.9^{+2.7}_{-1.8}$ |
| SR-Gbb-VC | 0.50 (0.00) | 0.08 | 3.0 | $4.6^{+2.0}_{-1.3}$ |

**Table 8.** The $p_0$-values and $Z$ (the number of equivalent Gaussian standard deviations), the 95% CL upper limits on the visible cross-section ($\sigma_{\mathrm{vis}}^{95}$), and the observed and expected 95% CL upper limits on the number of BSM events ($S_{obs}^{95}$ and $S_{\exp}^{95}$). The maximum allowed $p_0$-value is truncated at 0.5.

are used for this purpose, to aid in the reintepretation of these limits. Limits are obtained with a fit in each SR which proceeds in the same way as the fit used to predict the background, except that the number of events observed in the SR is added as an input to the fit. Also, an additional parameter for the non-SM signal strength, constrained to be non-negative, is fit. Upper limits on the visible BSM cross-section ($\sigma_{\mathrm{vis}}^{95}$) are obtained by dividing the observed upper limits on the number of BSM events with the integrated luminosity. The results are given in table 8, where the $p_0$-values, which represent the probability of the SM background alone to fluctuate to the observed number of events or higher, are also provided.

## 9.2 Model-dependent exclusion limits

The results are used to place exclusion limits on various signal models. The results are obtained using the CL$_s$ prescription in the asymptotic approximation [92]. The expected and observed limits were compared to the CL$_s$ calculated from pseudoexperiments and found to be compatible. The signal contamination in the CRs and the experimental systematic uncertainties in the signal are taken into account for this calculation. All the regions of the multi-bin analysis are statistically combined to set model-dependent upper limits on the Gbb, Gtt and variable branching ratio models.

The 95% CL observed and expected exclusion limits for the Gtt and Gbb models are shown in the LSP and gluino mass plane in figures 10a and 10b, respectively. The $\pm 1\sigma_{theory}^{SUSY}$ lines around the observed limits are obtained by changing the SUSY cross-section by one standard deviation ($\pm 1\sigma$), as described in section 4. The yellow band around the expected limit shows the $\pm 1\sigma$ uncertainty, including all statistical and systematic
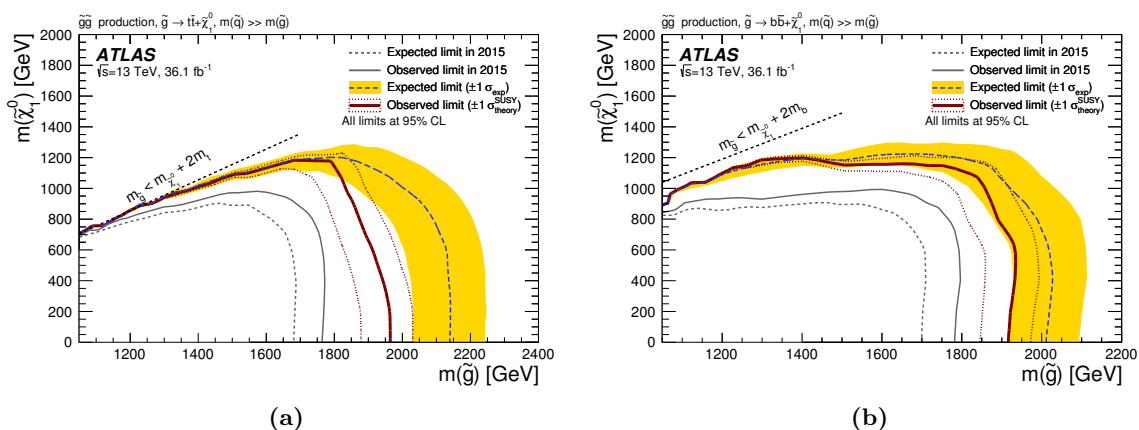
**Figure 10.** Exclusion limits in the $\tilde{\chi}_1^0$ and $\tilde{g}$ mass plane for the (a) Gtt and (b) Gbb models obtained in the context of the multi-bin analysis. The dashed and solid bold lines show the 95% CL expected and observed limits, respectively. The shaded bands around the expected limits show the impact of the experimental and background uncertainties. The dotted lines show the impact on the observed limit of the variation of the nominal signal cross-section by $\pm 1\sigma$ of its theoretical uncertainty. The 95% CL expected and observed limits from the ATLAS search based on 2015 data [19] are also shown.

uncertainties except the theoretical uncertainties in the SUSY cross-section. Compared to the previous results [19], the gluino mass sensitivities of the current search (assuming massless LSPs) have improved by 300 GeV and 450 GeV for the Gbb and Gtt models, respectively. Gluinos with masses below 1.97 (1.92) TeV are excluded at 95% CL for neutralino masses lower than 300 GeV in the Gtt (Gbb) model. The observed limit for the Gtt model at high gluino mass is weaker than the expected limits due to the mild excesses observed in the signal regions SR-0L-HH and SR-1L-HI of the multi-bin fit analysis. The best exclusion limit on the LSP mass is approximately 1.19 (1.20) TeV, which is reached for a gluino mass of approximately 1.40 (1.68) TeV for Gbb and Gtt models, respectively.

Limits are also set in the signal model described in section 2 for which the branching ratios of the gluinos to $t\bar{b}\tilde{\chi}_1^-$ (with $\tilde{\chi}_1^- \to f\bar{f}'\tilde{\chi}_1^0$), $t\bar{t}\tilde{\chi}_1^0$, and $b\bar{b}\tilde{\chi}_1^0$ are allowed to vary, with a unitarity constraint imposed on the sum of the three branching ratios. The expected and observed exclusions are shown in figure 11a for a fixed neutralino mass hypothesis ($m_{\tilde{\chi}_1^0} = 1$ GeV) and various gluino masses. The results are presented in the $B(\tilde{g} \to t\bar{t}\tilde{\chi}_1^0)$ vs. $B(\tilde{g} \to b\bar{b}\tilde{\chi}_1^0)$ plane, where the branching ratio for $\tilde{g} \to t\bar{b}\tilde{\chi}_1^-$ is equal to $1 - (B(\tilde{g} \to t\bar{t}\tilde{\chi}_1^0) + B(\tilde{g} \to b\bar{b}\tilde{\chi}_1^0))$. The exclusion limits are weaker in the lower left corner, where the branching ratio for $\tilde{g} \to t\bar{b}\tilde{\chi}_1^-$ is substantial, which is expected since these decays were not included in the optimisation procedure. Due to the mild excess observed in some regions of the multi-bin analysis and despite an expected sensitivity across the whole plane for a massless neutralino hypothesis, the 95% CL limit for a 1.8 TeV gluino is of $B(\tilde{g} \to t\bar{t}\tilde{\chi}_1^0) \geq 30\%$ ($B(\tilde{g} \to b\bar{b}\tilde{\chi}_1^0) \geq 40\%$) when assuming $B(\tilde{g} \to b\bar{b}\tilde{\chi}_1^0) = 0$ ($B(\tilde{g} \to t\bar{t}\tilde{\chi}_1^0) = 0$). None of the points in the plane are excluded for gluino masses larger than 2.0 TeV.
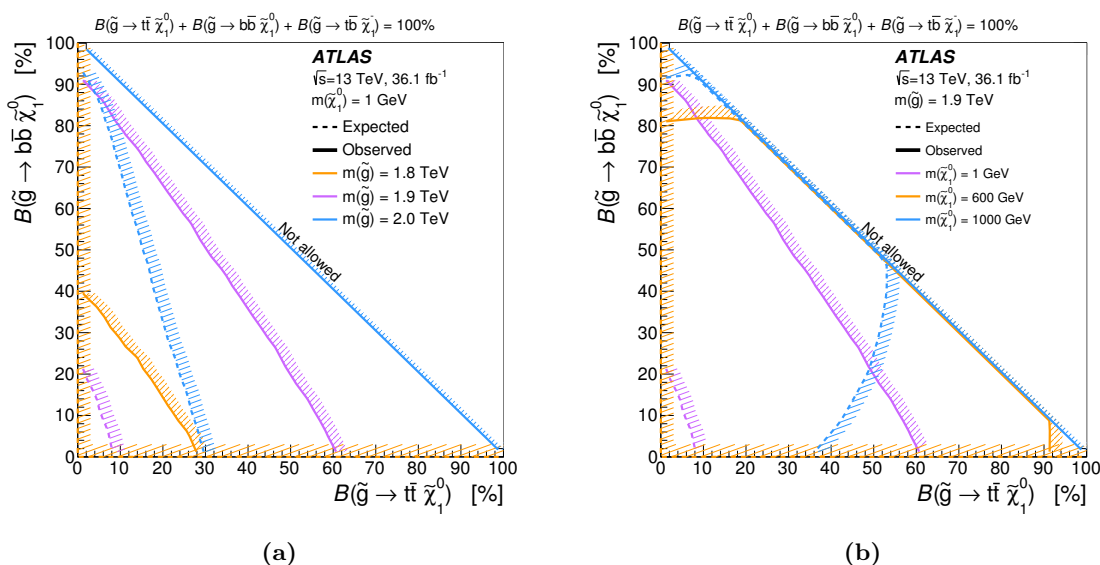
**Figure 11.** Exclusion limits in the $\tilde{g} \to t\bar{t}\tilde{\chi}_1^0$ and $\tilde{g} \to b\bar{b}\tilde{\chi}_1^0$ branching ratio plane assuming (a) a neutralino mass of 1 GeV and various gluino masses (1.8, 1.9 and 2.0 TeV) and (b) a gluino mass of 1.9 TeV and three neutralino masses (1, 600 and 1000 GeV). In (a), the expected limit for a gluino mass of 1.8 TeV follows the plot axes, meaning that the whole plane is expected to be excluded at 95% CL. The same is true in (b) for a neutralino mass of 600 GeV. The dashed and solid bold lines show the 95% CL expected and observed limits, respectively. The hashing indicates which side of the line is excluded. The upper right half of the plane is forbidden by the requirement that the sum of branching ratios does not exceed 100%.

Similar results are presented in figure 11b assuming a gluino mass of 1.9 TeV and scanning various neutralino masses (1, 600 and 1000 GeV). For neutralino masses between 1 and 600 GeV, most of the branching ratio plane is expected to be excluded at 95% CL. The observed limit is nevertheless worse due to the mild excess observed in the SRs. Thus, for instance, for a massless neutralino hypothesis, only the region with $B(\tilde{g} \to b\bar{b}\tilde{\chi}_1^0) > 90\%$ is excluded for all values of $B(\tilde{g} \to t\bar{t}\tilde{\chi}_1^0)$.

## 10 Conclusion

A search for pair-produced gluinos decaying via bottom or top squarks is presented. LHC proton-proton collision data from the full 2015 and 2016 data-taking periods are analysed, corresponding to an integrated luminosity of 36.1 fb$^{-1}$ collected at $\sqrt{s} = 13$ TeV by the ATLAS detector. The search uses multiple signal regions designed for different scenarios of gluino and LSP masses. The signal regions require several high-$p_T$ jets, of which at least three must be $b$-tagged, large $E_T^{miss}$ and either zero or at least one charged lepton. Two strategies are employed: one in which the signal regions are optimised for discovery, and another one in which several non-overlapping signal regions are fitted simultaneously to achieve optimal exclusion limits for benchmark signals. For all signal regions, the background is generally dominated by $t\bar{t}$+jets, which is normalised in dedicated control regions.

No excess is found above the predicted background in any of the signal regions. Model-independent limits are set on the visible cross-section for new physics processes. Exclusion limits are set on gluino and LSP masses in two simplified models where the gluino decays exclusively as $\tilde{g} \to b\bar{b}\tilde{\chi}_1^0$ or $\tilde{g} \to t\bar{t}\tilde{\chi}_1^0$. For LSP masses below approximately 300 GeV, gluino masses of less than 1.97 TeV and 1.92 TeV are excluded at the 95% CL for the $\tilde{g} \to t\bar{t}\tilde{\chi}_1^0$ and $\tilde{g} \to b\bar{b}\tilde{\chi}_1^0$ models, respectively. These results improve upon the exclusion limits obtained with the 2015 dataset alone. The results are also interpreted in a model with variable gluino branching ratios to $\tilde{g} \to b\bar{b}\tilde{\chi}_1^0$, $\tilde{g} \to t\bar{b}\tilde{\chi}_1^-$ and $\tilde{g} \to t\bar{t}\tilde{\chi}_1^0$. For example, a mass point with $m_{\tilde{g}} = 1.9$ TeV and $m_{\tilde{\chi}_1^0} = 1$ GeV is excluded at the 95% CL only if $B(\tilde{g} \to t\bar{b}\tilde{\chi}_1^-)$ ¡ 10%.

## Acknowledgments

# References

[1] Yu. A. Golfand and E.P. Likhtman, *Extension of the algebra of Poincaré group generators and violation of p invariance*, *JETP Lett.* **13** (1971) 323 [*Pisma Zh. Eksp. Teor. Fiz.* **13** (1971) 452] [INSPIRE].

[2] D.V. Volkov and V.P. Akulov, *Is the neutrino a Goldstone particle?*, *Phys. Lett.* **B 46** (1973) 109 [INSPIRE].

[3] J. Wess and B. Zumino, *Supergauge transformations in four-dimensions*, *Nucl. Phys.* **B 70** (1974) 39 [INSPIRE].

[4] J. Wess and B. Zumino, *Supergauge invariant extension of quantum electrodynamics*, *Nucl. Phys.* **B 78** (1974) 1 [INSPIRE].

[5] S. Ferrara and B. Zumino, *Supergauge invariant Yang-Mills theories*, *Nucl. Phys.* **B 79** (1974) 413 [INSPIRE].

[6] A. Salam and J.A. Strathdee, *Supersymmetry and non-Abelian gauges*, *Phys. Lett.* **B 51** (1974) 353 [INSPIRE].

[7] G.R. Farrar and P. Fayet, *Phenomenology of the production, decay and detection of new hadronic states associated with supersymmetry*, *Phys. Lett.* **B 76** (1978) 575 [INSPIRE].

[8] N. Sakai, *Naturalness in supersymmetric GUTs*, *Z. Phys.* **C 11** (1981) 153 [INSPIRE].

[9] S. Dimopoulos, S. Raby and F. Wilczek, *Supersymmetry and the scale of unification*, *Phys. Rev.* **D 24** (1981) 1681 [INSPIRE].

[10] L.E. Ibáñez and G.G. Ross, *Low-energy predictions in supersymmetric grand unified theories*, *Phys. Lett.* **B 105** (1981) 439 [INSPIRE].

[11] S. Dimopoulos and H. Georgi, *Softly broken supersymmetry and* SU(5), *Nucl. Phys.* **B 193** (1981) 150 [INSPIRE].

[12] K. Inoue, A. Kakuto, H. Komatsu and S. Takeshita, *Aspects of grand unified models with softly broken supersymmetry*, *Prog. Theor. Phys.* **68** (1982) 927 [*Erratum ibid.* **70** (1983) 330] [INSPIRE].

[13] J.R. Ellis and S. Rudaz, *Search for supersymmetry in toponium decays*, *Phys. Lett.* **B 128** (1983) 248 [INSPIRE].

[14] R. Barbieri and G.F. Giudice, *Upper bounds on supersymmetric particle masses*, *Nucl. Phys.* **B 306** (1988) 63 [INSPIRE].

[15] ATLAS collaboration, *The ATLAS experiment at the CERN Large Hadron Collider*, 2008 *JINST* **3** S08003 [INSPIRE].

[16] J. Alwall, M.-P. Le, M. Lisanti and J.G. Wacker, *Searching for directly decaying gluinos at the Tevatron*, *Phys. Lett.* **B 666** (2008) 34 [arXiv:0803.0019] [INSPIRE].

[17] J. Alwall, P. Schuster and N. Toro, *Simplified models for a first characterization of new physics at the LHC*, *Phys. Rev.* **D 79** (2009) 075020 [arXiv:0810.3921] [INSPIRE].

[18] LHC New Physics Working Group collaboration, D. Alves, *Simplified models for LHC new physics searches*, *J. Phys.* **G 39** (2012) 105005 [arXiv:1105.2838] [INSPIRE].

[19] ATLAS collaboration, *Search for pair production of gluinos decaying via stop and sbottom in events with b-jets and large missing transverse momentum in pp collisions at $\sqrt{s} = 13\,TeV$ with the ATLAS detector*, *Phys. Rev.* **D 94** (2016) 032003 [arXiv:1605.09318] [INSPIRE].

[20] ATLAS collaboration, *Search for supersymmetry at $\sqrt{s} = 13\,TeV$ in final states with jets and two same-sign leptons or three leptons with the ATLAS detector*, *Eur. Phys. J.* **C 76** (2016) 259 [arXiv:1602.09058] [INSPIRE].

[21] ATLAS collaboration, *Search for supersymmetry in final states with two same-sign or three leptons and jets using $36\,fb^{-1}$ of $\sqrt{s} = 13\,TeV$ pp collision data with the ATLAS detector*, *JHEP* **09** (2017) 084 [arXiv:1706.03731] [INSPIRE].

[22] CMS collaboration, *Search for physics beyond the Standard Model in events with two leptons of same sign, missing transverse momentum and jets in proton-proton collisions at $\sqrt{s} = 13\,TeV$*, *Eur. Phys. J.* **C 77** (2017) 578 [arXiv:1704.07323] [INSPIRE].

[23] CMS collaboration, *Search for supersymmetry in pp collisions at $\sqrt{s} = 13\,TeV$ in the single-lepton final state using the sum of masses of large-radius jets*, *Phys. Rev. Lett.* **119** (2017) 151802 [arXiv:1705.04673] [INSPIRE].

[24] CMS collaboration, *Search for supersymmetry in multijet events with missing transverse momentum in proton-proton collisions at $13\,TeV$*, *Phys. Rev.* **D 96** (2017) 032003 [arXiv:1704.07781] [INSPIRE].

[25] CMS collaboration, *Search for new phenomena with the $M_{T2}$ variable in the all-hadronic final state produced in proton-proton collisions at $\sqrt{s} = 13\,TeV$*, *Eur. Phys. J.* **C 77** (2017) 710 [arXiv:1705.04650] [INSPIRE].

[26] ATLAS collaboration, *Search for strong production of supersymmetric particles in final states with missing transverse momentum and at least three b-jets at $\sqrt{s} = 8\,TeV$ proton-proton collisions with the ATLAS detector*, *JHEP* **10** (2014) 024 [arXiv:1407.0600] [INSPIRE].

[27] CMS collaboration, *Inclusive search for supersymmetry using razor variables in pp collisions at $\sqrt{s} = 13\,TeV$*, *Phys. Rev.* **D 95** (2017) 012003 [arXiv:1609.07658] [INSPIRE].

[28] ATLAS collaboration, *ATLAS insertable B-layer technical design report*, CERN-LHCC-2010-013, CERN, Geneva, Switzerland, (2010) [ATLAS-TDR-19].

[29] ATLAS collaboration, *Performance of the ATLAS trigger system in* 2015, *Eur. Phys. J.* **C 77** (2017) 317 [arXiv:1611.09661] [INSPIRE].

[30] ATLAS collaboration, *Luminosity determination in pp collisions at $\sqrt{s} = 8\,TeV$ using the ATLAS detector at the LHC*, *Eur. Phys. J.* **C 76** (2016) 653 [arXiv:1608.03953] [INSPIRE].

[31] J. Alwall et al., *The automated computation of tree-level and next-to-leading order differential cross sections and their matching to parton shower simulations*, *JHEP* **07** (2014) 079 [arXiv:1405.0301] [INSPIRE].

[32] R.D. Ball et al., *Parton distributions with LHC data*, *Nucl. Phys.* **B 867** (2013) 244 [arXiv:1207.1303] [INSPIRE].

[33] T. Sjöstrand, S. Mrenna and P.Z. Skands, *A brief introduction to PYTHIA 8.1*, *Comput. Phys. Commun.* **178** (2008) 852 [arXiv:0710.3820] [INSPIRE].

[34] S. Alioli, P. Nason, C. Oleari and E. Re, *A general framework for implementing NLO calculations in shower Monte Carlo programs: the POWHEG BOX*, *JHEP* **06** (2010) 043 [arXiv:1002.2581] [INSPIRE].

[35] H.-L. Lai et al., *New parton distributions for collider physics*, *Phys. Rev.* **D 82** (2010) 074024 [arXiv:1007.2241] [INSPIRE].

[36] P. Artoisenet, R. Frederix, O. Mattelaer and R. Rietkerk, *Automatic spin-entangled decays of heavy resonances in Monte Carlo simulations*, *JHEP* **03** (2013) 015 [arXiv:1212.3460] [INSPIRE].

[37] T. Sjöstrand, S. Mrenna and P.Z. Skands, *PYTHIA 6.4 physics and manual*, *JHEP* **05** (2006) 026 [hep-ph/0603175] [INSPIRE].

[38] J. Pumplin, D.R. Stump, J. Huston, H.L. Lai, P.M. Nadolsky and W.K. Tung, *New generation of parton distributions with uncertainties from global QCD analysis*, *JHEP* **07** (2002) 012 [hep-ph/0201195] [INSPIRE].

[39] M. Bahr et al., *HERWIG++ physics and manual*, *Eur. Phys. J.* **C 58** (2008) 639 [arXiv:0803.0883] [INSPIRE].

[40] ATLAS collaboration, *Modelling of the $t\bar{t}H$ and $t\bar{t}V$ ($V = W, Z$) processes for $\sqrt{s} = 13$ TeV ATLAS analyses*, ATL-PHYS-PUB-2016-005, CERN, Geneva, Switzerland, (2016).

[41] T. Gleisberg et al., *Event generation with SHERPA 1.1*, *JHEP* **02** (2009) 007 [arXiv:0811.4622] [INSPIRE].

[42] T. Gleisberg and S. Höche, *Comix, a new matrix element generator*, *JHEP* **12** (2008) 039 [arXiv:0808.3674] [INSPIRE].

[43] F. Cascioli, P. Maierhofer and S. Pozzorini, *Scattering amplitudes with open loops*, *Phys. Rev. Lett.* **108** (2012) 111601 [arXiv:1111.5206] [INSPIRE].

[44] S. Schumann and F. Krauss, *A parton shower algorithm based on Catani-Seymour dipole factorisation*, *JHEP* **03** (2008) 038 [arXiv:0709.1027] [INSPIRE].

[45] S. Höche, F. Krauss, M. Schönherr and F. Siegert, *QCD matrix elements + parton showers: the NLO case*, *JHEP* **04** (2013) 027 [arXiv:1207.5030] [INSPIRE].

[46] PARTICLE DATA GROUP collaboration, C. Patrignani et al., *Review of particle physics*, *Chin. Phys.* **C 40** (2016) 100001 [INSPIRE].

[47] ATLAS collaboration, *Multi-boson simulation for 13 TeV ATLAS analyses*, ATL-PHYS-PUB-2016-002, CERN, Geneva, Switzerland, (2016).

[48] NNPDF collaboration, R.D. Ball et al., *Parton distributions for the LHC run II*, *JHEP* **04** (2015) 040 [arXiv:1410.8849] [INSPIRE].

[49] D.J. Lange, *The EvtGen particle decay simulation package*, *Nucl. Instrum. Meth.* **A 462** (2001) 152 [INSPIRE].

[50] P.Z. Skands, *Tuning Monte Carlo generators: the Perugia tunes*, *Phys. Rev.* **D 82** (2010) 074018 [arXiv:1005.3457] [INSPIRE].

[51] ATLAS collaboration, *ATLAS run 1 PYTHIA8 tunes*, ATL-PHYS-PUB-2014-021, CERN, Geneva, Switzerland, (2014).

[52] S. Gieseke, C. Rohr and A. Siodmok, *Colour reconnections in HERWIG++*, *Eur. Phys. J.* **C 72** (2012) 2225 [arXiv:1206.0041] [INSPIRE].

[53] ATLAS collaboration, *Summary of ATLAS PYTHIA 8 tunes*, ATL-PHYS-PUB-2012-003, CERN, Geneva, Switzerland, (2012).

[54] A.D. Martin, W.J. Stirling, R.S. Thorne and G. Watt, *Parton distributions for the LHC*, *Eur. Phys. J.* **C 63** (2009) 189 [arXiv:0901.0002] [INSPIRE].

[55] GEANT4 collaboration, S. Agostinelli et al., *GEANT4: a simulation toolkit*, *Nucl. Instrum. Meth.* **A 506** (2003) 250 [inSPIRE].

[56] ATLAS collaboration, *The simulation principle and performance of the ATLAS fast calorimeter simulation FastCaloSim*, ATL-PHYS-PUB-2010-013, CERN, Geneva, Switzerland, (2010).

[57] W. Beenakker, R. Hopker, M. Spira and P.M. Zerwas, *Squark and gluino production at hadron colliders*, *Nucl. Phys.* **B 492** (1997) 51 [hep-ph/9610490] [inSPIRE].

[58] A. Kulesza and L. Motyka, *Threshold resummation for squark-antisquark and gluino-pair production at the LHC*, *Phys. Rev. Lett.* **102** (2009) 111802 [arXiv:0807.2405] [inSPIRE].

[59] A. Kulesza and L. Motyka, *Soft gluon resummation for the production of gluino-gluino and squark-antisquark pairs at the LHC*, *Phys. Rev.* **D 80** (2009) 095004 [arXiv:0905.4749] [inSPIRE].

[60] W. Beenakker, S. Brensing, M. Krämer, A. Kulesza, E. Laenen and I. Niessen, *Soft-gluon resummation for squark and gluino hadroproduction*, *JHEP* **12** (2009) 041 [arXiv:0909.4418] [inSPIRE].

[61] W. Beenakker et al., *Squark and gluino hadroproduction*, *Int. J. Mod. Phys.* **A 26** (2011) 2637 [arXiv:1105.1110] [inSPIRE].

[62] C. Borschensky et al., *Squark and gluino production cross sections in pp collisions at $\sqrt{s} = 13$, 14, 33 and 100 TeV*, *Eur. Phys. J.* **C 74** (2014) 3174 [arXiv:1407.5066] [inSPIRE].

[63] ATLAS collaboration, *Search for squarks and gluinos with the ATLAS detector in final states with jets and missing transverse momentum using $4.7\,fb^{-1}$ of $\sqrt{s} = 7\,TeV$ proton-proton collision data*, *Phys. Rev.* **D 87** (2013) 012008 [arXiv:1208.0949] [inSPIRE].

[64] M. Czakon and A. Mitov, *Top++: a program for the calculation of the top-pair cross-section at hadron colliders*, *Comput. Phys. Commun.* **185** (2014) 2930 [arXiv:1112.5675] [inSPIRE].

[65] N. Kidonakis, *NNLL resummation for s-channel single top quark production*, *Phys. Rev.* **D 81** (2010) 054028 [arXiv:1001.5034] [inSPIRE].

[66] N. Kidonakis, *Two-loop soft anomalous dimensions for single top quark associated production with a $W^-$ or $H^-$*, *Phys. Rev.* **D 82** (2010) 054018 [arXiv:1005.4451] [inSPIRE].

[67] N. Kidonakis, *Next-to-next-to-leading-order collinear and soft gluon corrections for t-channel single top quark production*, *Phys. Rev.* **D 83** (2011) 091503 [arXiv:1103.2792] [inSPIRE].

[68] LHC HIGGS CROSS SECTION WORKING GROUP collaboration, D. de Florian et al., *Handbook of LHC Higgs cross sections: 4. Deciphering the nature of the Higgs sector*, arXiv:1610.07922 [inSPIRE].

[69] LHC HIGGS CROSS SECTION WORKING GROUP collaboration, J.R. Andersen et al., *Handbook of LHC Higgs cross sections: 3. Higgs properties*, arXiv:1307.1347 [inSPIRE].

[70] S. Catani, L. Cieri, G. Ferrera, D. de Florian and M. Grazzini, *Vector boson production at hadron colliders: a fully exclusive QCD calculation at NNLO*, *Phys. Rev. Lett.* **103** (2009) 082001 [arXiv:0903.2120] [inSPIRE].

[71] ATLAS collaboration, *Vertex reconstruction performance of the ATLAS detector at $\sqrt{s} = 13\,TeV$*, ATL-PHYS-PUB-2015-026, CERN, Geneva, Switzerland, (2015).

[72] ATLAS collaboration, *Topological cell clustering in the ATLAS calorimeters and its performance in LHC run 1*, *Eur. Phys. J.* **C 77** (2017) 490 [arXiv:1603.02934] [inSPIRE].

[73] M. Cacciari, G.P. Salam and G. Soyez, *The anti-k_t jet clustering algorithm*, *JHEP* **04** (2008) 063 [arXiv:0802.1189] [INSPIRE].

[74] M. Cacciari, G.P. Salam and G. Soyez, *FastJet user manual*, *Eur. Phys. J.* **C 72** (2012) 1896 [arXiv:1111.6097] [INSPIRE].

[75] ATLAS collaboration, *Jet energy scale measurements and their systematic uncertainties in proton-proton collisions at $\sqrt{s} = 13\,TeV$ with the ATLAS detector*, *Phys. Rev.* **D 96** (2017) 072002 [arXiv:1703.09665] [INSPIRE].

[76] ATLAS collaboration, *Selection of jets produced in* 13 *TeV proton-proton collisions with the ATLAS detector*, ATLAS-CONF-2015-029, CERN, Geneva, Switzerland, (2015).

[77] ATLAS collaboration, *Performance of pile-up mitigation techniques for jets in pp collisions at $\sqrt{s} = 8\,TeV$ using the ATLAS detector*, *Eur. Phys. J.* **C 76** (2016) 581 [arXiv:1510.03823] [INSPIRE].

[78] ATLAS collaboration, *Performance of b-jet identification in the ATLAS experiment*, 2016 *JINST* **11** P04008 [arXiv:1512.01094] [INSPIRE].

[79] ATLAS collaboration, *Optimisation of the ATLAS b-tagging performance for the* 2016 *LHC run*, ATL-PHYS-PUB-2016-012, CERN, Geneva, Switzerland, (2016).

[80] B. Nachman, P. Nef, A. Schwartzman, M. Swiatlowski and C. Wanotayaroj, *Jets from jets: re-clustering as a tool for large radius jet reconstruction and grooming at the LHC*, *JHEP* **02** (2015) 075 [arXiv:1407.2922] [INSPIRE].

[81] D. Krohn, J. Thaler and L.-T. Wang, *Jet trimming*, *JHEP* **02** (2010) 084 [arXiv:0912.1342] [INSPIRE].

[82] ATLAS collaboration, *Performance of jet substructure techniques for large-R jets in proton-proton collisions at $\sqrt{s} = 7\,TeV$ using the ATLAS detector*, *JHEP* **09** (2013) 076 [arXiv:1306.4945] [INSPIRE].

[83] ATLAS collaboration, *Performance of top quark and W boson tagging in run* 2 *with ATLAS*, ATLAS-CONF-2017-064, CERN, Geneva, Switzerland, (2017).

[84] ATLAS collaboration, *Electron and photon energy calibration with the ATLAS detector using LHC run* 1 *data*, *Eur. Phys. J.* **C 74** (2014) 3071 [arXiv:1407.5063] [INSPIRE].

[85] ATLAS collaboration, *Electron efficiency measurements with the ATLAS detector using the* 2015 *LHC proton-proton collision data*, ATLAS-CONF-2016-024, CERN, Geneva, Switzerland, (2016).

[86] ATLAS collaboration, *Muon reconstruction performance of the ATLAS detector in proton-proton collision data at $\sqrt{s} = 13\,TeV$*, *Eur. Phys. J.* **C 76** (2016) 292 [arXiv:1603.05598] [INSPIRE].

[87] ATLAS collaboration, *Performance of missing transverse momentum reconstruction for the ATLAS detector in the first proton-proton collisions at at $\sqrt{s} = 13\,TeV$*, ATL-PHYS-PUB-2015-027, CERN, Geneva, Switzerland, (2015).

[88] ATLAS collaboration, *Expected performance of missing transverse momentum reconstruction for the ATLAS detector at $\sqrt{s} = 13\,TeV$*, ATL-PHYS-PUB-2015-023, CERN, Geneva, Switzerland, (2015).

[89] ATLAS collaboration, *Jet calibration and systematic uncertainties for jets reconstructed in the ATLAS detector at $\sqrt{s} = 13\,TeV$*, ATL-PHYS-PUB-2015-015, CERN, Geneva, Switzerland, (2015).

[90] ATLAS collaboration, *Measurements of fiducial cross-sections for $t\bar{t}$ production with one or two additional b-jets in pp collisions at $\sqrt{s} = 8\,TeV$ using the ATLAS detector*, *Eur. Phys. J.* **C 76** (2016) 11 [arXiv:1508.06868] [INSPIRE].

[91] P. Kant et al., *HatHor for single top-quark production: updated predictions and uncertainty estimates for single top-quark production in hadronic collisions*, *Comput. Phys. Commun.* **191** (2015) 74 [arXiv:1406.4403] [INSPIRE].

[92] G. Cowan, K. Cranmer, E. Gross and O. Vitells, *Asymptotic formulae for likelihood-based tests of new physics*, *Eur. Phys. J.* **C 71** (2011) 1554 [*Erratum ibid.* **C 73** (2013) 2501] [arXiv:1007.1727] [INSPIRE].

[93] M. Baak, G.J. Besjes, D. Côte, A. Koutsman, J. Lorenz and D. Short, *HistFitter software framework for statistical data analysis*, *Eur. Phys. J.* **C 75** (2015) 153 [arXiv:1410.1280] [INSPIRE].

[94] A.L. Read, *Presentation of search results: the $CL_s$ technique*, *J. Phys.* **G 28** (2002) 2693 [INSPIRE].

[95] ATLAS collaboration, *ATLAS computing acknowledgements*, ATL-GEN-PUB-2016-002, CERN, Geneva, Switzerland, (2016).

## The ATLAS collaboration

M. Aaboud[137d], G. Aad[88], B. Abbott[115], O. Abdinov[12,*], B. Abeloos[119], S.H. Abidi[161],
O.S. AbouZeid[139], N.L. Abraham[151], H. Abramowicz[155], H. Abreu[154], R. Abreu[118],
Y. Abulaiti[148a,148b], B.S. Acharya[167a,167b,a], S. Adachi[157], L. Adamczyk[41a], J. Adelman[110],
M. Adersberger[102], T. Adye[133], A.A. Affolder[139], T. Agatonovic-Jovin[14], C. Agheorghiesei[28c],
J.A. Aguilar-Saavedra[128a,128f], S.P. Ahlen[24], F. Ahmadov[68,b], G. Aielli[135a,135b], S. Akatsuka[71],
H. Akerstedt[148a,148b], T.P.A. Åkesson[84], E. Akilli[52], A.V. Akimov[98], G.L. Alberghi[22a,22b],
J. Albert[172], P. Albicocco[50], M.J. Alconada Verzini[74], S.C. Alderweireldt[108], M. Aleksa[32],
I.N. Aleksandrov[68], C. Alexa[28b], G. Alexander[155], T. Alexopoulos[10], M. Alhroob[115], B. Ali[130],
M. Aliev[76a,76b], G. Alimonti[94a], J. Alison[33], S.P. Alkire[38], B.M.M. Allbrooke[151], B.W. Allen[118],
P.P. Allport[19], A. Aloisio[106a,106b], A. Alonso[39], F. Alonso[74], C. Alpigiani[140], A.A. Alshehri[56],
M.I. Alstaty[88], B. Alvarez Gonzalez[32], D. Álvarez Piqueras[170], M.G. Alviggi[106a,106b],
B.T. Amadio[16], Y. Amaral Coutinho[26a], C. Amelung[25], D. Amidei[92],
S.P. Amor Dos Santos[128a,128c], A. Amorim[128a,128b], S. Amoroso[32], G. Amundsen[25],
C. Anastopoulos[141], L.S. Ancu[52], N. Andari[19], T. Andeen[11], C.F. Anders[60b], J.K. Anders[77],
K.J. Anderson[33], A. Andreazza[94a,94b], V. Andrei[60a], S. Angelidakis[9], I. Angelozzi[109],
A. Angerami[38], A.V. Anisenkov[111,c], N. Anjos[13], A. Annovi[126a,126b], C. Antel[60a], M. Antonelli[50],
A. Antonov[100,*], D.J. Antrim[166], F. Anulli[134a], M. Aoki[69], L. Aperio Bella[32], G. Arabidze[93],
Y. Arai[69], J.P. Araque[128a], V. Araujo Ferraz[26a], A.T.H. Arce[48], R.E. Ardell[80], F.A. Arduh[74],
J-F. Arguin[97], S. Argyropoulos[66], M. Arik[20a], A.J. Armbruster[32], L.J. Armitage[79], O. Arnaez[161],
H. Arnold[51], M. Arratia[30], O. Arslan[23], A. Artamonov[99], G. Artoni[122], S. Artz[86], S. Asai[157],
N. Asbah[45], A. Ashkenazi[155], L. Asquith[151], K. Assamagan[27], R. Astalos[146a], M. Atkinson[169],
N.B. Atlay[143], K. Augsten[130], G. Avolio[32], B. Axen[16], M.K. Ayoub[119], G. Azuelos[97,d],
A.E. Baas[60a], M.J. Baca[19], H. Bachacou[138], K. Bachas[76a,76b], M. Backes[122], M. Backhaus[32],
P. Bagnaia[134a,134b], M. Bahmani[42], H. Bahrasemani[144], J.T. Baines[133], M. Bajic[39],
O.K. Baker[179], E.M. Baldin[111,c], P. Balek[175], F. Balli[138], W.K. Balunas[124], E. Banas[42],
A. Bandyopadhyay[23], Sw. Banerjee[176,e], A.A.E. Bannoura[178], L. Barak[32], E.L. Barberio[91],
D. Barberis[53a,53b], M. Barbero[88], T. Barillari[103], M-S Barisits[32], J.T. Barkeloo[118], T. Barklow[145],
N. Barlow[30], S.L. Barnes[36c], B.M. Barnett[133], R.M. Barnett[16], Z. Barnovska-Blenessy[36a],
A. Baroncelli[136a], G. Barone[25], A.J. Barr[122], L. Barranco Navarro[170], F. Barreiro[85],
J. Barreiro Guimarães da Costa[35a], R. Bartoldus[145], A.E. Barton[75], P. Bartos[146a], A. Basalaev[125],
A. Bassalat[119,f], R.L. Bates[56], S.J. Batista[161], J.R. Batley[30], M. Battaglia[139], M. Bauce[134a,134b],
F. Bauer[138], H.S. Bawa[145,g], J.B. Beacham[113], M.D. Beattie[75], T. Beau[83], P.H. Beauchemin[165],
P. Bechtle[23], H.P. Beck[18,h], H.C. Beck[57], K. Becker[122], M. Becker[86], M. Beckingham[173],
C. Becot[112], A.J. Beddall[20e], A. Beddall[20b], V.A. Bednyakov[68], M. Bedognetti[109], C.P. Bee[150],
T.A. Beermann[32], M. Begalli[26a], M. Begel[27], J.K. Behr[45], A.S. Bell[81], G. Bella[155],
L. Bellagamba[22a], A. Bellerive[31], M. Bellomo[154], K. Belotskiy[100], O. Beltramello[32],
N.L. Belyaev[100], O. Benary[155,*], D. Benchekroun[137a], M. Bender[102], K. Bendtz[148a,148b],
N. Benekos[10], Y. Benhammou[155], E. Benhar Noccioli[179], J. Benitez[66], D.P. Benjamin[48],
M. Benoit[52], J.R. Bensinger[25], S. Bentvelsen[109], L. Beresford[122], M. Beretta[50], D. Berge[109],
E. Bergeaas Kuutmann[168], N. Berger[5], J. Beringer[16], S. Berlendis[58], N.R. Bernard[89],
G. Bernardi[83], C. Bernius[145], F.U. Bernlochner[23], T. Berry[80], P. Berta[131], C. Bertella[35a],
G. Bertoli[148a,148b], F. Bertolucci[126a,126b], I.A. Bertram[75], C. Bertsche[45], D. Bertsche[115],
G.J. Besjes[39], O. Bessidskaia Bylund[148a,148b], M. Bessner[45], N. Besson[138], C. Betancourt[51],
A. Bethani[87], S. Bethke[103], A.J. Bevan[79], J. Beyer[103], R.M. Bianchi[127], O. Biebel[102],
D. Biedermann[17], R. Bielski[87], K. Bierwagen[86], N.V. Biesuz[126a,126b], M. Biglietti[136a],
T.R.V. Billoud[97], H. Bilokon[50], M. Bindi[57], A. Bingul[20b], C. Bini[134a,134b], S. Biondi[22a,22b],

T. Bisanz[57], C. Bittrich[47], D.M. Bjergaard[48], C.W. Black[152], J.E. Black[145], K.M. Black[24],
R.E. Blair[6], T. Blazek[146a], I. Bloch[45], C. Blocker[25], A. Blue[56], W. Blum[86,*], U. Blumenschein[79],
S. Blunier[34a], G.J. Bobbink[109], V.S. Bobrovnikov[111,c], S.S. Bocchetta[84], A. Bocci[48], C. Bock[102],
M. Boehler[51], D. Boerner[178], D. Bogavac[102], A.G. Bogdanchikov[111], C. Bohm[148a], V. Boisvert[80],
P. Bokan[168,i], T. Bold[41a], A.S. Boldyrev[101], A.E. Bolz[60b], M. Bomben[83], M. Bona[79],
M. Boonekamp[138], A. Borisov[132], G. Borissov[75], J. Bortfeldt[32], D. Bortoletto[122], V. Bortolotto[62a],
D. Boscherini[22a], M. Bosman[13], J.D. Bossio Sola[29], J. Boudreau[127], J. Bouffard[2],
E.V. Bouhova-Thacker[75], D. Boumediene[37], C. Bourdarios[119], S.K. Boutle[56], A. Boveia[113],
J. Boyd[32], I.R. Boyko[68], J. Bracinik[19], A. Brandt[8], G. Brandt[57], O. Brandt[60a], U. Bratzler[158],
B. Brau[89], J.E. Brau[118], W.D. Breaden Madden[56], K. Brendlinger[45], A.J. Brennan[91],
L. Brenner[109], R. Brenner[168], S. Bressler[175], D.L. Briglin[19], T.M. Bristow[49], D. Britton[56],
D. Britzger[45], F.M. Brochu[30], I. Brock[23], R. Brock[93], G. Brooijmans[38], T. Brooks[80],
W.K. Brooks[34b], J. Brosamer[16], E. Brost[110], J.H Broughton[19], P.A. Bruckman de Renstrom[42],
D. Bruncko[146b], A. Bruni[22a], G. Bruni[22a], L.S. Bruni[109], BH Brunt[30], M. Bruschi[22a],
N. Bruscino[23], P. Bryant[33], L. Bryngemark[45], T. Buanes[15], Q. Buat[144], P. Buchholz[143],
A.G. Buckley[56], I.A. Budagov[68], F. Buehrer[51], M.K. Bugge[121], O. Bulekov[100], D. Bullock[8],
T.J. Burch[110], S. Burdin[77], C.D. Burgard[51], A.M. Burger[5], B. Burghgrave[110], K. Burka[42],
S. Burke[133], I. Burmeister[46], J.T.P. Burr[122], E. Busato[37], D. Büscher[51], V. Büscher[86],
P. Bussey[56], J.M. Butler[24], C.M. Buttar[56], J.M. Butterworth[81], P. Butti[32], W. Buttinger[27],
A. Buzatu[35c], A.R. Buzykaev[111,c], S. Cabrera Urbán[170], D. Caforio[130], V.M. Cairo[40a,40b],
O. Cakir[4a], N. Calace[52], P. Calafiura[16], A. Calandri[88], G. Calderini[83], P. Calfayan[64],
G. Callea[40a,40b], L.P. Caloba[26a], S. Calvente Lopez[85], D. Calvet[37], S. Calvet[37], T.P. Calvet[88],
R. Camacho Toro[33], S. Camarda[32], P. Camarri[135a,135b], D. Cameron[121],
R. Caminal Armadans[169], C. Camincher[58], S. Campana[32], M. Campanelli[81], A. Camplani[94a,94b],
A. Campoverde[143], V. Canale[106a,106b], M. Cano Bret[36c], J. Cantero[116], T. Cao[155],
M.D.M. Capeans Garrido[32], I. Caprini[28b], M. Caprini[28b], M. Capua[40a,40b], R.M. Carbone[38],
R. Cardarelli[135a], F. Cardillo[51], I. Carli[131], T. Carli[32], G. Carlino[106a], B.T. Carlson[127],
L. Carminati[94a,94b], R.M.D. Carney[148a,148b], S. Caron[108], E. Carquin[34b], S. Carrá[94a,94b],
G.D. Carrillo-Montoya[32], J. Carvalho[128a,128c], D. Casadei[19], M.P. Casado[13,j], M. Casolino[13],
D.W. Casper[166], R. Castelijn[109], V. Castillo Gimenez[170], N.F. Castro[128a,k], A. Catinaccio[32],
J.R. Catmore[121], A. Cattai[32], J. Caudron[23], V. Cavaliere[169], E. Cavallaro[13], D. Cavalli[94a],
M. Cavalli-Sforza[13], V. Cavasinni[126a,126b], E. Celebi[20d], F. Ceradini[136a,136b], L. Cerda Alberich[170],
A.S. Cerqueira[26b], A. Cerri[151], L. Cerrito[135a,135b], F. Cerutti[16], A. Cervelli[18], S.A. Cetin[20d],
A. Chafaq[137a], D. Chakraborty[110], S.K. Chan[59], W.S. Chan[109], Y.L. Chan[62a], P. Chang[169],
J.D. Chapman[30], D.G. Charlton[19], C.C. Chau[161], C.A. Chavez Barajas[151], S. Che[113],
S. Cheatham[167a,167c], A. Chegwidden[93], S. Chekanov[6], S.V. Chekulaev[163a], G.A. Chelkov[68,l],
M.A. Chelstowska[32], C. Chen[67], H. Chen[27], J. Chen[36a], S. Chen[35b], S. Chen[157], X. Chen[35c,m],
Y. Chen[70], H.C. Cheng[92], H.J. Cheng[35a,35d], A. Cheplakov[68], E. Cheremushkina[132],
R. Cherkaoui El Moursli[137e], E. Cheu[7], K. Cheung[63], L. Chevalier[138], V. Chiarella[50],
G. Chiarelli[126a,126b], G. Chiodini[76a], A.S. Chisholm[32], A. Chitan[28b], Y.H. Chiu[172],
M.V. Chizhov[68], K. Choi[64], A.R. Chomont[37], S. Chouridou[156], V. Christodoulou[81],
D. Chromek-Burckhart[32], M.C. Chu[62a], J. Chudoba[129], A.J. Chuinard[90], J.J. Chwastowski[42],
L. Chytka[117], A.K. Ciftci[4a], D. Cinca[46], V. Cindro[78], I.A. Cioara[23], C. Ciocca[22a,22b], A. Ciocio[16],
F. Cirotto[106a,106b], Z.H. Citron[175], M. Citterio[94a], M. Ciubancan[28b], A. Clark[52], B.L. Clark[59],
M.R. Clark[38], P.J. Clark[49], R.N. Clarke[16], C. Clement[148a,148b], Y. Coadou[88], M. Cobal[167a,167c],
A. Coccaro[52], J. Cochran[67], L. Colasurdo[108], B. Cole[38], A.P. Colijn[109], J. Collot[58],
T. Colombo[166], P. Conde Muiño[128a,128b], E. Coniavitis[51], S.H. Connell[147b], I.A. Connelly[87],
S. Constantinescu[28b], G. Conti[32], F. Conventi[106a,n], M. Cooke[16], A.M. Cooper-Sarkar[122],

F. Cormier[171], K.J.R. Cormier[161], M. Corradi[134a,134b], F. Corriveau[90,o], A. Cortes-Gonzalez[32],
G. Cortiana[103], G. Costa[94a], M.J. Costa[170], D. Costanzo[141], G. Cottin[30], G. Cowan[80],
B.E. Cox[87], K. Cranmer[112], S.J. Crawley[56], R.A. Creager[124], G. Cree[31], S. Crépé-Renaudin[58],
F. Crescioli[83], W.A. Cribbs[148a,148b], M. Cristinziani[23], V. Croft[108], G. Crosetti[40a,40b], A. Cueto[85],
T. Cuhadar Donszelmann[141], A.R. Cukierman[145], J. Cummings[179], M. Curatolo[50], J. Cúth[86],
P. Czodrowski[32], G. D'amen[22a,22b], S. D'Auria[56], L. D'eramo[83], M. D'Onofrio[77],
M.J. Da Cunha Sargedas De Sousa[128a,128b], C. Da Via[87], W. Dabrowski[41a], T. Dado[146a],
T. Dai[92], O. Dale[15], F. Dallaire[97], C. Dallapiccola[89], M. Dam[39], J.R. Dandoy[124], M.F. Daneri[29],
N.P. Dang[176], A.C. Daniells[19], N.S. Dann[87], M. Danninger[171], M. Dano Hoffmann[138], V. Dao[150],
G. Darbo[53a], S. Darmora[8], J. Dassoulas[3], A. Dattagupta[118], T. Daubney[45], W. Davey[23],
C. David[45], T. Davidek[131], D.R. Davis[48], P. Davison[81], E. Dawe[91], I. Dawson[141], K. De[8],
R. de Asmundis[106a], A. De Benedetti[115], S. De Castro[22a,22b], S. De Cecco[83], N. De Groot[108],
P. de Jong[109], H. De la Torre[93], F. De Lorenzi[67], A. De Maria[57], D. De Pedis[134a],
A. De Salvo[134a], U. De Sanctis[135a,135b], A. De Santo[151], K. De Vasconcelos Corga[88],
J.B. De Vivie De Regie[119], W.J. Dearnaley[75], R. Debbe[27], C. Debenedetti[139], D.V. Dedovich[68],
N. Dehghanian[3], I. Deigaard[109], M. Del Gaudio[40a,40b], J. Del Peso[85], D. Delgove[119], F. Deliot[138],
C.M. Delitzsch[52], A. Dell'Acqua[32], L. Dell'Asta[24], M. Dell'Orso[126a,126b], M. Della Pietra[106a,106b],
D. della Volpe[52], M. Delmastro[5], C. Delporte[119], P.A. Delsart[58], D.A. DeMarco[161], S. Demers[179],
M. Demichev[68], A. Demilly[83], S.P. Denisov[132], D. Denysiuk[138], D. Derendarz[42],
J.E. Derkaoui[137d], F. Derue[83], P. Dervan[77], K. Desch[23], C. Deterre[45], K. Dette[46], M.R. Devesa[29],
P.O. Deviveiros[32], A. Dewhurst[133], S. Dhaliwal[25], F.A. Di Bello[52], A. Di Ciaccio[135a,135b],
L. Di Ciaccio[5], W.K. Di Clemente[124], C. Di Donato[106a,106b], A. Di Girolamo[32], B. Di Girolamo[32],
B. Di Micco[136a,136b], R. Di Nardo[32], K.F. Di Petrillo[59], A. Di Simone[51], R. Di Sipio[161],
D. Di Valentino[31], C. Diaconu[88], M. Diamond[161], F.A. Dias[39], M.A. Diaz[34a], E.B. Diehl[92],
J. Dietrich[17], S. Díez Cornell[45], A. Dimitrievska[14], J. Dingfelder[23], P. Dita[28b], S. Dita[28b],
F. Dittus[32], F. Djama[88], T. Djobava[54b], J.I. Djuvsland[60a], M.A.B. do Vale[26c], D. Dobos[32],
M. Dobre[28b], C. Doglioni[84], J. Dolejsi[131], Z. Dolezal[131], M. Donadelli[26d], S. Donati[126a,126b],
P. Dondero[123a,123b], J. Donini[37], J. Dopke[133], A. Doria[106a], M.T. Dova[74], A.T. Doyle[56],
E. Drechsler[57], M. Dris[10], Y. Du[36b], J. Duarte-Campderros[155], A. Dubreuil[52], E. Duchovni[175],
G. Duckeck[102], A. Ducourthial[83], O.A. Ducu[97,p], D. Duda[109], A. Dudarev[32], A.Chr. Dudder[86],
E.M. Duffield[16], L. Duflot[119], M. Dührssen[32], M. Dumancic[175], A.E. Dumitriu[28b],
A.K. Duncan[56], M. Dunford[60a], H. Duran Yildiz[4a], M. Düren[55], A. Durglishvili[54b],
D. Duschinger[47], B. Dutta[45], D. Duvnjak[1], B.S. Dziedzic[42], C. Eckardt[45],
K.M. Ecker[103], R.C. Edgar[92], T. Eifert[32], G. Eigen[15], K. Einsweiler[16], T. Ekelof[168],
M. El Kacimi[137c], R. El Kosseifi[88], V. Ellajosyula[88], M. Ellert[168], S. Elles[5], F. Ellinghaus[178],
A.A. Elliot[172], N. Ellis[32], J. Elmsheuser[27], M. Elsing[32], D. Emeliyanov[133], Y. Enari[157],
O.C. Endner[86], J.S. Ennis[173], J. Erdmann[46], A. Ereditato[18], M. Ernst[27], S. Errede[169],
M. Escalier[119], C. Escobar[170], B. Esposito[50], O. Estrada Pastor[170], A.I. Etienvre[138], E. Etzion[155],
H. Evans[64], A. Ezhilov[125], M. Ezzi[137e], F. Fabbri[22a,22b], L. Fabbri[22a,22b], V. Fabiani[108],
G. Facini[81], R.M. Fakhrutdinov[132], S. Falciano[134a], R.J. Falla[81], J. Faltova[32], Y. Fang[35a],
M. Fanti[94a,94b], A. Farbin[8], A. Farilla[136a], C. Farina[127], E.M. Farina[123a,123b], T. Farooque[93],
S. Farrell[16], S.M. Farrington[173], P. Farthouat[32], F. Fassi[137e], P. Fassnacht[32], D. Fassouliotis[9],
M. Faucci Giannelli[80], A. Favareto[53a,53b], W.J. Fawcett[122], L. Fayard[119], O.L. Fedin[125,q],
W. Fedorko[171], S. Feigl[121], L. Feligioni[88], C. Feng[36b], E.J. Feng[32], H. Feng[92], M.J. Fenton[56],
A.B. Fenyuk[132], L. Feremenga[8], P. Fernandez Martinez[170], S. Fernandez Perez[13], J. Ferrando[45],
A. Ferrari[168], P. Ferrari[109], R. Ferrari[123a], D.E. Ferreira de Lima[60b], A. Ferrer[170], D. Ferrere[52],
C. Ferretti[92], F. Fiedler[86], A. Filipčič[78], M. Filipuzzi[45], F. Filthaut[108], M. Fincke-Keeler[172],
K.D. Finelli[152], M.C.N. Fiolhais[128a,128c,r], L. Fiorini[170], A. Fischer[2], C. Fischer[13], J. Fischer[178],

W.C. Fisher[93], N. Flaschel[45], I. Fleck[143], P. Fleischmann[92], R.R.M. Fletcher[124], T. Flick[178],
B.M. Flierl[102], L.R. Flores Castillo[62a], M.J. Flowerdew[103], G.T. Forcolin[87], A. Formica[138],
F.A. Förster[13], A. Forti[87], A.G. Foster[19], D. Fournier[119], H. Fox[75], S. Fracchia[141],
P. Francavilla[83], M. Franchini[22a,22b], S. Franchino[60a], D. Francis[32], L. Franconi[121], M. Franklin[59],
M. Frate[166], M. Fraternali[123a,123b], D. Freeborn[81], S.M. Fressard-Batraneanu[32], B. Freund[97],
D. Froidevaux[32], J.A. Frost[122], C. Fukunaga[158], T. Fusayasu[104], J. Fuster[170], C. Gabaldon[58],
O. Gabizon[154], A. Gabrielli[22a,22b], A. Gabrielli[16], G.P. Gach[41a], S. Gadatsch[32], S. Gadomski[80],
G. Gagliardi[53a,53b], L.G. Gagnon[97], C. Galea[108], B. Galhardo[128a,128c], E.J. Gallas[122],
B.J. Gallop[133], P. Gallus[130], G. Galster[39], K.K. Gan[113], S. Ganguly[37], Y. Gao[77], Y.S. Gao[145,g],
F.M. Garay Walls[49], C. García[170], J.E. García Navarro[170], J.A. García Pascual[35a],
M. Garcia-Sciveres[16], R.W. Gardner[33], N. Garelli[145], V. Garonne[121], A. Gascon Bravo[45],
K. Gasnikova[45], C. Gatti[50], A. Gaudiello[53a,53b], G. Gaudio[123a], I.L. Gavrilenko[98], C. Gay[171],
G. Gaycken[23], E.N. Gazis[10], C.N.P. Gee[133], J. Geisen[57], M. Geisen[86], M.P. Geisler[60a],
K. Gellerstedt[148a,148b], C. Gemme[53a], M.H. Genest[58], C. Geng[92], S. Gentile[134a,134b],
C. Gentsos[156], S. George[80], D. Gerbaudo[13], A. Gershon[155], G. Geßner[46], S. Ghasemi[143],
M. Ghneimat[23], B. Giacobbe[22a], S. Giagu[134a,134b], N. Giangiacomi[22a,22b], P. Giannetti[126a,126b],
S.M. Gibson[80], M. Gignac[171], M. Gilchriese[16], D. Gillberg[31], G. Gilles[178], D.M. Gingrich[3,d],
N. Giokaris[9,*], M.P. Giordani[167a,167c], F.M. Giorgi[22a], P.F. Giraud[138], P. Giromini[59],
G. Giugliarelli[167a,167c], D. Giugni[94a], F. Giuli[122], C. Giuliani[103], M. Giulini[60b], B.K. Gjelsten[121],
S. Gkaitatzis[156], I. Gkialas[9,s], E.L. Gkougkousis[139], P. Gkountoumis[10], L.K. Gladilin[101],
C. Glasman[85], J. Glatzer[13], P.C.F. Glaysher[45], A. Glazov[45], M. Goblirsch-Kolb[25], J. Godlewski[42],
S. Goldfarb[91], T. Golling[52], D. Golubkov[132], A. Gomes[128a,128b,128d], R. Gonçalo[128a],
R. Goncalves Gama[26a], J. Goncalves Pinto Firmino Da Costa[138], G. Gonella[51], L. Gonella[19],
A. Gongadze[68], S. González de la Hoz[170], S. Gonzalez-Sevilla[52], L. Goossens[32],
P.A. Gorbounov[99], H.A. Gordon[27], I. Gorelov[107], B. Gorini[32], E. Gorini[76a,76b], A. Gorišek[78],
A.T. Goshaw[48], C. Gössling[46], M.I. Gostkin[68], C.A. Gottardo[23], C.R. Goudet[119],
D. Goujdami[137c], A.G. Goussiou[140], N. Govender[147b,t], E. Gozani[154], L. Graber[57],
I. Grabowska-Bold[41a], P.O.J. Gradin[168], J. Gramling[166], E. Gramstad[121], S. Grancagnolo[17],
V. Gratchev[125], P.M. Gravila[28f], C. Gray[56], H.M. Gray[16], Z.D. Greenwood[82,u], C. Grefe[23],
K. Gregersen[81], I.M. Gregor[45], P. Grenier[145], K. Grevtsov[5], J. Griffiths[8], A.A. Grillo[139],
K. Grimm[75], S. Grinstein[13,v], Ph. Gris[37], J.-F. Grivaz[119], S. Groh[86], E. Gross[175],
J. Grosse-Knetter[57], G.C. Grossi[82], Z.J. Grout[81], A. Grummer[107], L. Guan[92], W. Guan[176],
J. Guenther[65], F. Guescini[163a], D. Guest[166], O. Gueta[155], B. Gui[113], E. Guido[53a,53b],
T. Guillemin[5], S. Guindon[2], U. Gul[56], C. Gumpert[32], J. Guo[36c], W. Guo[92], Y. Guo[36a,w],
R. Gupta[43], S. Gupta[122], G. Gustavino[134a,134b], P. Gutierrez[115], N.G. Gutierrez Ortiz[81],
C. Gutschow[81], C. Guyot[138], M.P. Guzik[41a], C. Gwenlan[122], C.B. Gwilliam[77], A. Haas[112],
C. Haber[16], H.K. Hadavand[8], N. Haddad[137e], A. Hadef[88], S. Hageböck[23], M. Hagihara[164],
H. Hakobyan[180,*], M. Haleem[45], J. Haley[116], G. Halladjian[93], G.D. Hallewell[88], K. Hamacher[178],
P. Hamal[117], K. Hamano[172], A. Hamilton[147a], G.N. Hamity[141], P.G. Hamnett[45], L. Han[36a],
S. Han[35a,35d], K. Hanagaki[69,x], K. Hanawa[157], M. Hance[139], B. Haney[124], P. Hanke[60a],
J.B. Hansen[39], J.D. Hansen[39], M.C. Hansen[23], P.H. Hansen[39], K. Hara[164], A.S. Hard[176],
T. Harenberg[178], F. Hariri[119], S. Harkusha[95], R.D. Harrington[49], P.F. Harrison[173],
N.M. Hartmann[102], M. Hasegawa[70], Y. Hasegawa[142], A. Hasib[49], S. Hassani[138], S. Haug[18],
R. Hauser[93], L. Hauswald[47], L.B. Havener[38], M. Havranek[130], C.M. Hawkes[19], R.J. Hawkings[32],
D. Hayakawa[159], D. Hayden[93], C.P. Hays[122], J.M. Hays[79], H.S. Hayward[77], S.J. Haywood[133],
S.J. Head[19], T. Heck[86], V. Hedberg[84], L. Heelan[8], S. Heer[23], K.K. Heidegger[51], S. Heim[45],
T. Heim[16], B. Heinemann[45,y], J.J. Heinrich[102], L. Heinrich[112], C. Heinz[55], J. Hejbal[129],
L. Helary[32], A. Held[171], S. Hellman[148a,148b], C. Helsens[32], R.C.W. Henderson[75], Y. Heng[176],

S. Henkelmann[171], A.M. Henriques Correia[32], S. Henrot-Versille[119], G.H. Herbert[17], H. Herde[25],
V. Herget[177], Y. Hernández Jiménez[147c], H. Herr[86], G. Herten[51], R. Hertenberger[102], L. Hervas[32],
T.C. Herwig[124], G.G. Hesketh[81], N.P. Hessey[163a], J.W. Hetherly[43], S. Higashino[69],
E. Higón-Rodriguez[170], K. Hildebrand[33], E. Hill[172], J.C. Hill[30], K.H. Hiller[45], S.J. Hillier[19],
M. Hils[47], I. Hinchliffe[16], M. Hirose[51], D. Hirschbuehl[178], B. Hiti[78], O. Hladik[129], X. Hoad[49],
J. Hobbs[150], N. Hod[163a], M.C. Hodgkinson[141], P. Hodgson[141], A. Hoecker[32], M.R. Hoeferkamp[107],
F. Hoenig[102], D. Hohn[23], T.R. Holmes[33], M. Homann[46], S. Honda[164], T. Honda[69], T.M. Hong[127],
B.H. Hooberman[169], W.H. Hopkins[118], Y. Horii[105], A.J. Horton[144], J-Y. Hostachy[58], S. Hou[153],
A. Hoummada[137a], J. Howarth[87], J. Hoya[74], M. Hrabovsky[117], J. Hrdinka[32], I. Hristova[17],
J. Hrivnac[119], T. Hryn'ova[5], A. Hrynevich[96], P.J. Hsu[63], S.-C. Hsu[140], Q. Hu[36a], S. Hu[36c],
Y. Huang[35a], Z. Hubacek[130], F. Hubaut[88], F. Huegging[23], T.B. Huffman[122], E.W. Hughes[38],
G. Hughes[75], M. Huhtinen[32], P. Huo[150], N. Huseynov[68,b], J. Huston[93], J. Huth[59], G. Iacobucci[52],
G. Iakovidis[27], I. Ibragimov[143], L. Iconomidou-Fayard[119], Z. Idrissi[137e], P. Iengo[32],
O. Igonkina[109,z], T. Iizawa[174], Y. Ikegami[69], M. Ikeno[69], Y. Ilchenko[11,aa], D. Iliadis[156], N. Ilic[145],
G. Introzzi[123a,123b], P. Ioannou[9,*], M. Iodice[136a], K. Iordanidou[38], V. Ippolito[59], M.F. Isacson[168],
N. Ishijima[120], M. Ishino[157], M. Ishitsuka[159], C. Issever[122], S. Istin[20a], F. Ito[164],
J.M. Iturbe Ponce[62a], R. Iuppa[162a,162b], H. Iwasaki[69], J.M. Izen[44], V. Izzo[106a], S. Jabbar[3],
P. Jackson[1], R.M. Jacobs[23], V. Jain[2], K.B. Jakobi[86], K. Jakobs[51], S. Jakobsen[65], T. Jakoubek[129],
D.O. Jamin[116], D.K. Jana[82], R. Jansky[52], J. Janssen[23], M. Janus[57], P.A. Janus[41a], G. Jarlskog[84],
N. Javadov[68,b], T. Javůrek[51], M. Javurkova[51], F. Jeanneau[138], L. Jeanty[16], J. Jejelava[54a,ab],
A. Jelinskas[173], P. Jenni[51,ac], C. Jeske[173], S. Jézéquel[5], H. Ji[176], J. Jia[150], H. Jiang[67], Y. Jiang[36a],
Z. Jiang[145], S. Jiggins[81], J. Jimenez Pena[170], S. Jin[35a], A. Jinaru[28b], O. Jinnouchi[159], H. Jivan[147c],
P. Johansson[141], K.A. Johns[7], C.A. Johnson[64], W.J. Johnson[140], K. Jon-And[148a,148b],
R.W.L. Jones[75], S.D. Jones[151], S. Jones[7], T.J. Jones[77], J. Jongmanns[60a], P.M. Jorge[128a,128b],
J. Jovicevic[163a], X. Ju[176], A. Juste Rozas[13,v], M.K. Köhler[175], A. Kaczmarska[42], M. Kado[119],
H. Kagan[113], M. Kagan[145], S.J. Kahn[88], T. Kaji[174], E. Kajomovitz[48], C.W. Kalderon[84],
A. Kaluza[86], S. Kama[43], A. Kamenshchikov[132], N. Kanaya[157], L. Kanjir[78], V.A. Kantserov[100],
J. Kanzaki[69], B. Kaplan[112], L.S. Kaplan[176], D. Kar[147c], K. Karakostas[10], N. Karastathis[10],
M.J. Kareem[57], E. Karentzos[10], S.N. Karpov[68], Z.M. Karpova[68], K. Karthik[112],
V. Kartvelishvili[75], A.N. Karyukhin[132], K. Kasahara[164], L. Kashif[176], R.D. Kass[113],
A. Kastanas[149], Y. Kataoka[157], C. Kato[157], A. Katre[52], J. Katzy[45], K. Kawade[70], K. Kawagoe[73],
T. Kawamoto[157], G. Kawamura[57], E.F. Kay[77], V.F. Kazanin[111,c], R. Keeler[172], R. Kehoe[43],
J.S. Keller[31], J.J. Kempster[80], J Kendrick[19], H. Keoshkerian[161], O. Kepka[129], B.P. Kerševan[78],
S. Kersten[178], R.A. Keyes[90], M. Khader[169], F. Khalil-zada[12], A. Khanov[116], A.G. Kharlamov[111,c],
T. Kharlamova[111,c], A. Khodinov[160], T.J. Khoo[52], V. Khovanskiy[99,*], E. Khramov[68],
J. Khubua[54b,ad], S. Kido[70], C.R. Kilby[80], H.Y. Kim[8], S.H. Kim[164], Y.K. Kim[33], N. Kimura[156],
O.M. Kind[17], B.T. King[77], D. Kirchmeier[47], J. Kirk[133], A.E. Kiryunin[103], T. Kishimoto[157],
D. Kisielewska[41a], V. Kitali[45], K. Kiuchi[164], O. Kivernyk[5], E. Kladiva[146b],
T. Klapdor-Kleingrothaus[51], M.H. Klein[92], M. Klein[77], U. Klein[77], K. Kleinknecht[86],
P. Klimek[110], A. Klimentov[27], R. Klingenberg[46], T. Klingl[23], T. Klioutchnikova[32], E.-E. Kluge[60a],
P. Kluit[109], S. Kluth[103], E. Kneringer[65], E.B.F.G. Knoops[88], A. Knue[103], A. Kobayashi[157],
D. Kobayashi[159], T. Kobayashi[157], M. Kobel[47], M. Kocian[145], P. Kodys[131], T. Koffas[31],
E. Koffeman[109], N.M. Köhler[103], T. Koi[145], M. Kolb[60b], I. Koletsou[5], A.A. Komar[98,*],
Y. Komori[157], T. Kondo[69], N. Kondrashova[36c], K. Köneke[51], A.C. König[108], T. Kono[69,ae],
R. Konoplich[112,af], N. Konstantinidis[81], R. Kopeliansky[64], S. Koperny[41a], A.K. Kopp[51],
K. Korcyl[42], K. Kordas[156], A. Korn[81], A.A. Korol[111,c], I. Korolkov[13], E.V. Korolkova[141],
O. Kortner[103], S. Kortner[103], T. Kosek[131], V.V. Kostyukhin[23], A. Kotwal[48], A. Koulouris[10],
A. Kourkoumeli-Charalampidi[123a,123b], C. Kourkoumelis[9], E. Kourlitis[141], V. Kouskoura[27],

A.B. Kowalewska[42], R. Kowalewski[172], T.Z. Kowalski[41a], C. Kozakai[157], W. Kozanecki[138],
A.S. Kozhin[132], V.A. Kramarenko[101], G. Kramberger[78], D. Krasnopevtsev[100], M.W. Krasny[83],
A. Krasznahorkay[32], D. Krauss[103], J.A. Kremer[41a], J. Kretzschmar[77], K. Kreutzfeldt[55],
P. Krieger[161], K. Krizka[33], K. Kroeninger[46], H. Kroha[103], J. Kroll[129], J. Kroll[124], J. Kroseberg[23],
J. Krstic[14], U. Kruchonak[68], H. Krüger[23], N. Krumnack[67], M.C. Kruse[48], T. Kubota[91],
H. Kucuk[81], S. Kuday[4b], J.T. Kuechler[178], S. Kuehn[32], A. Kugel[60a], F. Kuger[177], T. Kuhl[45],
V. Kukhtin[68], R. Kukla[88], Y. Kulchitsky[95], S. Kuleshov[34b], Y.P. Kulinich[169], M. Kuna[134a,134b],
T. Kunigo[71], A. Kupco[129], T. Kupfer[46], O. Kuprash[155], H. Kurashige[70], L.L. Kurchaninov[163a],
Y.A. Kurochkin[95], M.G. Kurth[35a,35d], V. Kus[129], E.S. Kuwertz[172], M. Kuze[159], J. Kvita[117],
T. Kwan[172], D. Kyriazopoulos[141], A. La Rosa[103], J.L. La Rosa Navarro[26d], L. La Rotonda[40a,40b],
F. La Ruffa[40a,40b], C. Lacasta[170], F. Lacava[134a,134b], J. Lacey[45], H. Lacker[17], D. Lacour[83],
E. Ladygin[68], R. Lafaye[5], B. Laforge[83], T. Lagouri[179], S. Lai[57], S. Lammers[64], W. Lampl[7],
E. Lançon[27], U. Landgraf[51], M.P.J. Landon[79], M.C. Lanfermann[52], V.S. Lang[60a], J.C. Lange[13],
R.J. Langenberg[32], A.J. Lankford[166], F. Lanni[27], K. Lantzsch[23], A. Lanza[123a],
A. Lapertosa[53a,53b], S. Laplace[83], J.F. Laporte[138], T. Lari[94a], F. Lasagni Manghi[22a,22b],
M. Lassnig[32], P. Laurelli[50], W. Lavrijsen[16], A.T. Law[139], P. Laycock[77], T. Lazovich[59],
M. Lazzaroni[94a,94b], B. Le[91], O. Le Dortz[83], E. Le Guirriec[88], E.P. Le Quilleuc[138], M. LeBlanc[172],
T. LeCompte[6], F. Ledroit-Guillon[58], C.A. Lee[27], G.R. Lee[133,ag], S.C. Lee[153], L. Lee[59],
B. Lefebvre[90], G. Lefebvre[83], M. Lefebvre[172], F. Legger[102], C. Leggett[16], G. Lehmann Miotto[32],
X. Lei[7], W.A. Leight[45], M.A.L. Leite[26d], R. Leitner[131], D. Lellouch[175], B. Lemmer[57],
K.J.C. Leney[81], T. Lenz[23], B. Lenzi[32], R. Leone[7], S. Leone[126a,126b], C. Leonidopoulos[49],
G. Lerner[151], C. Leroy[97], A.A.J. Lesage[138], C.G. Lester[30], M. Levchenko[125], J. Levêque[5],
D. Levin[92], L.J. Levinson[175], M. Levy[19], D. Lewis[79], B. Li[36a,w], C.-Q. Li[36a], H. Li[150], L. Li[36c],
Q. Li[35a,35d], S. Li[48], X. Li[36c], Y. Li[143], Z. Liang[35a], B. Liberti[135a], A. Liblong[161], K. Lie[62c],
J. Liebal[23], W. Liebig[15], A. Limosani[152], S.C. Lin[182], T.H. Lin[86], R.A. Linck[64], B.E. Lindquist[150],
A.E. Lionti[52], E. Lipeles[124], A. Lipniacka[15], M. Lisovyi[60b], T.M. Liss[169,ah], A. Lister[171],
A.M. Litke[139], B. Liu[153,ai], H. Liu[92], H. Liu[27], J.K.K. Liu[122], J. Liu[36b], J.B. Liu[36a], K. Liu[88],
L. Liu[169], M. Liu[36a], Y.L. Liu[36a], Y. Liu[36a], M. Livan[123a,123b], A. Lleres[58], J. Llorente Merino[35a],
S.L. Lloyd[79], C.Y. Lo[62b], F. Lo Sterzo[153], E.M. Lobodzinska[45], P. Loch[7], F.K. Loebinger[87],
A. Loesle[51], K.M. Loew[25], A. Loginov[179,*], T. Lohse[17], K. Lohwasser[141], M. Lokajicek[129],
B.A. Long[24], J.D. Long[169], R.E. Long[75], L. Longo[76a,76b], K.A. Looper[113], J.A. Lopez[34b],
D. Lopez Mateos[59], I. Lopez Paz[13], A. Lopez Solis[83], J. Lorenz[102], N. Lorenzo Martinez[5],
M. Losada[21], P.J. Lösel[102], X. Lou[35a], A. Lounis[119], J. Love[6], P.A. Love[75], H. Lu[62a], N. Lu[92],
Y.J. Lu[63], H.J. Lubatti[140], C. Luci[134a,134b], A. Lucotte[58], C. Luedtke[51], F. Luehring[64],
W. Lukas[65], L. Luminari[134a], O. Lundberg[148a,148b], B. Lund-Jensen[149], M.S. Lutz[89], P.M. Luzi[83],
D. Lynn[27], R. Lysak[129], E. Lytken[84], F. Lyu[35a], V. Lyubushkin[68], H. Ma[27], L.L. Ma[36b],
Y. Ma[36b], G. Maccarrone[50], A. Macchiolo[103], C.M. Macdonald[141], B. Maček[78],
J. Machado Miguens[124,128b], D. Madaffari[170], R. Madar[37], W.F. Mader[47], A. Madsen[45],
J. Maeda[70], S. Maeland[15], T. Maeno[27], A.S. Maevskiy[101], V. Magerl[51], J. Mahlstedt[109],
C. Maiani[119], C. Maidantchik[26a], A.A. Maier[103], T. Maier[102], A. Maio[128a,128b,128d],
O. Majersky[146a], S. Majewski[118], Y. Makida[69], N. Makovec[119], B. Malaescu[83], Pa. Malecki[42],
V.P. Maleev[125], F. Malek[58], U. Mallik[66], D. Malon[6], C. Malone[30], S. Maltezos[10], S. Malyukov[32],
J. Mamuzic[170], G. Mancini[50], I. Mandić[78], J. Maneira[128a,128b], L. Manhaes de Andrade Filho[26b],
J. Manjarres Ramos[47], K.H. Mankinen[84], A. Mann[102], A. Manousos[32], B. Mansoulie[138],
J.D. Mansour[35a], R. Mantifel[90], M. Mantoani[57], S. Manzoni[94a,94b], L. Mapelli[32], G. Marceca[29],
L. March[52], L. Marchese[122], G. Marchiori[83], M. Marcisovsky[129], M. Marjanovic[37], D.E. Marley[92],
F. Marroquim[26a], S.P. Marsden[87], Z. Marshall[16], M.U.F Martensson[168], S. Marti-Garcia[170],
C.B. Martin[113], T.A. Martin[173], V.J. Martin[49], B. Martin dit Latour[15], M. Martinez[13,v],

V.I. Martinez Outschoorn[169], S. Martin-Haugh[133], V.S. Martoiu[28b], A.C. Martyniuk[81],
A. Marzin[32], L. Masetti[86], T. Mashimo[157], R. Mashinistov[98], J. Masik[87], A.L. Maslennikov[111,c],
L. Massa[135a,135b], P. Mastrandrea[5], A. Mastroberardino[40a,40b], T. Masubuchi[157], P. Mättig[178],
J. Maurer[28b], S.J. Maxfield[77], D.A. Maximov[111,c], R. Mazini[153], I. Maznas[156], S.M. Mazza[94a,94b],
N.C. Mc Fadden[107], G. Mc Goldrick[161], S.P. Mc Kee[92], A. McCarn[92], R.L. McCarthy[150],
T.G. McCarthy[103], L.I. McClymont[81], E.F. McDonald[91], J.A. Mcfayden[81], G. Mchedlidze[57],
S.J. McMahon[133], P.C. McNamara[91], R.A. McPherson[172,o], S. Meehan[140], T.J. Megy[51],
S. Mehlhase[102], A. Mehta[77], T. Meideck[58], K. Meier[60a], B. Meirose[44], D. Melini[170,aj],
B.R. Mellado Garcia[147c], J.D. Mellenthin[57], M. Melo[146a], F. Meloni[18], A. Melzer[23],
S.B. Menary[87], L. Meng[77], X.T. Meng[92], A. Mengarelli[22a,22b], S. Menke[103], E. Meoni[40a,40b],
S. Mergelmeyer[17], P. Mermod[52], L. Merola[106a,106b], C. Meroni[94a], F.S. Merritt[33],
A. Messina[134a,134b], J. Metcalfe[6], A.S. Mete[166], C. Meyer[124], J-P. Meyer[138], J. Meyer[109],
H. Meyer Zu Theenhausen[60a], F. Miano[151], R.P. Middleton[133], S. Miglioranzi[53a,53b], L. Mijović[49],
G. Mikenberg[175], M. Mikestikova[129], M. Mikuž[78], M. Milesi[91], A. Milic[161], D.W. Miller[33],
C. Mills[49], A. Milov[175], D.A. Milstead[148a,148b], A.A. Minaenko[132], Y. Minami[157],
I.A. Minashvili[54b], A.I. Mincer[112], B. Mindur[41a], M. Mineev[68], Y. Minegishi[157], Y. Ming[176],
L.M. Mir[13], K.P. Mistry[124], T. Mitani[174], J. Mitrevski[102], V.A. Mitsou[170], A. Miucci[18],
P.S. Miyagawa[141], A. Mizukami[69], J.U. Mjörnmark[84], T. Mkrtchyan[180], M. Mlynarikova[131],
T. Moa[148a,148b], K. Mochizuki[97], P. Mogg[51], S. Mohapatra[38], S. Molander[148a,148b],
R. Moles-Valls[23], R. Monden[71], M.C. Mondragon[93], K. Mönig[45], J. Monk[39], E. Monnier[88],
A. Montalbano[150], J. Montejo Berlingen[32], F. Monticelli[74], S. Monzani[94a,94b], R.W. Moore[3],
N. Morange[119], D. Moreno[21], M. Moreno Llácer[32], P. Morettini[53a], S. Morgenstern[32], D. Mori[144],
T. Mori[157], M. Morii[59], M. Morinaga[157], V. Morisbak[121], A.K. Morley[32], G. Mornacchi[32],
J.D. Morris[79], L. Morvaj[150], P. Moschovakos[10], M. Mosidze[54b], H.J. Moss[141], J. Moss[145,ak],
K. Motohashi[159], R. Mount[145], E. Mountricha[27], E.J.W. Moyse[89], S. Muanza[88], F. Mueller[103],
J. Mueller[127], R.S.P. Mueller[102], D. Muenstermann[75], P. Mullen[56], G.A. Mullier[18],
F.J. Munoz Sanchez[87], W.J. Murray[173,133], H. Musheghyan[32], M. Muškinja[78],
A.G. Myagkov[132,al], M. Myska[130], B.P. Nachman[16], O. Nackenhorst[52], K. Nagai[122],
R. Nagai[69,ae], K. Nagano[69], Y. Nagasaka[61], K. Nagata[164], M. Nagel[51], E. Nagy[88], A.M. Nairz[32],
Y. Nakahama[105], K. Nakamura[69], T. Nakamura[157], I. Nakano[114], R.F. Naranjo Garcia[45],
R. Narayan[11], D.I. Narrias Villar[60a], I. Naryshkin[125], T. Naumann[45], G. Navarro[21], R. Nayyar[7],
H.A. Neal[92], P.Yu. Nechaeva[98], T.J. Neep[138], A. Negri[123a,123b], M. Negrini[22a], S. Nektarijevic[108],
C. Nellist[119], A. Nelson[166], M.E. Nelson[122], S. Nemecek[129], P. Nemethy[112], M. Nessi[32,am],
M.S. Neubauer[169], M. Neumann[178], P.R. Newman[19], T.Y. Ng[62c], T. Nguyen Manh[97],
R.B. Nickerson[122], R. Nicolaidou[138], J. Nielsen[139], V. Nikolaenko[132,al], I. Nikolic-Audit[83],
K. Nikolopoulos[19], J.K. Nilsen[121], P. Nilsson[27], Y. Ninomiya[157], A. Nisati[134a], N. Nishu[35c],
R. Nisius[103], I. Nitsche[46], T. Nitta[174], T. Nobe[157], Y. Noguchi[71], M. Nomachi[120], I. Nomidis[31],
M.A. Nomura[27], T. Nooney[79], M. Nordberg[32], N. Norjoharuddeen[122], O. Novgorodova[47],
M. Nozaki[69], L. Nozka[117], K. Ntekas[166], E. Nurse[81], F. Nuti[91], K. O'connor[25], D.C. O'Neil[144],
A.A. O'Rourke[45], V. O'Shea[56], F.G. Oakham[31,d], H. Oberlack[103], T. Obermann[23], J. Ocariz[83],
A. Ochi[70], I. Ochoa[38], J.P. Ochoa-Ricoux[34a], S. Oda[73], S. Odaka[69], A. Oh[87], S.H. Oh[48],
C.C. Ohm[16], H. Ohman[168], H. Oide[53a,53b], H. Okawa[164], Y. Okumura[157], T. Okuyama[69],
A. Olariu[28b], L.F. Oleiro Seabra[128a], S.A. Olivares Pino[49], D. Oliveira Damazio[27], A. Olszewski[42],
J. Olszowska[42], A. Onofre[128a,128e], K. Onogi[105], P.U.E. Onyisi[11,aa], H. Oppen[121], M.J. Oreglia[33],
Y. Oren[155], D. Orestano[136a,136b], N. Orlando[62b], R.S. Orr[161], B. Osculati[53a,53b,*], R. Ospanov[36a],
G. Otero y Garzon[29], H. Otono[73], M. Ouchrif[137d], F. Ould-Saada[121], A. Ouraou[138],
K.P. Oussoren[109], Q. Ouyang[35a], M. Owen[56], R.E. Owen[19], V.E. Ozcan[20a], N. Ozturk[8],
K. Pachal[144], A. Pacheco Pages[13], L. Pacheco Rodriguez[138], C. Padilla Aranda[13],

S. Pagan Griso[16], M. Paganini[179], F. Paige[27], G. Palacino[64], S. Palazzo[40a,40b], S. Palestini[32],
M. Palka[41b], D. Pallin[37], E.St. Panagiotopoulou[10], I. Panagoulias[10], C.E. Pandini[83],
J.G. Panduro Vazquez[80], P. Pani[32], S. Panitkin[27], D. Pantea[28b], L. Paolozzi[52],
Th.D. Papadopoulou[10], K. Papageorgiou[9,s], A. Paramonov[6], D. Paredes Hernandez[179],
A.J. Parker[75], M.A. Parker[30], K.A. Parker[45], F. Parodi[53a,53b], J.A. Parsons[38], U. Parzefall[51],
V.R. Pascuzzi[161], J.M. Pasner[139], E. Pasqualucci[134a], S. Passaggio[53a], Fr. Pastore[80],
S. Pataraia[86], J.R. Pater[87], T. Pauly[32], B. Pearson[103], S. Pedraza Lopez[170], R. Pedro[128a,128b],
S.V. Peleganchuk[111,c], O. Penc[129], C. Peng[35a,35d], H. Peng[36a], J. Penwell[64], B.S. Peralva[26b],
M.M. Perego[138], D.V. Perepelitsa[27], F. Peri[17], L. Perini[94a,94b], H. Pernegger[32],
S. Perrella[106a,106b], R. Peschke[45], V.D. Peshekhonov[68,*], K. Peters[45], R.F.Y. Peters[87],
B.A. Petersen[32], T.C. Petersen[39], E. Petit[58], A. Petridis[1], C. Petridou[156], P. Petroff[119],
E. Petrolo[134a], M. Petrov[122], F. Petrucci[136a,136b], N.E. Pettersson[89], A. Peyaud[138], R. Pezoa[34b],
F.H. Phillips[93], P.W. Phillips[133], G. Piacquadio[150], E. Pianori[173], A. Picazio[89], E. Piccaro[79],
M.A. Pickering[122], R. Piegaia[29], J.E. Pilcher[33], A.D. Pilkington[87], A.W.J. Pin[87],
M. Pinamonti[135a,135b], J.L. Pinfold[3], H. Pirumov[45], M. Pitt[175], L. Plazak[146a], M.-A. Pleier[27],
V. Pleskot[86], E. Plotnikova[68], D. Pluth[67], P. Podberezko[111], R. Poettgen[148a,148b],
R. Poggi[123a,123b], L. Poggioli[119], D. Pohl[23], G. Polesello[123a], A. Poley[45], A. Policicchio[40a,40b],
R. Polifka[32], A. Polini[22a], C.S. Pollard[56], V. Polychronakos[27], K. Pommès[32], D. Ponomarenko[100],
L. Pontecorvo[134a], G.A. Popeneciu[28d], A. Poppleton[32], S. Pospisil[130], K. Potamianos[16],
I.N. Potrap[68], C.J. Potter[30], G. Poulard[32], T. Poulsen[84], J. Poveda[32], M.E. Pozo Astigarraga[32],
P. Pralavorio[88], A. Pranko[16], S. Prell[67], D. Price[87], M. Primavera[76a], S. Prince[90], N. Proklova[100],
K. Prokofiev[62c], F. Prokoshin[34b], S. Protopopescu[27], J. Proudfoot[6], M. Przybycien[41a], A. Puri[169],
P. Puzo[119], J. Qian[92], G. Qin[56], Y. Qin[87], A. Quadt[57], M. Queitsch-Maitland[45], D. Quilty[56],
S. Raddum[121], V. Radeka[27], V. Radescu[122], S.K. Radhakrishnan[150], P. Radloff[118], P. Rados[91],
F. Ragusa[94a,94b], G. Rahal[181], J.A. Raine[87], S. Rajagopalan[27], C. Rangel-Smith[168], T. Rashid[119],
S. Raspopov[5], M.G. Ratti[94a,94b], D.M. Rauch[45], F. Rauscher[102], S. Rave[86], I. Ravinovich[175],
J.H. Rawling[87], M. Raymond[32], A.L. Read[121], N.P. Readioff[58], M. Reale[76a,76b],
D.M. Rebuzzi[123a,123b], A. Redelbach[177], G. Redlinger[27], R. Reece[139], R.G. Reed[147c], K. Reeves[44],
L. Rehnisch[17], J. Reichert[124], A. Reiss[86], C. Rembser[32], H. Ren[35a,35d], M. Rescigno[134a],
S. Resconi[94a], E.D. Resseguie[124], S. Rettie[171], E. Reynolds[19], O.L. Rezanova[111,c], P. Reznicek[131],
R. Rezvani[97], R. Richter[103], S. Richter[81], E. Richter-Was[41b], O. Ricken[23], M. Ridel[83], P. Rieck[103],
C.J. Riegel[178], J. Rieger[57], O. Rifki[115], M. Rijssenbeek[150], A. Rimoldi[123a,123b], M. Rimoldi[18],
L. Rinaldi[22a], G. Ripellino[149], B. Ristić[32], E. Ritsch[32], I. Riu[13], F. Rizatdinova[116], E. Rizvi[79],
C. Rizzi[13], R.T. Roberts[87], S.H. Robertson[90,o], A. Robichaud-Veronneau[90], D. Robinson[30],
J.E.M. Robinson[45], A. Robson[56], E. Rocco[86], C. Roda[126a,126b], Y. Rodina[88,an],
S. Rodriguez Bosca[170], A. Rodriguez Perez[13], D. Rodriguez Rodriguez[170], S. Roe[32], C.S. Rogan[59],
O. Røhne[121], J. Roloff[59], A. Romaniouk[100], M. Romano[22a,22b], S.M. Romano Saez[37],
E. Romero Adam[170], N. Rompotis[77], M. Ronzani[51], L. Roos[83], S. Rosati[134a], K. Rosbach[51],
P. Rose[139], N.-A. Rosien[57], E. Rossi[106a,106b], L.P. Rossi[53a], J.H.N. Rosten[30], R. Rosten[140],
M. Rotaru[28b], J. Rothberg[140], D. Rousseau[119], A. Rozanov[88], Y. Rozen[154], X. Ruan[147c],
F. Rubbo[145], F. Rühr[51], A. Ruiz-Martinez[31], Z. Rurikova[51], N.A. Rusakovich[68], H.L. Russell[90],
J.P. Rutherfoord[7], N. Ruthmann[32], Y.F. Ryabov[125], M. Rybar[169], G. Rybkin[119], S. Ryu[6],
A. Ryzhov[132], G.F. Rzehorz[57], A.F. Saavedra[152], G. Sabato[109], S. Sacerdoti[29],
H.F-W. Sadrozinski[139], R. Sadykov[68], F. Safai Tehrani[134a], P. Saha[110], M. Sahinsoy[60a],
M. Saimpert[45], M. Saito[157], T. Saito[157], H. Sakamoto[157], Y. Sakurai[174], G. Salamanna[136a,136b],
J.E. Salazar Loyola[34b], D. Salek[109], P.H. Sales De Bruin[168], D. Salihagic[103], A. Salnikov[145],
J. Salt[170], D. Salvatore[40a,40b], F. Salvatore[151], A. Salvucci[62a,62b,62c], A. Salzburger[32],
D. Sammel[51], D. Sampsonidis[156], D. Sampsonidou[156], J. Sánchez[170], V. Sanchez Martinez[170],

A. Sanchez Pineda[167a,167c], H. Sandaker[121], R.L. Sandbach[79], C.O. Sander[45], M. Sandhoff[178],
C. Sandoval[21], D.P.C. Sankey[133], M. Sannino[53a,53b], Y. Sano[105], A. Sansoni[50], C. Santoni[37],
H. Santos[128a], I. Santoyo Castillo[151], A. Sapronov[68], J.G. Saraiva[128a,128d], B. Sarrazin[23],
O. Sasaki[69], K. Sato[164], E. Sauvan[5], G. Savage[80], P. Savard[161,d], N. Savic[103], C. Sawyer[133],
L. Sawyer[82,u], J. Saxon[33], C. Sbarra[22a], A. Sbrizzi[22a,22b], T. Scanlon[81], D.A. Scannicchio[166],
M. Scarcella[152], J. Schaarschmidt[140], P. Schacht[103], B.M. Schachtner[102], D. Schaefer[32],
L. Schaefer[124], R. Schaefer[45], J. Schaeffer[86], S. Schaepe[23], S. Schaetzel[60b], U. Schäfer[86],
A.C. Schaffer[119], D. Schaile[102], R.D. Schamberger[150], V.A. Schegelsky[125], D. Scheirich[131],
M. Schernau[166], C. Schiavi[53a,53b], S. Schier[139], L.K. Schildgen[23], C. Schillo[51], M. Schioppa[40a,40b],
S. Schlenker[32], K.R. Schmidt-Sommerfeld[103], K. Schmieden[32], C. Schmitt[86], S. Schmitt[45],
S. Schmitz[86], U. Schnoor[51], L. Schoeffel[138], A. Schoening[60b], B.D. Schoenrock[93], E. Schopf[23],
M. Schott[86], J.F.P. Schouwenberg[108], J. Schovancova[32], S. Schramm[52], N. Schuh[86], A. Schulte[86],
M.J. Schultens[23], H.-C. Schultz-Coulon[60a], H. Schulz[17], M. Schumacher[51], B.A. Schumm[139],
Ph. Schune[138], A. Schwartzman[145], T.A. Schwarz[92], H. Schweiger[87], Ph. Schwemling[138],
R. Schwienhorst[93], J. Schwindling[138], A. Sciandra[23], G. Sciolla[25], M. Scornajenghi[40a,40b],
F. Scuri[126a,126b], F. Scutti[91], J. Searcy[92], P. Seema[23], S.C. Seidel[107], A. Seiden[139], J.M. Seixas[26a],
G. Sekhniaidze[106a], K. Sekhon[92], S.J. Sekula[43], N. Semprini-Cesari[22a,22b], S. Senkin[37],
C. Serfon[121], L. Serin[119], L. Serkin[167a,167b], M. Sessa[136a,136b], R. Seuster[172], H. Severini[115],
T. Sfiligoj[78], F. Sforza[32], A. Sfyrla[52], E. Shabalina[57], N.W. Shaikh[148a,148b], L.Y. Shan[35a],
R. Shang[169], J.T. Shank[24], M. Shapiro[16], P.B. Shatalov[99], K. Shaw[167a,167b], S.M. Shaw[87],
A. Shcherbakova[148a,148b], C.Y. Shehu[151], Y. Shen[115], N. Sherafati[31], P. Sherwood[81], L. Shi[153,ao],
S. Shimizu[70], C.O. Shimmin[179], M. Shimojima[104], I.P.J. Shipsey[122], S. Shirabe[73],
M. Shiyakova[68,ap], J. Shlomi[175], A. Shmeleva[98], D. Shoaleh Saadi[97], M.J. Shochet[33], S. Shojaii[94a],
D.R. Shope[115], S. Shrestha[113], E. Shulga[100], M.A. Shupe[7], P. Sicho[129], A.M. Sickles[169],
P.E. Sidebo[149], E. Sideras Haddad[147c], O. Sidiropoulou[177], A. Sidoti[22a,22b], F. Siegert[47],
Dj. Sijacki[14], J. Silva[128a,128d], S.B. Silverstein[148a], V. Simak[130], L. Simic[14], S. Simion[119],
E. Simioni[86], B. Simmons[81], M. Simon[86], P. Sinervo[161], N.B. Sinev[118], M. Sioli[22a,22b],
G. Siragusa[177], I. Siral[92], S.Yu. Sivoklokov[101], J. Sjölin[148a,148b], M.B. Skinner[75], P. Skubic[115],
M. Slater[19], T. Slavicek[130], M. Slawinska[42], K. Sliwa[165], R. Slovak[131], V. Smakhtin[175],
B.H. Smart[5], J. Smiesko[146a], N. Smirnov[100], S.Yu. Smirnov[100], Y. Smirnov[100],
L.N. Smirnova[101,aq], O. Smirnova[84], J.W. Smith[57], M.N.K. Smith[38], R.W. Smith[38],
M. Smizanska[75], K. Smolek[130], A.A. Snesarev[98], I.M. Snyder[118], S. Snyder[27], R. Sobie[172,o],
F. Socher[47], A. Soffer[155], A. Søgaard[49], D.A. Soh[153], G. Sokhrannyi[78], C.A. Solans Sanchez[32],
M. Solar[130], E.Yu. Soldatov[100], U. Soldevila[170], A.A. Solodkov[132], A. Soloshenko[68],
O.V. Solovyanov[132], V. Solovyev[125], P. Sommer[51], H. Son[165], A. Sopczak[130], D. Sosa[60b],
C.L. Sotiropoulou[126a,126b], R. Soualah[167a,167c], A.M. Soukharev[111,c], D. South[45], B.C. Sowden[80],
S. Spagnolo[76a,76b], M. Spalla[126a,126b], M. Spangenberg[173], F. Spanò[80], D. Sperlich[17],
F. Spettel[103], T.M. Spieker[60a], R. Spighi[22a], G. Spigo[32], L.A. Spiller[91], M. Spousta[131],
R.D. St. Denis[56,*], A. Stabile[94a], R. Stamen[60a], S. Stamm[17], E. Stanecka[42], R.W. Stanek[6],
C. Stanescu[136a], M.M. Stanitzki[45], B.S. Stapf[109], S. Stapnes[121], E.A. Starchenko[132], G.H. Stark[33],
J. Stark[58], S.H Stark[39], P. Staroba[129], P. Starovoitov[60a], S. Stärz[32], R. Staszewski[42],
P. Steinberg[27], B. Stelzer[144], H.J. Stelzer[32], O. Stelzer-Chilton[163a], H. Stenzel[55], G.A. Stewart[56],
M.C. Stockton[118], M. Stoebe[90], G. Stoicea[28b], P. Stolte[57], S. Stonjek[103], A.R. Stradling[8],
A. Straessner[47], M.E. Stramaglia[18], J. Strandberg[149], S. Strandberg[148a,148b], M. Strauss[115],
P. Strizenec[146b], R. Ströhmer[177], D.M. Strom[118], R. Stroynowski[43], A. Strubig[49], S.A. Stucci[27],
B. Stugu[15], N.A. Styles[45], D. Su[145], J. Su[127], S. Suchek[60a], Y. Sugaya[120], M. Suk[130],
V.V. Sulin[98], DMS Sultan[162a,162b], S. Sultansoy[4c], T. Sumida[71], S. Sun[59], X. Sun[3], K. Suruliz[151],
C.J.E. Suster[152], M.R. Sutton[151], S. Suzuki[69], M. Svatos[129], M. Swiatlowski[33], S.P. Swift[2],

I. Sykora[146a], T. Sykora[131], D. Ta[51], K. Tackmann[45], J. Taenzer[155], A. Taffard[166],
R. Tafirout[163a], N. Taiblum[155], H. Takai[27], R. Takashima[72], E.H. Takasugi[103], T. Takeshita[142],
Y. Takubo[69], M. Talby[88], A.A. Talyshev[111,c], J. Tanaka[157], M. Tanaka[159], R. Tanaka[119],
S. Tanaka[69], R. Tanioka[70], B.B. Tannenwald[113], S. Tapia Araya[34b], S. Tapprogge[86], S. Tarem[154],
G.F. Tartarelli[94a], P. Tas[131], M. Tasevsky[129], T. Tashiro[71], E. Tassi[40a,40b],
A. Tavares Delgado[128a,128b], Y. Tayalati[137e], A.C. Taylor[107], G.N. Taylor[91], P.T.E. Taylor[91],
W. Taylor[163b], P. Teixeira-Dias[80], D. Temple[144], H. Ten Kate[32], P.K. Teng[153], J.J. Teoh[120],
F. Tepel[178], S. Terada[69], K. Terashi[157], J. Terron[85], S. Terzo[13], M. Testa[50], R.J. Teuscher[161,o],
T. Theveneaux-Pelzer[88], F. Thiele[39], J.P. Thomas[19], J. Thomas-Wilsker[80], P.D. Thompson[19],
A.S. Thompson[56], L.A. Thomsen[179], E. Thomson[124], M.J. Tibbetts[16], R.E. Ticse Torres[88],
V.O. Tikhomirov[98,ar], Yu.A. Tikhonov[111,c], S. Timoshenko[100], P. Tipton[179], S. Tisserant[88],
K. Todome[159], S. Todorova-Nova[5], S. Todt[47], J. Tojo[73], S. Tokár[146a], K. Tokushuku[69],
E. Tolley[113], L. Tomlinson[87], M. Tomoto[105], L. Tompkins[145,as], K. Toms[107], B. Tong[59],
P. Tornambe[51], E. Torrence[118], H. Torres[144], E. Torró Pastor[140], J. Toth[88,at], F. Touchard[88],
D.R. Tovey[141], C.J. Treado[112], T. Trefzger[177], F. Tresoldi[151], A. Tricoli[27], I.M. Trigger[163a],
S. Trincaz-Duvoid[83], M.F. Tripiana[13], W. Trischuk[161], B. Trocmé[58], A. Trofymov[45],
C. Troncon[94a], M. Trottier-McDonald[16], M. Trovatelli[172], L. Truong[147b], M. Trzebinski[42],
A. Trzupek[42], K.W. Tsang[62a], J.C-L. Tseng[122], P.V. Tsiareshka[95], G. Tsipolitis[10],
N. Tsirintanis[9], S. Tsiskaridze[13], V. Tsiskaridze[51], E.G. Tskhadadze[54a], K.M. Tsui[62a],
I.I. Tsukerman[99], V. Tsulaia[16], S. Tsuno[69], D. Tsybychev[150], Y. Tu[62b], A. Tudorache[28b],
V. Tudorache[28b], T.T. Tulbure[28a], A.N. Tuna[59], S.A. Tupputi[22a,22b], S. Turchikhin[68],
D. Turgeman[175], I. Turk Cakir[4b,au], R. Turra[94a], P.M. Tuts[38], G. Ucchielli[22a,22b], I. Ueda[69],
M. Ughetto[148a,148b], F. Ukegawa[164], G. Unal[32], A. Undrus[27], G. Unel[166], F.C. Ungaro[91],
Y. Unno[69], C. Unverdorben[102], J. Urban[146b], P. Urquijo[91], P. Urrejola[86], G. Usai[8], J. Usui[69],
L. Vacavant[88], V. Vacek[130], B. Vachon[90], K.O.H. Vadla[121], A. Vaidya[81], C. Valderanis[102],
E. Valdes Santurio[148a,148b], S. Valentinetti[22a,22b], A. Valero[170], L. Valéry[13], S. Valkar[131],
A. Vallier[5], J.A. Valls Ferrer[170], W. Van Den Wollenberg[109], H. van der Graaf[109],
P. van Gemmeren[6], J. Van Nieuwkoop[144], I. van Vulpen[109], M.C. van Woerden[109],
M. Vanadia[135a,135b], W. Vandelli[32], A. Vaniachine[160], P. Vankov[109], G. Vardanyan[180], R. Vari[134a],
E.W. Varnes[7], C. Varni[53a,53b], T. Varol[43], D. Varouchas[119], A. Vartapetian[8], K.E. Varvell[152],
J.G. Vasquez[179], G.A. Vasquez[34b], F. Vazeille[37], T. Vazquez Schroeder[90], J. Veatch[57],
V. Veeraraghavan[7], L.M. Veloce[161], F. Veloso[128a,128c], S. Veneziano[134a], A. Ventura[76a,76b],
M. Venturi[172], N. Venturi[32], A. Venturini[25], V. Vercesi[123a], M. Verducci[136a,136b], W. Verkerke[109],
A.T. Vermeulen[109], J.C. Vermeulen[109], M.C. Vetterli[144,d], N. Viaux Maira[34b], O. Viazlo[84],
I. Vichou[169,*], T. Vickey[141], O.E. Vickey Boeriu[141], G.H.A. Viehhauser[122], S. Viel[16], L. Vigani[122],
M. Villa[22a,22b], M. Villaplana Perez[94a,94b], E. Vilucchi[50], M.G. Vincter[31], V.B. Vinogradov[68],
A. Vishwakarma[45], C. Vittori[22a,22b], I. Vivarelli[151], S. Vlachos[10], M. Vogel[178], P. Vokac[130],
G. Volpi[126a,126b], H. von der Schmitt[103], E. von Toerne[23], V. Vorobel[131], K. Vorobev[100],
M. Vos[170], R. Voss[32], J.H. Vossebeld[77], N. Vranjes[14], M. Vranjes Milosavljevic[14], V. Vrba[130],
M. Vreeswijk[109], R. Vuillermet[32], I. Vukotic[33], P. Wagner[23], W. Wagner[178], J. Wagner-Kuhr[102],
H. Wahlberg[74], S. Wahrmund[47], J. Wakabayashi[105], J. Walder[75], R. Walker[102], W. Walkowiak[143],
V. Wallangen[148a,148b], C. Wang[35b], C. Wang[36b,av], F. Wang[176], H. Wang[16], H. Wang[3],
J. Wang[45], J. Wang[152], Q. Wang[115], R. Wang[6], S.M. Wang[153], T. Wang[38], W. Wang[153,aw],
W. Wang[36a,ax], Z. Wang[36c], C. Wanotayaroj[118], A. Warburton[90], C.P. Ward[30], D.R. Wardrope[81],
A. Washbrook[49], P.M. Watkins[19], A.T. Watson[19], M.F. Watson[19], G. Watts[140], S. Watts[87],
B.M. Waugh[81], A.F. Webb[11], S. Webb[86], M.S. Weber[18], S.W. Weber[177], S.A. Weber[31],
J.S. Webster[6], A.R. Weidberg[122], B. Weinert[64], J. Weingarten[57], M. Weirich[86], C. Weiser[51],
H. Weits[109], P.S. Wells[32], T. Wenaus[27], T. Wengler[32], S. Wenig[32], N. Wermes[23], M.D. Werner[67],

P. Werner[32], M. Wessels[60a], K. Whalen[118], N.L. Whallon[140], A.M. Wharton[75], A.S. White[92],
A. White[8], M.J. White[1], R. White[34b], D. Whiteson[166], B.W. Whitmore[75], F.J. Wickens[133],
W. Wiedenmann[176], M. Wielers[133], C. Wiglesworth[39], L.A.M. Wiik-Fuchs[51], A. Wildauer[103],
F. Wilk[87], H.G. Wilkens[32], H.H. Williams[124], S. Williams[109], C. Willis[93], S. Willocq[89],
J.A. Wilson[19], I. Wingerter-Seez[5], E. Winkels[151], F. Winklmeier[118], O.J. Winston[151],
B.T. Winter[23], M. Wittgen[145], M. Wobisch[82,u], T.M.H. Wolf[109], R. Wolff[88], M.W. Wolter[42],
H. Wolters[128a,128c], V.W.S. Wong[171], S.D. Worm[19], B.K. Wosiek[42], J. Wotschack[32],
K.W. Wozniak[42], M. Wu[33], S.L. Wu[176], X. Wu[52], Y. Wu[92], T.R. Wyatt[87], B.M. Wynne[49],
S. Xella[39], Z. Xi[92], L. Xia[35c], D. Xu[35a], L. Xu[27], T. Xu[138], B. Yabsley[152], S. Yacoob[147a],
D. Yamaguchi[159], Y. Yamaguchi[120], A. Yamamoto[69], S. Yamamoto[157], T. Yamanaka[157],
M. Yamatani[157], K. Yamauchi[105], Y. Yamazaki[70], Z. Yan[24], H. Yang[36c], H. Yang[16], Y. Yang[153],
Z. Yang[15], W-M. Yao[16], Y.C. Yap[83], Y. Yasu[69], E. Yatsenko[5], K.H. Yau Wong[23], J. Ye[43], S. Ye[27],
I. Yeletskikh[68], E. Yigitbasi[24], E. Yildirim[86], K. Yorita[174], K. Yoshihara[124], C. Young[145],
C.J.S. Young[32], J. Yu[8], J. Yu[67], S.P.Y. Yuen[23], I. Yusuff[30,ay], B. Zabinski[42], G. Zacharis[10],
R. Zaidan[13], A.M. Zaitsev[132,al], N. Zakharchuk[45], J. Zalieckas[15], A. Zaman[150], S. Zambito[59],
D. Zanzi[91], C. Zeitnitz[178], G. Zemaityte[122], A. Zemla[41a], J.C. Zeng[169], Q. Zeng[145], O. Zenin[132],
T. Ženiš[146a], D. Zerwas[119], D. Zhang[92], F. Zhang[176], G. Zhang[36a,ax], H. Zhang[35b], J. Zhang[6],
L. Zhang[51], L. Zhang[36a], M. Zhang[169], P. Zhang[35b], R. Zhang[23], R. Zhang[36a,av], X. Zhang[36b],
Y. Zhang[35a,35d], Z. Zhang[119], X. Zhao[43], Y. Zhao[36b,az], Z. Zhao[36a], A. Zhemchugov[68], B. Zhou[92],
C. Zhou[176], L. Zhou[43], M. Zhou[35a,35d], M. Zhou[150], N. Zhou[35c], C.G. Zhu[36b], H. Zhu[35a], J. Zhu[92],
Y. Zhu[36a], X. Zhuang[35a], K. Zhukov[98], A. Zibell[177], D. Zieminska[64], N.I. Zimine[68],
C. Zimmermann[86], S. Zimmermann[51], Z. Zinonos[103], M. Zinser[86], M. Ziolkowski[143], L. Živković[14],
G. Zobernig[176], A. Zoccoli[22a,22b], R. Zou[33], M. zur Nedden[17] and L. Zwalinski[32]

1   *Department of Physics, University of Adelaide, Adelaide, Australia*
2   *Physics Department, SUNY Albany, Albany NY, United States of America*
3   *Department of Physics, University of Alberta, Edmonton AB, Canada*
4   [(a)] *Department of Physics, Ankara University, Ankara;* [(b)] *Istanbul Aydin University, Istanbul;* [(c)]
    *Division of Physics, TOBB University of Economics and Technology, Ankara, Turkey*
5   *LAPP, CNRS/IN2P3 and Université Savoie Mont Blanc, Annecy-le-Vieux, France*
6   *High Energy Physics Division, Argonne National Laboratory, Argonne IL, United States of America*
7   *Department of Physics, University of Arizona, Tucson AZ, United States of America*
8   *Department of Physics, The University of Texas at Arlington, Arlington TX, United States of*
    *America*
9   *Physics Department, National and Kapodistrian University of Athens, Athens, Greece*
10  *Physics Department, National Technical University of Athens, Zografou, Greece*
11  *Department of Physics, The University of Texas at Austin, Austin TX, United States of America*
12  *Institute of Physics, Azerbaijan Academy of Sciences, Baku, Azerbaijan*
13  *Institut de Física d'Altes Energies (IFAE), The Barcelona Institute of Science and Technology,*
    *Barcelona, Spain*
14  *Institute of Physics, University of Belgrade, Belgrade, Serbia*
15  *Department for Physics and Technology, University of Bergen, Bergen, Norway*
16  *Physics Division, Lawrence Berkeley National Laboratory and University of California, Berkeley*
    *CA, United States of America*
17  *Department of Physics, Humboldt University, Berlin, Germany*
18  *Albert Einstein Center for Fundamental Physics and Laboratory for High Energy Physics,*
    *University of Bern, Bern, Switzerland*
19  *School of Physics and Astronomy, University of Birmingham, Birmingham, United Kingdom*
20  [(a)] *Department of Physics, Bogazici University, Istanbul;* [(b)] *Department of Physics Engineering,*
    *Gaziantep University, Gaziantep;* [(d)] *Istanbul Bilgi University, Faculty of Engineering and Natural*

Sciences, Istanbul; [e] *Bahcesehir University, Faculty of Engineering and Natural Sciences, Istanbul, Turkey*

21 *Centro de Investigaciones, Universidad Antonio Narino, Bogota, Colombia*

22 [a] *INFN Sezione di Bologna*; [b] *Dipartimento di Fisica e Astronomia, Università di Bologna, Bologna, Italy*

23 *Physikalisches Institut, University of Bonn, Bonn, Germany*

24 *Department of Physics, Boston University, Boston MA, United States of America*

25 *Department of Physics, Brandeis University, Waltham MA, United States of America*

26 [a] *Universidade Federal do Rio De Janeiro COPPE/EE/IF, Rio de Janeiro*; [b] *Electrical Circuits Department, Federal University of Juiz de Fora (UFJF), Juiz de Fora*; [c] *Federal University of Sao Joao del Rei (UFSJ), Sao Joao del Rei*; [d] *Instituto de Fisica, Universidade de Sao Paulo, Sao Paulo, Brazil*

27 *Physics Department, Brookhaven National Laboratory, Upton NY, United States of America*

28 [a] *Transilvania University of Brasov, Brasov*; [b] *Horia Hulubei National Institute of Physics and Nuclear Engineering, Bucharest*; [c] *Department of Physics, Alexandru Ioan Cuza University of Iasi, Iasi*; [d] *National Institute for Research and Development of Isotopic and Molecular Technologies, Physics Department, Cluj Napoca*; [e] *University Politehnica Bucharest, Bucharest*; [f] *West University in Timisoara, Timisoara, Romania*

29 *Departamento de Física, Universidad de Buenos Aires, Buenos Aires, Argentina*

30 *Cavendish Laboratory, University of Cambridge, Cambridge, United Kingdom*

31 *Department of Physics, Carleton University, Ottawa ON, Canada*

32 *CERN, Geneva, Switzerland*

33 *Enrico Fermi Institute, University of Chicago, Chicago IL, United States of America*

34 [a] *Departamento de Física, Pontificia Universidad Católica de Chile, Santiago*; [b] *Departamento de Física, Universidad Técnica Federico Santa María, Valparaíso, Chile*

35 [a] *Institute of High Energy Physics, Chinese Academy of Sciences, Beijing*; [b] *Department of Physics, Nanjing University, Jiangsu*; [c] *Physics Department, Tsinghua University, Beijing 100084*; [d] *University of Chinese Academy of Science (UCAS), Beijing, China*

36 [a] *Department of Modern Physics and State Key Laboratory of Particle Detection and Electronics, University of Science and Technology of China, Anhui*; [b] *School of Physics, Shandong University, Shandong*; [c] *Department of Physics and Astronomy, Key Laboratory for Particle Physics, Astrophysics and Cosmology, Ministry of Education; Shanghai Key Laboratory for Particle Physics and Cosmology, Shanghai Jiao Tong University, Shanghai(also at PKU-CHEP), China*

37 *Université Clermont Auvergne, CNRS/IN2P3, LPC, Clermont-Ferrand, France*

38 *Nevis Laboratory, Columbia University, Irvington NY, United States of America*

39 *Niels Bohr Institute, University of Copenhagen, Kobenhavn, Denmark*

40 [a] *INFN Gruppo Collegato di Cosenza, Laboratori Nazionali di Frascati*; [b] *Dipartimento di Fisica, Università della Calabria, Rende, Italy*

41 [a] *AGH University of Science and Technology, Faculty of Physics and Applied Computer Science, Krakow*; [b] *Marian Smoluchowski Institute of Physics, Jagiellonian University, Krakow, Poland*

42 *Institute of Nuclear Physics Polish Academy of Sciences, Krakow, Poland*

43 *Physics Department, Southern Methodist University, Dallas TX, United States of America*

44 *Physics Department, University of Texas at Dallas, Richardson TX, United States of America*

45 *DESY, Hamburg and Zeuthen, Germany*

46 *Lehrstuhl für Experimentelle Physik IV, Technische Universität Dortmund, Dortmund, Germany*

47 *Institut für Kern- und Teilchenphysik, Technische Universität Dresden, Dresden, Germany*

48 *Department of Physics, Duke University, Durham NC, United States of America*

49 *SUPA - School of Physics and Astronomy, University of Edinburgh, Edinburgh, United Kingdom*

50 *INFN e Laboratori Nazionali di Frascati, Frascati, Italy*

51 *Fakultät für Mathematik und Physik, Albert-Ludwigs-Universität, Freiburg, Germany*

52 *Departement de Physique Nucleaire et Corpusculaire, Université de Genève, Geneva, Switzerland*

53 [a] *INFN Sezione di Genova*; [b] *Dipartimento di Fisica, Università di Genova, Genova, Italy*

54 (a) *E. Andronikashvili Institute of Physics, Iv. Javakhishvili Tbilisi State University, Tbilisi;* (b) *High Energy Physics Institute, Tbilisi State University, Tbilisi, Georgia*

55 *II Physikalisches Institut, Justus-Liebig-Universität Giessen, Giessen, Germany*

56 *SUPA - School of Physics and Astronomy, University of Glasgow, Glasgow, United Kingdom*

57 *II Physikalisches Institut, Georg-August-Universität, Göttingen, Germany*

58 *Laboratoire de Physique Subatomique et de Cosmologie, Université Grenoble-Alpes, CNRS/IN2P3, Grenoble, France*

59 *Laboratory for Particle Physics and Cosmology, Harvard University, Cambridge MA, United States of America*

60 (a) *Kirchhoff-Institut für Physik, Ruprecht-Karls-Universität Heidelberg, Heidelberg;* (b) *Physikalisches Institut, Ruprecht-Karls-Universität Heidelberg, Heidelberg, Germany*

61 *Faculty of Applied Information Science, Hiroshima Institute of Technology, Hiroshima, Japan*

62 (a) *Department of Physics, The Chinese University of Hong Kong, Shatin, N.T., Hong Kong;* (b) *Department of Physics, The University of Hong Kong, Hong Kong;* (c) *Department of Physics and Institute for Advanced Study, The Hong Kong University of Science and Technology, Clear Water Bay, Kowloon, Hong Kong, China*

63 *Department of Physics, National Tsing Hua University, Taiwan, Taiwan*

64 *Department of Physics, Indiana University, Bloomington IN, United States of America*

65 *Institut für Astro- und Teilchenphysik, Leopold-Franzens-Universität, Innsbruck, Austria*

66 *University of Iowa, Iowa City IA, United States of America*

67 *Department of Physics and Astronomy, Iowa State University, Ames IA, United States of America*

68 *Joint Institute for Nuclear Research, JINR Dubna, Dubna, Russia*

69 *KEK, High Energy Accelerator Research Organization, Tsukuba, Japan*

70 *Graduate School of Science, Kobe University, Kobe, Japan*

71 *Faculty of Science, Kyoto University, Kyoto, Japan*

72 *Kyoto University of Education, Kyoto, Japan*

73 *Research Center for Advanced Particle Physics and Department of Physics, Kyushu University, Fukuoka, Japan*

74 *Instituto de Física La Plata, Universidad Nacional de La Plata and CONICET, La Plata, Argentina*

75 *Physics Department, Lancaster University, Lancaster, United Kingdom*

76 (a) *INFN Sezione di Lecce;* (b) *Dipartimento di Matematica e Fisica, Università del Salento, Lecce, Italy*

77 *Oliver Lodge Laboratory, University of Liverpool, Liverpool, United Kingdom*

78 *Department of Experimental Particle Physics, Jožef Stefan Institute and Department of Physics, University of Ljubljana, Ljubljana, Slovenia*

79 *School of Physics and Astronomy, Queen Mary University of London, London, United Kingdom*

80 *Department of Physics, Royal Holloway University of London, Surrey, United Kingdom*

81 *Department of Physics and Astronomy, University College London, London, United Kingdom*

82 *Louisiana Tech University, Ruston LA, United States of America*

83 *Laboratoire de Physique Nucléaire et de Hautes Energies, UPMC and Université Paris-Diderot and CNRS/IN2P3, Paris, France*

84 *Fysiska institutionen, Lunds universitet, Lund, Sweden*

85 *Departamento de Fisica Teorica C-15, Universidad Autonoma de Madrid, Madrid, Spain*

86 *Institut für Physik, Universität Mainz, Mainz, Germany*

87 *School of Physics and Astronomy, University of Manchester, Manchester, United Kingdom*

88 *CPPM, Aix-Marseille Université and CNRS/IN2P3, Marseille, France*

89 *Department of Physics, University of Massachusetts, Amherst MA, United States of America*

90 *Department of Physics, McGill University, Montreal QC, Canada*

91 *School of Physics, University of Melbourne, Victoria, Australia*

92 *Department of Physics, The University of Michigan, Ann Arbor MI, United States of America*

93 *Department of Physics and Astronomy, Michigan State University, East Lansing MI, United States of America*

94 <sup>(a)</sup> *INFN Sezione di Milano;* <sup>(b)</sup> *Dipartimento di Fisica, Università di Milano, Milano, Italy*

95 *B.I. Stepanov Institute of Physics, National Academy of Sciences of Belarus, Minsk, Republic of Belarus*

96 *Research Institute for Nuclear Problems of Byelorussian State University, Minsk, Republic of Belarus*

97 *Group of Particle Physics, University of Montreal, Montreal QC, Canada*

98 *P.N. Lebedev Physical Institute of the Russian Academy of Sciences, Moscow, Russia*

99 *Institute for Theoretical and Experimental Physics (ITEP), Moscow, Russia*

100 *National Research Nuclear University MEPhI, Moscow, Russia*

101 *D.V. Skobeltsyn Institute of Nuclear Physics, M.V. Lomonosov Moscow State University, Moscow, Russia*

102 *Fakultät für Physik, Ludwig-Maximilians-Universität München, München, Germany*

103 *Max-Planck-Institut für Physik (Werner-Heisenberg-Institut), München, Germany*

104 *Nagasaki Institute of Applied Science, Nagasaki, Japan*

105 *Graduate School of Science and Kobayashi-Maskawa Institute, Nagoya University, Nagoya, Japan*

106 <sup>(a)</sup> *INFN Sezione di Napoli;* <sup>(b)</sup> *Dipartimento di Fisica, Università di Napoli, Napoli, Italy*

107 *Department of Physics and Astronomy, University of New Mexico, Albuquerque NM, United States of America*

108 *Institute for Mathematics, Astrophysics and Particle Physics, Radboud University Nijmegen/Nikhef, Nijmegen, Netherlands*

109 *Nikhef National Institute for Subatomic Physics and University of Amsterdam, Amsterdam, Netherlands*

110 *Department of Physics, Northern Illinois University, DeKalb IL, United States of America*

111 *Budker Institute of Nuclear Physics, SB RAS, Novosibirsk, Russia*

112 *Department of Physics, New York University, New York NY, United States of America*

113 *Ohio State University, Columbus OH, United States of America*

114 *Faculty of Science, Okayama University, Okayama, Japan*

115 *Homer L. Dodge Department of Physics and Astronomy, University of Oklahoma, Norman OK, United States of America*

116 *Department of Physics, Oklahoma State University, Stillwater OK, United States of America*

117 *Palacký University, RCPTM, Olomouc, Czech Republic*

118 *Center for High Energy Physics, University of Oregon, Eugene OR, United States of America*

119 *LAL, Univ. Paris-Sud, CNRS/IN2P3, Université Paris-Saclay, Orsay, France*

120 *Graduate School of Science, Osaka University, Osaka, Japan*

121 *Department of Physics, University of Oslo, Oslo, Norway*

122 *Department of Physics, Oxford University, Oxford, United Kingdom*

123 <sup>(a)</sup> *INFN Sezione di Pavia;* <sup>(b)</sup> *Dipartimento di Fisica, Università di Pavia, Pavia, Italy*

124 *Department of Physics, University of Pennsylvania, Philadelphia PA, United States of America*

125 *National Research Centre "Kurchatov Institute" B.P.Konstantinov Petersburg Nuclear Physics Institute, St. Petersburg, Russia*

126 <sup>(a)</sup> *INFN Sezione di Pisa;* <sup>(b)</sup> *Dipartimento di Fisica E. Fermi, Università di Pisa, Pisa, Italy*

127 *Department of Physics and Astronomy, University of Pittsburgh, Pittsburgh PA, United States of America*

128 <sup>(a)</sup> *Laboratório de Instrumentação e Física Experimental de Partículas - LIP, Lisboa;* <sup>(b)</sup> *Faculdade de Ciências, Universidade de Lisboa, Lisboa;* <sup>(c)</sup> *Department of Physics, University of Coimbra, Coimbra;* <sup>(d)</sup> *Centro de Física Nuclear da Universidade de Lisboa, Lisboa;* <sup>(e)</sup> *Departamento de Fisica, Universidade do Minho, Braga;* <sup>(f)</sup> *Departamento de Fisica Teorica y del Cosmos, Universidad de Granada, Granada;* <sup>(g)</sup> *Dep Fisica and CEFITEC of Faculdade de Ciencias e Tecnologia, Universidade Nova de Lisboa, Caparica, Portugal*

129 *Institute of Physics, Academy of Sciences of the Czech Republic, Praha, Czech Republic*

130 *Czech Technical University in Prague, Praha, Czech Republic*

131 *Charles University, Faculty of Mathematics and Physics, Prague, Czech Republic*

132 *State Research Center Institute for High Energy Physics (Protvino), NRC KI, Russia*

133 *Particle Physics Department, Rutherford Appleton Laboratory, Didcot, United Kingdom*

134 [a] *INFN Sezione di Roma;* [b] *Dipartimento di Fisica, Sapienza Università di Roma, Roma, Italy*

135 [a] *INFN Sezione di Roma Tor Vergata;* [b] *Dipartimento di Fisica, Università di Roma Tor Vergata, Roma, Italy*

136 [a] *INFN Sezione di Roma Tre;* [b] *Dipartimento di Matematica e Fisica, Università Roma Tre, Roma, Italy*

137 [a] *Faculté des Sciences Ain Chock, Réseau Universitaire de Physique des Hautes Energies - Université Hassan II, Casablanca;* [b] *Centre National de l'Energie des Sciences Techniques Nucleaires, Rabat;* [c] *Faculté des Sciences Semlalia, Université Cadi Ayyad, LPHEA-Marrakech;* [d] *Faculté des Sciences, Université Mohamed Premier and LPTPM, Oujda;* [e] *Faculté des sciences, Université Mohammed V, Rabat, Morocco*

138 *DSM/IRFU (Institut de Recherches sur les Lois Fondamentales de l'Univers), CEA Saclay (Commissariat à l'Energie Atomique et aux Energies Alternatives), Gif-sur-Yvette, France*

139 *Santa Cruz Institute for Particle Physics, University of California Santa Cruz, Santa Cruz CA, United States of America*

140 *Department of Physics, University of Washington, Seattle WA, United States of America*

141 *Department of Physics and Astronomy, University of Sheffield, Sheffield, United Kingdom*

142 *Department of Physics, Shinshu University, Nagano, Japan*

143 *Department Physik, Universität Siegen, Siegen, Germany*

144 *Department of Physics, Simon Fraser University, Burnaby BC, Canada*

145 *SLAC National Accelerator Laboratory, Stanford CA, United States of America*

146 [a] *Faculty of Mathematics, Physics & Informatics, Comenius University, Bratislava;* [b] *Department of Subnuclear Physics, Institute of Experimental Physics of the Slovak Academy of Sciences, Kosice, Slovak Republic*

147 [a] *Department of Physics, University of Cape Town, Cape Town;* [b] *Department of Physics, University of Johannesburg, Johannesburg;* [c] *School of Physics, University of the Witwatersrand, Johannesburg, South Africa*

148 [a] *Department of Physics, Stockholm University;* [b] *The Oskar Klein Centre, Stockholm, Sweden*

149 *Physics Department, Royal Institute of Technology, Stockholm, Sweden*

150 *Departments of Physics & Astronomy and Chemistry, Stony Brook University, Stony Brook NY, United States of America*

151 *Department of Physics and Astronomy, University of Sussex, Brighton, United Kingdom*

152 *School of Physics, University of Sydney, Sydney, Australia*

153 *Institute of Physics, Academia Sinica, Taipei, Taiwan*

154 *Department of Physics, Technion: Israel Institute of Technology, Haifa, Israel*

155 *Raymond and Beverly Sackler School of Physics and Astronomy, Tel Aviv University, Tel Aviv, Israel*

156 *Department of Physics, Aristotle University of Thessaloniki, Thessaloniki, Greece*

157 *International Center for Elementary Particle Physics and Department of Physics, The University of Tokyo, Tokyo, Japan*

158 *Graduate School of Science and Technology, Tokyo Metropolitan University, Tokyo, Japan*

159 *Department of Physics, Tokyo Institute of Technology, Tokyo, Japan*

160 *Tomsk State University, Tomsk, Russia*

161 *Department of Physics, University of Toronto, Toronto ON, Canada*

162 [a] *INFN-TIFPA;* [b] *University of Trento, Trento, Italy*

163 [a] *TRIUMF, Vancouver BC;* [b] *Department of Physics and Astronomy, York University, Toronto ON, Canada*

164 *Faculty of Pure and Applied Sciences, and Center for Integrated Research in Fundamental Science and Engineering, University of Tsukuba, Tsukuba, Japan*

165 *Department of Physics and Astronomy, Tufts University, Medford MA, United States of America*

166 *Department of Physics and Astronomy, University of California Irvine, Irvine CA, United States of*

*America*

167 $^{(a)}$ *INFN Gruppo Collegato di Udine, Sezione di Trieste, Udine;* $^{(b)}$ *ICTP, Trieste;* $^{(c)}$ *Dipartimento di Chimica, Fisica e Ambiente, Università di Udine, Udine, Italy*

168 *Department of Physics and Astronomy, University of Uppsala, Uppsala, Sweden*

169 *Department of Physics, University of Illinois, Urbana IL, United States of America*

170 *Instituto de Fisica Corpuscular (IFIC), Centro Mixto Universidad de Valencia - CSIC, Spain*

171 *Department of Physics, University of British Columbia, Vancouver BC, Canada*

172 *Department of Physics and Astronomy, University of Victoria, Victoria BC, Canada*

173 *Department of Physics, University of Warwick, Coventry, United Kingdom*

174 *Waseda University, Tokyo, Japan*

175 *Department of Particle Physics, The Weizmann Institute of Science, Rehovot, Israel*

176 *Department of Physics, University of Wisconsin, Madison WI, United States of America*

177 *Fakultät für Physik und Astronomie, Julius-Maximilians-Universität, Würzburg, Germany*

178 *Fakultät für Mathematik und Naturwissenschaften, Fachgruppe Physik, Bergische Universität Wuppertal, Wuppertal, Germany*

179 *Department of Physics, Yale University, New Haven CT, United States of America*

180 *Yerevan Physics Institute, Yerevan, Armenia*

181 *Centre de Calcul de l'Institut National de Physique Nucléaire et de Physique des Particules (IN2P3), Villeurbanne, France*

182 *Academia Sinica Grid Computing, Institute of Physics, Academia Sinica, Taipei, Taiwan*

$^a$ *Also at Department of Physics, King's College London, London, United Kingdom*

$^b$ *Also at Institute of Physics, Azerbaijan Academy of Sciences, Baku, Azerbaijan*

$^c$ *Also at Novosibirsk State University, Novosibirsk, Russia*

$^d$ *Also at TRIUMF, Vancouver BC, Canada*

$^e$ *Also at Department of Physics & Astronomy, University of Louisville, Louisville, KY, United States of America*

$^f$ *Also at Physics Department, An-Najah National University, Nablus, Palestine*

$^g$ *Also at Department of Physics, California State University, Fresno CA, United States of America*

$^h$ *Also at Department of Physics, University of Fribourg, Fribourg, Switzerland*

$^i$ *Also at II Physikalisches Institut, Georg-August-Universität, Göttingen, Germany*

$^j$ *Also at Departament de Fisica de la Universitat Autonoma de Barcelona, Barcelona, Spain*

$^k$ *Also at Departamento de Fisica e Astronomia, Faculdade de Ciencias, Universidade do Porto, Portugal*

$^l$ *Also at Tomsk State University, Tomsk, and Moscow Institute of Physics and Technology State University, Dolgoprudny, Russia*

$^m$ *Also at The Collaborative Innovation Center of Quantum Matter (CICQM), Beijing, China*

$^n$ *Also at Universita di Napoli Parthenope, Napoli, Italy*

$^o$ *Also at Institute of Particle Physics (IPP), Canada*

$^p$ *Also at Horia Hulubei National Institute of Physics and Nuclear Engineering, Bucharest, Romania*

$^q$ *Also at Department of Physics, St. Petersburg State Polytechnical University, St. Petersburg, Russia*

$^r$ *Also at Borough of Manhattan Community College, City University of New York, New York City, United States of America*

$^s$ *Also at Department of Financial and Management Engineering, University of the Aegean, Chios, Greece*

$^t$ *Also at Centre for High Performance Computing, CSIR Campus, Rosebank, Cape Town, South Africa*

$^u$ *Also at Louisiana Tech University, Ruston LA, United States of America*

$^v$ *Also at Institucio Catalana de Recerca i Estudis Avancats, ICREA, Barcelona, Spain*

$^w$ *Also at Department of Physics, The University of Michigan, Ann Arbor MI, United States of America*

[x] Also at Graduate School of Science, Osaka University, Osaka, Japan

[y] Also at Fakultät für Mathematik und Physik, Albert-Ludwigs-Universität, Freiburg, Germany

[z] Also at Institute for Mathematics, Astrophysics and Particle Physics, Radboud University Nijmegen/Nikhef, Nijmegen, Netherlands

[aa] Also at Department of Physics, The University of Texas at Austin, Austin TX, United States of America

[ab] Also at Institute of Theoretical Physics, Ilia State University, Tbilisi, Georgia

[ac] Also at CERN, Geneva, Switzerland

[ad] Also at Georgian Technical University (GTU),Tbilisi, Georgia

[ae] Also at Ochadai Academic Production, Ochanomizu University, Tokyo, Japan

[af] Also at Manhattan College, New York NY, United States of America

[ag] Also at Departamento de Física, Pontificia Universidad Católica de Chile, Santiago, Chile

[ah] Also at The City College of New York, New York NY, United States of America

[ai] Also at School of Physics, Shandong University, Shandong, China

[aj] Also at Departamento de Fisica Teorica y del Cosmos, Universidad de Granada, Granada, Portugal

[ak] Also at Department of Physics, California State University, Sacramento CA, United States of America

[al] Also at Moscow Institute of Physics and Technology State University, Dolgoprudny, Russia

[am] Also at Departement de Physique Nucleaire et Corpusculaire, Université de Genève, Geneva, Switzerland

[an] Also at Institut de Física d'Altes Energies (IFAE), The Barcelona Institute of Science and Technology, Barcelona, Spain

[ao] Also at School of Physics, Sun Yat-sen University, Guangzhou, China

[ap] Also at Institute for Nuclear Research and Nuclear Energy (INRNE) of the Bulgarian Academy of Sciences, Sofia, Bulgaria

[aq] Also at Faculty of Physics, M.V.Lomonosov Moscow State University, Moscow, Russia

[ar] Also at National Research Nuclear University MEPhI, Moscow, Russia

[as] Also at Department of Physics, Stanford University, Stanford CA, United States of America

[at] Also at Institute for Particle and Nuclear Physics, Wigner Research Centre for Physics, Budapest, Hungary

[au] Also at Giresun University, Faculty of Engineering, Turkey

[av] Also at CPPM, Aix-Marseille Université and CNRS/IN2P3, Marseille, France

[aw] Also at Department of Physics, Nanjing University, Jiangsu, China

[ax] Also at Institute of Physics, Academia Sinica, Taipei, Taiwan

[ay] Also at University of Malaya, Department of Physics, Kuala Lumpur, Malaysia

[az] Also at LAL, Univ. Paris-Sud, CNRS/IN2P3, Université Paris-Saclay, Orsay, France

[*] Deceased